A Constitutively Consistent Lower Bound, Direct Shakedown and Ratchet Method

Alan Jappy

PhD Thesis

Department of Mechanical and Aerospace Engineering

The University of Strathclyde

Glasgow

June 2014

Abstract

When a structure is subject to cyclic loads there is a possibility of it failing due to ratchet or incremental collapse. In many engineering structures the demonstration of non-ratcheting behaviour is a fundamental requirement of the design and assessment process. Whilst it is possible to use incremental finite element analysis to simulate the cyclic response for a given load case to demonstrate shakedown or ratchet, it does not yield any information on the safety factor. In addition, there are several practical problems in using this approach to determine whether or not a component has achieved shakedown. Consequently several direct methods which find the loads at the shakedown and ratchet boundaries have been developed in the past 3 decades.

In general, lower bound methods are preferred for design and assessment methodologies. However, to date, the lower bound methods which have been proposed for shakedown and ratchet analysis have not been fully reliable and accurate. In this thesis a lower bound shakedown and ratchet method which is both reliable and accurate is proposed.

Previously proposed elastic plastic lower bound ratchet methods are revisited and modified to understand the limitations in current methods. From this, Melan's theorem is reinterpreted in terms of plasticity modelling and shown to have the same form as a non-smooth multi yield surface plasticity model. A new shakedown method is then proposed based on the non-smooth multi yield surface plasticity model. The new shakedown method is extended using a two stage process to determine the ratchet boundary for cyclic loads in excess of the alternating plasticity boundary. Two simplified variants of the ratchet method are also proposed to decrease the computational expense of the proposed ratchet method.

Through several common benchmark problems the proposed methods are shown to give excellent agreement with the current upper bound methods which have been demonstrated to be accurate. The flexibility of the shakedown method is demonstrated by extending the method to incorporate temperature dependent yield, hardening and simplified non-linear geometric effects.

This thesis is the result of the author's original research. It has been composed by the author and has not been previously submitted for examination which has led to the award of a degree.

Acknowledgments

The three years of this PhD course of study have been interesting to say the least. There have been fun times, hard times, moments of shear frustration and some of pure elation. During these times I have had the support of some great people.

I would like to extend my thanks to the University of Strathclyde for funding my research through their scholarship scheme. I would also like to thank the staff of the Mechanical and Aerospace Engineering Department.

I would like to say a huge thank you to Prof. Donald Mackenzie, who despite having a packed schedule, was able to provide continued support and guidance throughout the PhD. Without his level head and experience I would not have been able to achieve all I have during the past three years. I would also like to acknowledge his efforts in proof reading this thesis.

I would also like to acknowledge the members of the Linear Matching Research team. Specifically my peers James Ure and Micheal Lytwyn, who were/are also undertaking PhDs in the topic of shakedown and ratchet, for being there to bounce ideas of and sharing in the learning curve for Fortran, ABAQUS and user subroutines.

I would also like to extend thanks to my family for their continued and enduring support throughout my time at university, especially my Father for taking the time to proof read this thesis.

Without the friends who provided many enjoyable and uplifting moments I would not have enjoyed the experience as much, specifically a thank you to Martin Van-Zyl, Lewis Brown, James Ure, Micheal Lytwyn, Jamie Frame and Hugh Macknally.

Contents

1 Introduction

This thesis presents the development of an accurate, reliable, strict lower bound direct shakedown and ratchet method. In general, the demonstration of the shakedown behaviour of a structure is an important part of the design process, as the alternative ratcheting behaviour can be a serious form of failure and is generally catastrophic in nature. Therefore having both accurate and reliable methods for ascertaining if a structure has achieved shakedown is of interest in many engineering sectors, in particular the electricity generation and nuclear sectors.

Given the current simulation/analysis capabilities of commercial finite element software, it might be difficult to understand why showing shakedown behaviour requires the use of specialist methods such as those proposed here. However there are a number of difficulties in using the Finite Element Method for the demonstration of shakedown behaviour:

It can require a large number of cycles. If using standard incremental Finite Element Method the number of cycles that may be necessary to show a strict shakedown behaviour can be large, sometimes thousands or tens of thousands of load cycles.

What is a suitable criteria for shakedown? When using finite elements the software will generally report on the plastic strains in the structure. To show shakedown it must be demonstrated that there is no accumulation in net plastic strains from one cycle to the next cycle. However given that the procedure is always subject to numerical error it is necessary to define sufficient criteria for the check on plastic strains.

It can be computationally expensive. Due to the two problems mentioned above, the overall cost of demonstrating shakedown behaviour can be computationally expensive compared to specialist shakedown and ratchet methods.

A method which can accurately determine whether or not shakedown has been achieved in a computationally efficient manner would be beneficial to the design and structural integrity assessment processes.

This thesis is separated into 6 sections which demonstrate the progression of the research from understanding the current methods through to development of a new approach to the lower bound shakedown and ratchet problems:

Section 2 introduces the phenomena of shakedown and ratchet. The section describes the mechanisms involved in shakedown and ratchet and discusses using Finite

Element Analysis (FEA) to determine the shakedown/ratchet behaviour. The idea of bounding theorems is introduced and the section concludes with a review of the various analysis methods currently used to determine shakedown and ratchet boundaries.

Section 3 proposes and implements a method similar to the current "state of the art" elastic-plastic lower bound methods, to explore the reasons for current elastic-plastic lower bound methods being unreliable. The shakedown and ratchet problem is posed in a manner in which it may be solved using the Finite Element Method. Several benchmark problems are studied to identify the likely source of instability and errors in the results obtained by the method.

Section 4 builds on the findings of Section 3. Melan's theorem is revisited and discussed in the context of material behaviour and finite element modelling. By defining a material model from Melan's theorem and plasticity theory, the lower bound shakedown and ratchet problems are shown to have the same form as a particular class of material model. Section 4 continues by proposing the residual stress condition as a stress state which is shared by all of the load cases considered in the shakedown and ratchet problem, which is important for the application of the material model in a FEA.

Section 5 proposes and implements a new shakedown method based on the class of material model which was demonstrated to have the same form as the lower bound shakedown theorem in Section 4. The proposed method is tested with several common benchmark problems. After demonstrating the accuracy of the new shakedown method it is extended to include temperature dependent yield, hardening effects and simplified non-linear geometry effects.

Section 6 extends the shakedown method developed in Section 5 to the ratchet boundary beyond the alternating plasticity boundary. The proposed method is tested with several common benchmark problems. After demonstrating the accuracy of the new ratchet method it is extended to include temperature dependent yield strength.

Notation

In this thesis it has been necessary to use mixed notation. The tensor notation used is the indicial notation, where indices are repeated Einstein summation is assumed. Matrices are denoted by [ ] for square matrices and { } for vectors. For square matrices

subscripts are used in some cases when a particular element of the matrix is being referred to i.e. $[A]_{\alpha\beta}$ is the element in matrix $[A]$ at row α and column β.

2 Shakedown and Ratchet

The review of literature here gives a general background to the shakedown and ratchet problem along with key topics such as bounding theorems and methods for finding the load condition at the various shakedown and ratchet boundaries. As the focus of this research is the development of a ratchet method, the review of the current methods focuses on the "augmented limit" methods, as these are the only methods which are currently able to give the elastic and plastic ratchet boundaries. Other literature covered is intended as an overview of other areas of interest but not discussed in detail.

2.1 Bree Diagram

Shakedown and ratchet are terms used to describe the long term elastic or elastic-plastic response of a structure subject to cyclic loads. These behaviours are usually introduced through the Bree Problem (Bree 1967). The Bree problem is a common benchmark used in shakedown and ratchet research as it represents a simple analytical problem which demonstrates all 5 idealised long term responses a structure may exhibit under cyclic loading.

The Bree problem was designed to consider the shakedown/ratchet behavior of a pressurized shell, of elastic-perfectly plastic material, subject to cyclic thermal gradient. In order to allow analytical solution of the system, it is simplified to a plane stress plate with a cyclic thermal gradient through its thickness and constant uni-axial tension. To give cyclic thermal stresses due to the cyclic thermal gradient, the plate is constrained to remain in plane section. A schematic diagram of the Bree problem is given in figure 1a.

Under the constant load from the uni-axial tension and the cyclic load from the cyclic thermal gradient, the Bree problem can exhibit 5 long term elastic or elastic-plastic cyclic responses. The responses are generally shown on a graph of normalised constant load v.s. normalised thermal load, in both cases normalised against the yield strength of the material making up the plate. A typical graph for the Bree Cylinder with each type of cyclic response identified is shown in figure 1b. The 5 responses may be defined as follows:

Elastic During the initial cycle of load the stress everywhere in the structure remains in the elastic domain and no yielding occurs. A time independent state of plastic strain exists i.e. $\varepsilon_{ij}^{p}(t) = 0$ everywhere in the structure with a cyclic stress such that $|\sigma_{ij}(t)| \leq \sigma^{y}$.

Elastic shakedown During the initial load cycles the the structure undergoes plastic straining but does not collapse. After a finite number of load cycles the stress everywhere in the structure remains within the elastic domain during the whole load cycle i.e. $|\sigma_{ij}(t)| \leq \sigma^y$ and the plastic strain becomes time invariant $\varepsilon_{ij}^p(t) =$ Constant everywhere in the structure.

Plastic shakedown During the initial load cycles the structure undergoes plastic straining but does not collapse. After a finite number of load cycles a closed plastic strain cycle exist somewhere in the structure i.e. $\varepsilon_{ij}{}^p(t+\varphi) = \varepsilon_{ij}{}^p(t)$ where φ is the period of a load cycle. Everywhere else in the structure, the stresses cycle within the elastic domain and a time invariant plastic strain exists.

Ratchet or incremental collapse During the initial load cycles the structure undergoes plastic straining but does not collapse. During each successive cycle of load there is an increase in the plastic strain over every point in a section of the structure.

Limit or collapse During the initial cycle of load the structure collapses due to gross plastic deformation.

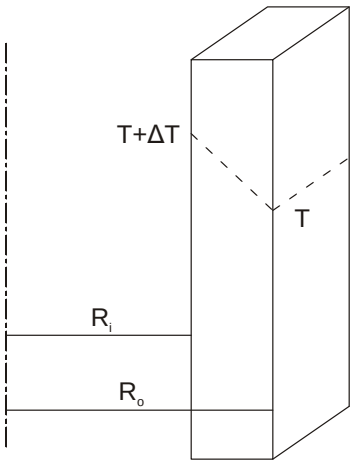

(a) Schematic

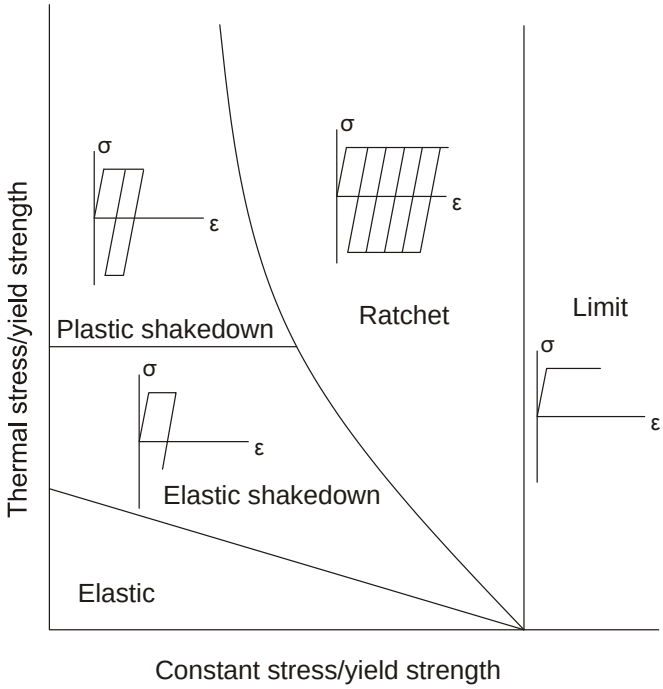

(b) Bree Diagram with inset cyclic responses

Figure 1: Bree Problem

2.1.1 Effect of Hardening On Shakedown Boundaries

The basic Bree problem considers prefect plasticity. In certain situations this may be overly conservative. The effect of unlimited hardening was considered by Melan (1938), Maier (1972) and Ponter (1975). When considering hardening there are two basic groupings of the hardening behaviour. Isotropic hardening increases the magnitude of the yield stress and kinematic hardening allows the yield surface to displace in stress space to accommodate increased stresses.

The effect of unlimited isotropic hardening is to result in elastic shakedown behaviour under all circumstances; i.e. there would be no alternating plasticity or ratchet boundary in the Bree diagram. This is due to the yield surface being able to increase in size to accommodate any magnitude of elastic stress range. When considering unlimited kinematic hardening the yield surface remains the same size, thus the elastic range of the material remains the same and therefore the alternating plasticity limit will remain as for the perfect plasticity case. Ratchet will however never occur under the effects of unlimited hardening as an alternating plasticity mechanism will always be able to develop, which results in a stabilised plastic strain cycle.

The use of unlimited hardening leads to the conclusion that ratchet would never occur in a structure. However ratchet has been observed in practice (see for example Indermohan and Reinhardt 2012), therefore it is known that the behaviour described by unlimited hardening is unrealistic. Limited hardening has been consider by a number of sources (see for example Weichert and Gross-Weege 1988, Polizzotto et al. 1991, Corigliano et al. 1995a, Corigliano et al. 1995b, Nguyen and and Pham 2005). Under the effects of limited isotropic hardening the elastic range of the material is bounded by twice the hardened yield strength. Thus there will be an alternating plasticity boundary. As the hardening is limited the maximum stress that can be support by a section is limited, if this limit is reached over an entire section of the component for any combination of load points ratchet will occur. With limited kinematic hardening the elastic range of the material remains unchanged thus the alternating plasticity limit will be the same as for the perfectly plastic case. The limited hardening does however result in a limit to the maximum stress which can be supported by a section of the component. If this maximum stress is reached over an entire section of a component for any combination of load cases, ratchet will occur.

The description of shakedown/ratchet provided by limited hardening is more consistent with observed component behaviour than unlimited hardening. However, recently the usefulness of this description has been questioned, see (Indermohan and

Reinhardt 2012). It was noted in (Indermohan and Reinhardt 2012) that under the effect of limited hardening, whilst ratchet will be predicted the plastic strains at the resulting ratchet boundary can be large. Practically, if large plastic strains are necessary to allow shakedown to occur it should be questioned whether shakedown would be achieved before some other failure mechanism occurrs. In such circumstances accurate predictions of plastic strains would be useful when considering structural deformation and rupture. However, few methods provide accurate plastic strains when considering hardening, as the link between hardening and plastic strains are ignored. Therefore at present it is not clear if the use of hardening in shakedown/ratchet methods is fully developed and applicable to practical design considerations.

2.2 Boundary Names

There is no general consensus in the literature for the names given to the different boundaries on the Bree diagram. Figure 2 shows a collection of Bree diagrams with various different names given to the boundaries commonly in use. As is evident from the figures, some naming conventions use the name ratchet boundary to mean different parts of the ratchet response.

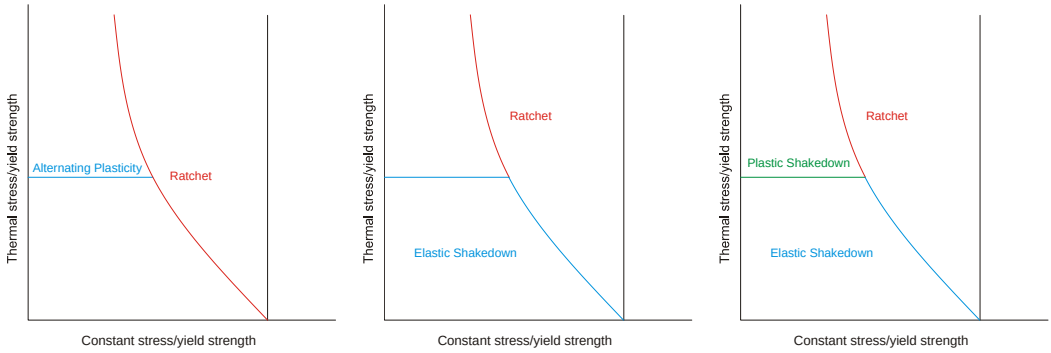

Figure 2: Differing Boundary Names

As shakedown and ratchet are discussed individually in this thesis, it is at times necessary to separate the ratchet boundary into 2 distinct parts: the elastic ratchet boundary and the plastic ratchet boundary (see figure 3), signifying which shakedown region they bound. This avoids confusion as to which part of the ratchet boundary is being referred to. In all cases, where reference is made to the ratchet boundary, it is meant that both the elastic and plastic ratchet boundaries are being referred to. In addition, it is necessary to separate the elastic shakedown boundary into the alternating plasticity boundary and the elastic ratchet boundary. The names of the various boundaries used in this thesis are summarised in figure 3.

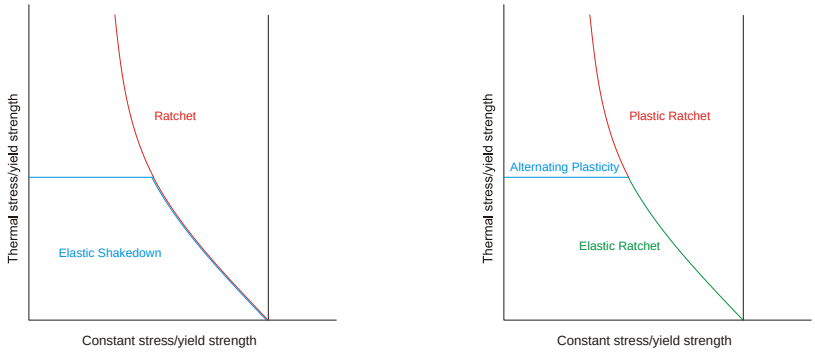

Figure 3: Naming Convention for Boundaries

2.3 Using FEA for Shakedown and Ratchet Analysis

Demonstrating shakedown or ratchet behaviour is, fundamentally, a plasticity problem. Whilst most of the theorems in the field (see Section 2.4) are based on stress or strain

energy, the fundamental formulations of the theorems are based on plasticity arguments. With the technology available today (i.e. the Finite Element Method), and increasing computational abilities making elastic plastic analysis ever cheaper, it might be difficult to understand why an engineer seeking to determine the shakedown or ratchet behaviour would not just use elastic plastic FEA.

In some cases using elastic plastic FEA might be the most appropriate solution method, however there are a number of limitations with that approach. Consider a structure subject to an arbitrary cyclic load case. Assume that the structure was simulated in an elastic plastic FEA for x cycles and demonstrated a shakedown behaviour. Whilst shakedown has been demonstrated, and this may satisfy some design codes, the safety factor against the onset of ratchet has not been determined. In general this is not possible from a single FEA. It is necessary to conduct several more elastic plastic analysis with higher loads to find the load case at which ratchet first occurs. This leads to relatively high computational expense and effort when trying to identify the ratchet boundary and thus obtain knowledge of safety factors.

Consider a situation where the structure is simulated for x cycles and does not show a strict shakedown behaviour. If this is the case it might be tempting to assume that the applied load lies outside the ratchet boundary. However this may not be the case. Depending on the complexity of the component and load cycle, showing strict shakedown in a component may require thousands of load cycles to be simulated. Only when a constant stabilised plastic strain increase over each cycle is found may the behaviour be identified as ratcheting. Thus complex components/load cycles may require large computational effort to identify the shakedown or ratchet behaviour for a single load case. Given that this does not give an indication as to the margin of safety to ratchet, several of these analysis will be needed to identify the ratchet boundary, leading to potentially excessive computational cost.

The difficulties of the two previous problems are exacerbated by the numerical accuracy of the computational solution methods. Any numerical solution method utilising computational methods is subject to the numerical accuracy possible with the computer architecture and hardware. Given the large number of iterations an elastic plastic FEA may take, accumulated numerical error can result. This can produce what appears to be a ratchet strain which is actually nothing more than accumulation in numerical error. This further complicates identifying the shakedown/ ratchet response. This also results in another problem. What should be the required level of accuracy when determining whether the magnitude of a plastic strain has stabilised from one load cycle to the next?

Given the potential problems when trying to identify the ratchet boundary using elastic plastic FEA, a method for finding the ratchet boundary directly in a single analysis would be beneficial. To do this the conditions which lead to the onset of ratchet must first be defined. This is the purpose of the bounding theorems for shakedown and ratchet.

2.4 The bounding theorems for shakedown and ratchet

The bounding theorems for shakedown and ratchet have been in development since the late 1930s, when they were used in analytical solutions for shakedown and ratchet. The lower bound theorems seek to define an equilibrium solution, for a given load case, for which a shakedown behaviour exists. The upper bound theorems seek a kinematic solution, for a given load case, which minimises the ratchet strain energy.

2.4.1 Elastic Shakedown

Melan's static shakedown theorem (Melan 1936), commonly referred to as Melan's lower bound shakedown theorem, considers time invariant equilibrium stress fields and may be expressed:

If a structure is subject to an arbitrary cyclic load case $P(t)$ which results in fully elastic stresses $\sigma^e_{ij}(t)$in equilibrium with that load case, the structure will shakedown if a time invariant residual stress field, ρ^c_{ij}, can be defined such that when superimposed with the elastic stresses $\sigma^e_{ij}(t)$, the resulting equivalent stress $|\rho^c_{ij} + \sigma^e_{ij}(t)|$ everywhere in the structure remains within the elastic region during the entire load cycle.

Koiter gave the general proof for the kinematic shakedown theorem (Koiter 1960), commonly referred to as Koiter's upper bound shakedown theorem, which considers kinematically admissible strains and may be expressed:

If, a set of cyclic external influences P_j applied on the surface S of the structure results in an admissible cyclic displacement field u_j on S, shakedown will not occur if the work dissipated W by a set of kinematically admissible plastic strains, ε^{p0}_{ij}, is less than the work done on the structure.

That is shakedown will not occur if:

$$\int\int P_j u_j dS dt > \int\int W(\varepsilon^{p0}_{ij}) dV dt \tag{1}$$

Thus the problem reduces to minimising the following inequality:

$$\int\int U\left(P_j u_j\right) dSdt \leq \int\int W(\varepsilon_{ij}^{p0}) dV dt$$

where $U\left(P_j u_j\right)$ is the work done in the structure by $(P_j u_j)$, $W(\varepsilon_{ij}^{p0})$ is the work energy dissipated by (ε_{ij}^{p0}) and V is the volume of the structure

Both the Melan and Koiter theorems assume linear kinematics and an elastic-perfectly plastic material and do not necessarily give appropriate shakedown boundaries for all practical situations, such as large structural deformations and strain softening materials. Several extensions to the Melan and Koiter formulations have been proposed to overcome these and other limitations, for example: unlimited kinematic hardening (Melan 1938, Maier 1972 and Ponter 1975); limited kinematic hardening (Weichert and Gross-Weege 1988, Polizzotto et al. 1991, Corigliano et al. 1995a, Corigliano et al. 1995b, Nguyen and and Pham 2005); geometric non-linearity (Maier 1972, Weichert 1986 and Gross-Weege 1990); material damage (Hachemi and Weichert 1992); non-associative flow rules, for example (Maier 1969 and Boulbibane and Weichert 1997) and cracked structures (Huang and Stein 1996 and Belouchrani et al. 2000).

2.4.2 Extended Shakedown Theorems

The elastic shakedown theorems are sufficient for cyclic loads below the alternating plasticity boundary. If the cyclic loads are higher than those necessary to cause a reverse plasticity mechanism in the structure, additional conditions must be placed on the plastic strain cycle.

Melan's elastic shakedown theorem was extended to allow for cyclic loads above the alternating plasticity boundary by Gokhfeld (1980). Gokhfeld's theorem applies to a structure subject to a load case $P(t)$ that must be separated into constant and cyclic components, P^c and $\hat{P}(t)$. Application of these loads results in development of fully elastic stresses σ_{ij}^c and $\hat{\sigma}_{ij}\left(t\right)$ in equilibrium with their respective load. The theorem states that the structure will shakedown if:

A time invariant residual stress field, $\rho_{ij}^c + \overline{\rho}_{ij}$, and time varying residual stress field, $\rho_{ij}^{\Delta}(t)$, can be found such that when superimposed on the elastic stresses σ_{ij}^c and $\hat{\sigma}_{ij}\left(t\right)$, the resulting equivalent stress $\left|\rho_{ij}^c + \overline{\rho}_{ij} + \rho_{ij}^{\Delta}(t) + \sigma_{ij}^c + \hat{\sigma}_{ij}\left(t\right)\right|$ remains within the elastic region during the entire load cycle everywhere in the structure with the additional constraint that the varying residual stress field is limited to the regions of the structure where the magnitude of the cyclic stresses are great enough to result in alternating plasticity and must vanish over the cycle i.e. $\rho_{ij}^{\Delta}(t) = \rho_{ij}^{\Delta}(t+\varphi)$ where φ is

the period of one cycle and k is an integer.

A detailed discussion of the static shakedown and static extended shakedown theorems and the necessary requirement of the closed cyclic solutions, or post transient plastic strains, may be found in (Pollizzotto 1993a,b,c,d).

A general extension to Koiter's upper bound shakedown theorem, to include the plastic ratchet boundary, has recently been given by Ponter and Chen (Ponter and Chen 2001). It may be summarised as follows:

If a structure is subject to a set of external influences, which results in a kinematically admissible strain history, for elastic or plastic shakedown to exist it must be shown that the plastic dissipation resulting from the stress-strain cycle does not exceed the structure's potential to dissipate that energy: therefore an upper bound ratchet multiplier Y^{rat} is given by:

$$\int \int \left(\sigma^y - Y^{rat} \hat{\sigma}_{ij} \right) \dot{\varepsilon}^p_{ij} dt dV = 0$$

2.4.3 Naming Convention for Methods Based on Bounding Theorems

Many sources refer to methods based on these bounding theorems as being lower bound "stress based" or upper bound "strain" based methods (within the usual limitations of the finite element method). However lower and upper bound have stricter definitions. For instance, a lower bound method should never give a converged solution above the actual ratchet/shakedown load.[1] Conversely in the case of an asymptotically converging upper bound it should approach the actual ratchet/shakedown load from above and never give a solution below the actual ratchet/shakedown load.

It is therefore necessary to have a means of representing this difference. If the method is based on stresses and is a "stress based" lower bound, it will be referred to as a lower bound method. If it satisfies the strict definition of the term "lower bound" then it will be referred to as a strict lower bound method. For upper bounds, those based on strain will be upper bound methods, if they satisfy the more stringent definition of "upper bound" they will then be referred to as strict upper bound methods.

2.5 Augmented Limit Methods

The methods which have so far been able to define the plastic ratchet boundary have been the methods which are based on performing an augmented limit analysis, by either repeated elastic analysis or elastic plastic analysis. This is due to it being shown that

[1] For an example of a "lower bound method" which gives non-conservative result see the ratchet boundary given by the lower bound Linear Matching Method in section 6.4.2 and appendix A.

the lower bounding theorems for limit, shakedown and ratchet are analogous to each other, where different load cases are used, (Melan 1938 and Ponter and Chen 2001).

In general, the augmented limit type ratchet methods use the same solution strategy. This requires the load to be decomposed into constant and cyclic parts. The post transient stresses and plastic strains are found for the cyclic loads to give a closed plastic strain cycle. These stresses are then added to the constant load and an augmented limit analysis is performed based on the combined post transient stresses and the constant stress. This is basically the method used in (Bree 1967), where analytical solutions for the cyclic stresses were known, and was suggested in (Gokhfeld 1980). The conditions for the post transient stresses and plastic strains and the use of a limit based shakedown solver for ratchet is given in (Polizzotto 1993c,d)

2.5.1 Elastic Compensation method

The elastic compensation method is a direct limit load method which was extended to be a shakedown method. This method does not give the plastic ratchet boundary however it forms the basic idea for a number of the direct ratchet methods. The elastic compensation method was developed from a concept given by Marriott (1988) and introduced by Mackenzie and Boyle (1993), also (Nadarajah et al. 1993 and Shi et al. 1993), as a direct limit method based on the lower bound limit theorem see (Lubliner 1990). In this method a series of linear elastic analysis are conducted with altered elastic modulus to approximate the stress redistribution due to plasticity, allowing the approximation of lower bound limit load multiplier.

The concept which leads to the elastic compensation method is relatively simple and may be summarised as follows; for static equilibrium to exist in a structure made from elastic-perfectly plastic material, the stress everywhere in the structure must be less than or equal to the yield strength of the material. Consider a structure subject to an arbitrary load P which results in a fully elastic stress of σ_{ij}. If the equivalent stress $|\sigma_{ij}| > \sigma^y$ the redistribution of stress in the structure may be approximated by reducing the elastic modulus, E, of the material according to:

$$E^n = E^{n-1} \frac{\sigma^r}{\left|\sigma_{ij}^{n-1}\right|} \tag{2}$$

where n is the current increment.

Thus for points in the structure where the equivalent stress is below the normalised stress σ^r the stiffness increases, and decreases for points in the structure where the equivalent stress is above the normalised stress σ^r. Therefore the stress will redistribute

from the higher stressed regions to the lower stressed regions as would be the case in an elastic plastic analysis.

To calculate the resulting limit load multiplier it is observed that the structure behaves in a linear manner for a given iteration. Therefore the limiting lower bound limit multiplier would be given by the point in the structure with the highest stress:

$$Y = \frac{\sigma^y}{max\left(\left|\sigma_{ij}^{n-1}\right|\right)}$$

By continuing this process of modifying the elastic modulus and calculating the limit load multiplier the stress should redistribute and produce larger limit load multipliers. The highest limit load multiplier calculated in this manner during the analysis is identified as the limit load multiplier for the structure subject to load P. More recent research on variations of this method can be found in (Yang et al. 2005, Chen et al. 2008).

The extension to shakedown, see (Mackenzie et al. 2000) assumes that the load case may be decomposed into a constant load P^c and a set of proportionally time varying loads $\hat{P}(t)$. Therefore to satisfy Melan's theorem the load case need only be checked at the mid point of the cycle, when the proportional loads are at their maximum, and at the end of the cycle, when only the constant load is applied to the structure[2].

By applying the load P^c to the structure the stress in the structure due to load P^c may be directly calculated. The stress due to both P^c and $\hat{P}(t)$ may be found by superposition of the fully elastic stress which results result from $\hat{P}(t)$ onto the stress caused by P^c. If the equivalent stress at either point exceeds yield, the stress due to P^c can be redistributed using the same modulus adjustment procedure as used in the limit load method.

The lower bound shakedown multiplier may then be calculated by scaling the elastic stresses in equilibrium with the constant load and the constant plus cyclic loads until they satisfy Melan's theorem for each material point. As in the limit method, the lowest shakedown multiplier in the structure for that given iteration is stored and the analysis continues to the next iteration. The highest of the stored limit load multipliers obtained during the analysis is identified as the lower bound shakedown multiplier.

2.5.2 Linear Matching Method (LMM)

As with the elastic compensation method, the Linear Matching Method (LMM) has it roots as a method for finding the limit state of the structure. In (Ponter and Carter

[2]For problems including transients, the stress may need to be checked at various other points when the magnitudes of stresses and/or plastic strains are at local maxima and minima in the history.

1996) an early form of the LMM is presented. It was demonstrated that the adjusted modulus methods could be interpreted as a non-linear programming technique and the strain fields resulting from an elastic analysis, similar to the elastic compensation method, may be used to calculate a monotonically reducing upper bound to the limit solution, based on the upper bound limit theorem (Martin 1975).

A number of key differences exist between the LMM and the elastic compensation method including the use of incompressible strain fields in the method given in (Ponter and Carter 1996) and the ability to prove convergence of the upper bound see (Ponter and Carter 1996). A similar proof for the convergence of the lower bound is not available, and there are examples, see (Yang et al. 2005 and Chen et al. 2008), of the lower bound multiplier being non-convergent.

The method was modified to give the elastic shakedown boundary in (Ponter and Carter 1997). In the implementation given in (Ponter and Carter 1997), the shakedown load cycle is decomposed into a constant load and a proportional time varying load. The stress resulting from the constant load only and the summation of the constant load and the maximum cyclic load is tested and the modulus is adjusted depending on whether one or both of the stress conditions violate Melan's theorem. As with the limit load version of the LMM, convergence of the upper bound shakedown multiplier can be proven (Ponter and Carter 1997).

In (Ponter et al. 2000), the method is generalised where both the strain rate of the linear elastic material is matched to the strain rate of the non-linear solution and the yield condition simultaneously. It was also discussed in (Ponter et al. 2000) that the method may be reinterpreted as a numerical programming technique in which a dual minimisation is applied to converge on a least upper bound of the shakedown problem. In (Ponter and Engelhardt 2000) this method is extended to the shakedown boundary. In this method the solution is matched as in (Ponter et al. 2000) for an arbitrary cyclic load case. A constant residual stress is calculated based on the matched values of shear modulus at the points on the cycle where Melan's theorem is violated and a corresponding strain field calculated. These solutions are then utilised in the calculation of the upper bound shakedown multiplier. This becomes the basis for the LMM.

In (Ponter and Chen 2001), Koiter's upper bound shakedown theorem is generalised to give an upper bounding theorem for the shakedown solution in excess of alternating plasticity, i.e. to give the ratchet boundary (see Section 2.4 for a discussion on the extended theorem). A method for applying the upper bound ratchet theorem of (Ponter and Chen 2001) was given in (Chen and Ponter 2001a). This is the ratchet variant of

the LMM.

The minimisation of the bounding theorem given in (Ponter and Chen 2001) requires that a closed plastic strain history can be found. This is difficult to do whilst also finding a constant residual stress and upper bound multiplier that leads to a minimisation in the inequality given in (Ponter and Chen 2001). Thus the ratchet variant of the LMM is split into two distinct stages. The first stage finds a closed plastic strain cycle which results from a prescribed cyclic load history by repeated matching of the load history in turn and accumulation of the ratchet strain per increment. The second stage of the ratchet form of the LMM is the addition of the constant load to the structure whilst minimising the inequality in (Ponter and Chen 2001) by the same process as used in the shakedown form of the LMM.

The LMM has seen continued development: see for example (Chen and Ponter 2001b) for the first published use in 3D, (Chen et al. 2003, Chen and Ponter 2004, Chen and Ponter 2005a, Chen and Ponter 2006, Chen et al. 2011 and Gorash and Chen 2012) for extensions to allow the assessment of creep effects and (Chen and Ponter 2005b and Ponter et al. 2006) for applications including contact.

The LMM's core is an upper bound method, however lower bound estimates were possible for the shakedown version of the LMM due to the proportionality of the load case. More recently a lower bound approximation to the ratchet form of the LMM has been proposed (Ure et al. 2011) and developed (Chen et al. 2013 and Ure et al. 2013). This approximation uses the residual stress fields and cyclic stresses generated by the upper bound LMM and scales the elastic cyclic stress solutions until the resulting total stress fields satisfy Melan's theorem. However cases have been found in which this lower bound produces results in excess of the upper bound solution, this is demonstrated in APPENDIX A, thus it is not a strict lower bound. The lower bound is dependent on the behaviour of the upper bound solution. This can lead to residual stress fields which are amenable to lower bound solution but which are not necessarily a good description of the physics of the problem.

The use of upper bound methods can result in a number of problems. For instance, an upper bound solution must be shown to be converged to result in a high level of confidence in the solution. In the case of the LMM, the method can show convergence for secondary ratchet mechanisms, i.e. ratchet mechanisms that take place at constant loads greater that the limiting ratchet case. In such cases convergence needs to be made stricter. This results in the problem of what convergence criteria are appropriate for all problems. The lower bound estimate was developed to increase the confidence in the upper bound solution but it has already been discussed that it is not entirely reliable.

Thus, whilst it has been shown that good agreement with non-linear FEAis possible, reliability in the accuracy is highly dependent on the convergence controls placed in the method.

2.5.3 Non-cyclic Method

The non-cyclic method was introduced in (Reinhardt 2008) as a lower bound alternative to the upper bound LMM. Reinhardt noted that an upper bound method can only be accepted if it has fully converged, which may result in a number of problems (this is demonstrated in APPENDIX A). A strict lower bound however would be beneficial as any solution found could be used in design. In practice this would be the highest load found.

The method proposed in (Reinhardt 2008) is based on the lower bound extended Melan's theorem, see (Gokhfeld 1980). The load history is decomposed into a constant load and a series of symmetric cyclic loads. Note that symmetric refers to the plastic strains which will result due to the load history, thus the general loading need not be fully symmetric, however the two points of interest must be. Therefore the two points in the load cycle reduce to a fully reversed stress cycle with zero mean stress. The symmetry of the load cycle, as the method is lower bound, implies that if the stress causes a reverse plasticity cycle the plastic strain caused by the positive part of the load cycle will be completely reversed by the negative part of the load cycle. However the stress distribution of the cyclic loads must still be found. For example, if the fully elastic cyclic stress range causes the equivalent stress to go beyond yield, the solution will not satisfy the extended Melan's theorem. Thus in the non-cyclic method of (Reinhardt 2008), the load range is applied to a finite element model with elastic perfectly plastic material properties. This redistributes the load throughout the structure such that the cyclic stress range is limited to yield, thus satisfying the extended Melan's theorem.

If m fully reversed load cycles are identified, the first reversed load cycle is applied to the structure in a FEA with elastic perfectly plastic material properties. The equivalent stress is then found. This equivalent stress is subtracted from the current yield strength of the material and the result becomes the new yield strength for the material. This process is repeated for the remaining reverse load cycles identified. If at any time collapse occurs, this indicates that the load cycle cannot result in a stable plastic strain cycle and ratchet is assumed, although this may not be the case as this approach is generally overly conservative. If collapse does not occur the constant load is added to the structure in a limit analysis using the yield strength from the last cyclic solution. The constant load which results in limit is identified as the constant load at ratchet.

In (Reinhardt 2008) this method was demonstrated as being lower bound, however numerical instability was likely due to the yield strength of the material being reduced to zero in parts of the structure in which a reverse plasticity cycle occurs.

In (Adibi-Asl and Reihardt 2008) the Elastic Modulus Adjustment Procedure (EMAP) was used to replace the elastic plastic limit analysis used in the original form of the method in (Reinhardt 2008). EMAP see (Adibi-Asl et al. 2006) is a repeated elastic analysis similar to those used in the elastic compensation method and the LMM thus is not subject to the same type of numerical instability as the traditional elastic plastic analysis techniques used in (Reinhardt 2008).

The EMAP procedure, like the LMM, uses incompressible strains during the analysis. The procedure used to match the response of the elastic analysis to the non-linear solution is not as robust as that of the LMM with only the stress being matched. This matching is obtained through the use of an adjusted elastic modulus: in this form of the EMAP the relationship used to adjust the elastic modulus is:

$$E^n = E^{n-1}\left(\frac{\sigma^{r^{n+1}}}{\left|\sigma_{ij}^{n-1}\right|}\right)^q$$

where

$$\sigma^{r^{n+1}} = \left(\frac{\int_V \left|\sigma_{ij}^{n-1}\right|^2 dV}{V}\right)^{1/2}$$

and

$$q = \frac{\ln\left(\frac{2(\sigma^r)^2}{\left|\sigma_{ij}^{n-1}\right|^2+(\sigma^r)^2}\right)}{\ln\left(\frac{\sigma^r}{\left|\sigma_{ij}^{n-1}\right|}\right)}$$

In the same manner as in the elastic compensation method, the modulus is adjusted for several iterations. During each iteration a lower bound limit load multiplier is calculated. The lowest multiplier in the structure calculated during the iteration is stored. Once the EMAP procedure has reached a "converged" state, the largest stored limit load multiplier is identified as the constant load ratchet multiplier.

The use of the EMAP in the limit analysis used to identify the constant load at the ratchet boundary provides a stable solution method. However there is no convergence proof for the lower bound multiplier calculated in this way, and based on the results given in (Adibi-Asl and Reihardt 2009) the convergence behaviour of the lower bound multiplier is relatively poor. Whilst this does not affect the suitability

of any of the calculated multipliers to be used as a lower bound, it does suggest that the results of the method may not reach full convergence, and thus the results could be overly conservative in certain conditions. Questions therefore still remain about the overall accuracy of this approach. Despite the use of EMAP, the method presented in (Adibi-Asl and Reihardt 2008) was shown to be generally overly conservative in multi-axial stress states as the addition of the stresses is based upon uniaxial arguments (Adibi-Asl and Reihardt 2009), thus any beneficial effects of a multi-axial stress state are not accounted for.

In (Adibi-Asl and Reihardt 2009) a number of developments were made to the method. The load history is decomposed into a constant load and a single fully reverse load cycle. That is, the extremes in the stress history must be described by just two points which give a maximum and minimum and the fully elastic stresses must be the negative of each other i.e. $\hat{\sigma}_{ij}^{max} = -\hat{\sigma}_{ij}^{min}$. The reduced yield strength is calculated on the addition of the cyclic and constant loads in a component basis, thus removing the possibility of overly conservative results of the method presented in (Reinhardt 2008). This form of the method is what is now most commonly referred to as the Non-Cyclic Method. Further details of the work are given in (Adibi-Asl and Reinhardt 2011a, Adibi-Asl and Reinhardt 2011b), in which reasonable agreement with the LMM was demonstrated. Due to the use of non-linear cyclic solutions and lower bound limit analysis, this method is a strict lower bound. However the requirement of separating the load cycle into just two extreme points is potentially limiting with regard to the assessment of complex structures/load cycles.

2.5.4 Hybrid Method

Whilst the non-cyclic method is a lower bound, which is advantageous to design, it has a number of limitations. It is limited to a fully reverse cyclic load case and the lower bound repeated elastic limit analysis does not necessarily converge. In (Martin and Rice 2009) the hybrid method was introduced as an adaptation of the non-cyclic methods presented in (Reinhardt 2008) and (Adibi-Asl and Reinhardt 2009).

The non-cyclic method was limited to a fully reversed load cycle to allow the stabilised cyclic stresses, (which satisfy the extended Melan's theorem), to be estimated using a single elastic-plastic FEA. However, for more complex structures/load histories it may be difficult or impossible to identify just two points in the load cycle which capture all the necessary maximums and minimums in the cyclic load history, stress history and plastic strain history. To overcome this limitation, the Hybrid Method decomposes the load history into a constant load and an arbitrary set of cyclic loads,

Direct Cyclic Analysis (DCA), see (Nguyen-Tajan et al. 2003), is then used to find the fully stabilised cyclic solution, if one exists, for the cyclic loads only. This is equivalent to finding the post transient solutions as suggested in (Polozzotto 1993c,d). By using DCA to find the stabilised cyclic solutions the method can consider an arbitrary set of cyclic loads. However to pass the solutions of the DCA step into the limit analysis a post processing step must take place, which results in a bottle neck in the process and can hamper the user-friendliness of the analysis.

Once the stabilised cyclic stresses are known, an augmented limit analysis is conducted to identify the additional constant load the structure can support without the onset of ratcheting. Repeated elastic analysis could be used, (several advantages and disadvantages to this have already been covered in this Section) but instead the Hybrid Method uses a reduced yield strength elastic plastic limit analysis as in (Reinhardt 2008), making use of a similar multi-axial summation of the stress components as in (Adibi-Asl and Reinhardt 2009). The Hybrid Method assumes the limit analysis used to obtain the constant load at ratchet may be conducted using the stresses from the constant load only whilst adjusting the yield stress based on the superposition of the stresses obtained from the cyclic solutions. For example consider Melan's theorem for a two point load cycle:

$$\left|\rho_{ij}^{c}+\sigma_{ij}^{c}+\left(\overline{\rho}_{ij}+\rho_{ij}^{\Delta,1}+\hat{\sigma}_{ij}^{1}\right)\right|\leq\sigma^{y}\quad,\quad\left|\rho_{ij}^{c}+\sigma_{ij}^{c}+\left(\overline{\rho}_{ij}+\rho_{ij}^{\Delta,2}+\hat{\sigma}_{ij}^{2}\right)\right|\leq\sigma^{y}$$

thus since $\left(\overline{\rho}_{ij}+\rho_{ij}^{\Delta,m}+\hat{\sigma}_{ij}^{m}\right)$ is known, a maximum allowable $\left|\left(\rho_{ij}^{c}+\hat{\sigma}_{ij}^{c}\right)\right|$ may be calculated and this maximum allowable is used as the yield strength in the elastic-plastic limit analysis. In the Hybrid Method, the maximum allowable $\left|\left(\rho_{ij}^{c}+\hat{\sigma}_{ij}^{c}\right)\right|$ is calculated at the beginning of the limit analysis only, and thus does not take into account any redistribution of stress in the structure due to plastic straining of the material. Thus the solutions may become non-conservative, see the results in (Martin and Rice 2009). The stress in the limit analysis, and thus the direction of the plastic strain, is based only on the constant load. Whilst this does not affect the applicability of the solutions to Melan's theorem, it may result in a plastic strain direction which does not limit the strain energy in the structure based on Melan's theorem and may not find the maximum allowable constant load as a result. Due to the possibility of non-conservative results this method is classified as a stress based lower bound.

2.5.5 UMY/LDYM

Both the isotropic Uniform Modified Yield method (UMY) and "anisotropic" Load Dependent Yield Modification method (LDYM), see (Abou-Hanna and McGreevy 2011), are numerical implementations of the simplified ratchet method proposed by Gokhfeld (1980). The simplification used in this method occurs during the cyclic analysis. In the other methods mentioned thus far, the cyclic solutions required a non-linear analysis to redistribute the cyclic stress such that it satisfied the Extended Melan's theorem completely. However in the UMY and LDYM methods a single elastic analysis is conducted for the cyclic solutions.

Consider a load case (as in the non-cyclic method) that may be decomposed into a fully reversed cyclic load and a constant load. In the UMY and LDYM method the cyclic load amplitude is applied to the structure and the resulting elastic stress distribution is stored. The stored stress field is analysed and at material points where the equivalent stress is beyond yield it is scaled back, to give an adjusted cyclic stress $\sigma_{ij}^{A,adj}$ which has an equivalent stress equal to yield strength of the material, i.e.

$$\sigma_{ij}^{A,adj}(t) = \begin{cases} \hat{\sigma}_{ij}^{A}(t) \quad \text{for} \quad \left|\hat{\sigma}_{ij}^{A}(t)\right| \leq \sigma^{y} \\ \\ Q\hat{\sigma}_{ij}^{A}(t) \quad \text{for} \quad \left|\hat{\sigma}_{ij}^{A}(t)\right| > \sigma^{y} \quad \text{where} \quad Q = \frac{\sigma^{y}}{\left|\hat{\sigma}_{ij}^{A}(t)\right|} \end{cases}$$

This approach simplifies the cyclic solutions; however by doing this the stress beyond yield is not redistributed to the rest of the structure. This results in a cyclic stress field which is not in equilibrium to the applied cyclic load and as a result, if the simplification is applied (i.e. if the cyclic stress is in the plastic shakedown region) then the cyclic stresses used in the ratchet analysis are not sufficient to satisfy the extended Melan's theorem. This was alluded to in (Gokhfeld 1980) with the statement being made that when using this approach there is the possibility of over estimation of the constant load at ratchet. Thus it would appear that this was a known issue. It is however not discussed in the literature concerning the UMY and LDYM methods. The results presented in (Abou-Hanna and McGreevy 2011) agree with this as they show results in excess of the upper bound LMM. This point is discussed further in Section 6.

Once the cyclic stresses are known, the UMY and LDYM methods calculate a modified yield strength as in the Hybrid Method. The UMY method calculates the modified yield strength at the start of the ratchet analysis only, thus may result in non-conservative or overly conservative results as is the case with the Hybrid Method. The LDYM method recalculates the modified yield strength at the beginning of each

iteration, thus removing the possibility of non-conservatism due to the changing of the constant stress direction. This does not remove the possibility of non-conservatism due to the simplified cyclic stress description.

In both the UMY and LDYM methods the ratchet analysis reduces to a limit analysis with reduced yield strength, as in the Hybrid method. The UMY and LDYM methods are therefore susceptible to the same instabilities as the other conventional elastic-plastic limit based ratchet methods. These instabilities stem from the use of the radial return method, (see Section 3.6 for further discussion). Thus whilst the UMY and LDYM methods are relatively computationally inexpensive, there are known issues with the approach which makes these methods insufficient as a strict lower bound. Thus they are only a stress based lower bound and non-conservative results may be given by these approaches.

2.5.6 General Observations for Augmented Limit Solution Methods

The augmented limit methods are currently the only methods available for finding the ratchet boundary for cyclic loads beyond the alternating plasticity boundary for structures where analytical solutions for the stress distribution that results from loading are not available. A conventional analysis is an approach where the loads are prescribed and the result, for those loads, is found by simulating the load history. The shakedown methods, however, are inverse methods. That is the loads, at which shakedown occurs, are found rather than being prescribed. Thus the shakedown methods are relatively computationally inexpensive. The ratchet solutions, in comparison, are not inverse as they require prescribed cyclic loads to be defined to allow the stabilised cyclic stresses to be found. The ratchet method can therefore be thought of as partially inverse, as the cyclic load must first be prescribed. This increases the computational cost relative to the shakedown methods, considerably so for the LMM and the Hybrid method.

This review of the current lower bound ratchet methods shows that a general, reliable, strictly lower bound ratchet method is not available. Whilst the upper bound methods are in most cases reliable, a partially inverse, accurate, strictly lower bound method would result in increased confidence in the calculated ratchet boundary. Such a method would be of practical interest to the designer and structural integrity engineer.

Generality in the methods, i.e. making the methods fully inverse, hardening etc., is currently difficult to achieve as all of the current solution strategies require the separation of constant and cyclic loads. In the case of the elastic-plastic methods the separation continues into the limit solution. To allow a general method to be developed for elastic-plastic solution strategies, it would be necessary to first devise a

method for consideration of both cyclic and constant loads during the limit solution. In addition, if the method can be defined such that it allows for the incorporation of more of the underlying mechanics then further extensions to improve upon the generality of the method, such as making the ratchet method fully inverse, hardening etc., should, theoretically, be possible. This additional requirement would suggest that an elastic-plastic method would be the most appropriate, as it allows for incorporation of implicitly integrated plastic strains and strain fields which are physically meaningful, rather than the kinematically admissible strain fields found by the repeated elastic solution methods.

The aim here is to provide a method to act as a coherent basis for a more general, fully inverse, elastic-plastic ratchet method. In particular the research will focus on the development of an elastic-plastic method which allows consideration of constant and cyclic loads during the limit solution used to find the constant load at ratchet.

2.6 Mathematical Programming Methods

There are a number of methods based on mathematical programming techniques. Here a brief overview of the methods are given with references to more detailed discussions of the methods.

2.6.1 Iterative penalization

The iterative penalization method reduces to minimising the dissipated energy in the strain cycle described by m admissible cyclic loads corresponding to vertices in the load history. The minimization of the dissipated energy takes place over m admissible cyclic loads with respect to the structural displacement and the plastic strain increments with constraints on the normalisation of external work and compatibility of the final strains. The minimisation is done over the whole volume of the structure with the summation of the dissipated energy obtained via a weighted Gauss summation. The solution to the minimisation problem can be achieved in a number of ways, see for example (Carvelli et al. 2000 and Maier et al. 2001)

2.6.2 The LISA Project

The European LISA project see (Staat and Heitzer 2001) defined a direct shakedown method based on the Primal-Dual algorithm. This algorithm utilises the duality in the upper and lower bound shakedown theorems to define a minimisation problem for the elastic shakedown boundary. The LISA project was defined for shakedown considering kinematic hardening using a two surface hardening model.

The two surface hardening model forgoes the usual relationship between the increment in plastic strain and the increment in backstress through a hardening modulus, instead using a bounded surface for the backstress. The resulting hardening modulus is referred to as the two surface model, the first surface being the yield surface displaced by the backstress and the second being the bounded surface, given by the maximum allowable backstress plus yield strength. Thus the yield surface is allowed to displace inside the bounded surface until the backstress becomes large enough that the yield surface touches the bounded surface and the magnitude of the backstress is then limited to the maximum value. This allows for a simplified incorporation of limited kinematic hardening into the shakedown method.

Further work based on the LISA project has been conducted by the originators, for example, comparisons to experimental tests to validate lower bound estimates given by the method (Lang et al. 2001), comparisons to experimental tests to validate hardening (Heitzer et al. 2003), the incorporation of temperature dependent yield strength (Vu and Staat 2007).

2.6.3 Interior Point Algorithm

This shakedown method, see (Simon and Weichert 2011) for recent developments, utilises the same primal dual relationship as is used in the LISA project, but solves the minimisation problem using the interior point algorithm. The interior point algorithm is of interest as it is capable of solving numerical problems involving large numbers of degrees of freedom in a relatively computationally efficient manner. The implementation given in (Simon and Weichert 2011) uses a tailored form of the interior point algorithm to achieve solution times which are many times quicker than other optimisation based mathematical programming methods. The drawback of this approach is that the incorporation of hardening and other effects such as in (Weichert and Gross-Weege 1988, Weichert 1986 and Hachemi and Weichert 1992) cannot be directly implemented in the method without reformulation of the method to allow for these effects.

2.6.4 General Comments

Numerical programming methods have thus far not been extended to the plastic ratchet boundary. This is a limitation in a number of applications of practical interest. Further, whilst the methods do provide a relatively efficient means of identifying the shakedown boundary, the methods don't model certain aspects of the problem. This may be illustrated with the extensions some of the methods have been given to include hardening.

Whilst the methods give a bounded result for the hardening behaviour, the actual hardening law is not considered and the relation between plastic strain and backstress through a hardening modulus is not considered. Some important physical information about the hardening behaviour is thus lost in the method. This could result in backstresses which are impossible to achieve in the "real" component as hardening models for use in shakedown problems must saturate (i.e. the hardening modulus reaches zero) leading to the possibility that the backstress is not necessarily associative to the total plastic strain after the hardening modulus has saturated.

2.7 Post Process Methods

The augmented limit methods and the mathematical programming methods require, to varying degrees, the use of user programming to be incorporated into conventional analysis methods, such as finite element software. The post processing methods however, do not require the use of user programmed functionality to be implemented in a standard Finite Element Method. They do however, generally, require the use of user programming in the post processing application. This is however generally an easier task than user programmed functionality for the FEA. As such the post processing methods are easier to implement that the augmented limit methods and the mathematical programming methods.

The non-linear superposition method was introduced in (Muscat et al. 2002, 2003). The method utilised non-linear analysis and superposition of elastic loads to estimate a lower bound ratchet boundary. A similar method more recently proposed by (Abdalla et al. 2006, 2007a, 2007b, 2007c, 2008, 2009) has seen limited development to include simplified hardening models. The method is a strictly lower bound method based on "built in" material models in most commercially available finite element software packages. The method is relatively simple. The load case is first separated into constant and fully reversed cyclic parts. The constant load is applied to the structure with an elastic plastic material model and in the next step the cyclic stress amplitude is added to the structure/component during an elastic perfectly plastic limit analysis. For each solution, the stress distribution is written to disk to allow post processing to take place. On completion of the limit analysis an elastic analysis is performed for the cyclic load range, this stress is also written to disk for post processing.

In the post processing procedure, the stress fields for the elastic-plastic analysis and elastic analysis are retrieved. Starting at the lowest cyclic load range the elastic cyclic load range is then scaled to the equivalent value it would have had during the elastic plastic analysis and subtracted from the elastic plastic stress field at the corresponding

cyclic elastic plastic stress solution. If the equivalent stress is less than yield, for that cyclic stress range, the system satisfies Melan's theorem and thus shakedown is achieved. By repeating this at successively higher cyclic load ranges the cyclic load at which shakedown does not occur can be found.

Whilst the post-processing methods are considerably easier to implement than the augmented limit analysis and the mathematical programming methods, there are a number of disadvantages. As the method finds the residual stress field by post process methods such that when the first unloading causes yielding in the structure the analysis identifies that loads as the shakedown load. However the stress at the unloaded state, in the case of the elastic ratchet boundary, will, in general, redistribute further to accommodate greater cyclic loads whilst satisfying Melan's theorem. As a consequence the elastic ratchet boundary is generally overly conservative when found by this method. Additionally, post-processing is, generally, relatively computationally expensive and may result in bottle necks in the assessment process.

3 Formulation of a Modified Yield Ratchet Method

In Section 2.5 it was noted that current lower bound methods are less accurate and reliable than the current upper bound methods. In this chapter a modified yield ratchet method, similar to the Hybrid Method, is formulated. The aim here is to remove a number of the assumptions that are included in the other methods of this type, see (Martin and Rice 2009 and Abou-Hanna and McGreevy 2011). By doing so the methods should consistently satisfy the extended Melan's theorem and remove the possibility of non conservative results discussed in Section 2.5. However it will be shown that whilst improvement can be made over the Hybrid Method there are still large errors in the calculated ratchet boundaries.

The work in this chapter requires a number of assumptions about the structure's behaviour to allow the formulation of the method. These assumptions are as follows:

Assumption 1 The load history can be partitioned into constant and cyclic parts

Assumption 2 The cyclic loads lie within the ratchet boundary

Assumption 3 The constant load is applied under load control

Assumption 4 Perfect plasticity is assumed throughout

Assumption 5 All material properties are temperature independent.

Assumption 6 The cyclic loads may be described by superimposed elastic stresses from the unstrained state, i.e non-linear geometry effects may be ignored

3.1 Separation of Constant and Cyclic Solutions

When considering ratcheting there are two unknown parts of the problem. Firstly, for a shakedown condition to exist it must be shown that the cyclic loads can be supported by the structure whilst resulting in a closed plastic strain cycle. The second part of the problem is to find the magnitude of constant load the structure can support without causing ratchet. When using conventional finite elements it is difficult to solve for both the cyclic and constant solutions at the same time. It is therefore necessary to separate the load case into cyclic and constant parts and consider their actions in two stages.

The load case must then be separated into both cyclic and constant parts. The requirement of a constant load for these methods to show a suitable safety margin against ratchet may, in some cases, render the method unsuitable for a particular problem. Such cases would be when the load case has no discernible constant load. In such cases it may be difficult to adequately define a constant load which would show a

suitable margin of safety against ratchet. However, developing a reliable lower bound method which requires the separation of constant and cyclic loads extends knowledge of the field of research.

The extended Melan's theorem requires that the stress in the structure at all times remains below the yield strength of the material. It is therefore theoretically necessary to know the full cyclic load history. This is, however, impractical. Given that the actual load history may not be known, or is difficult to define, a further decomposition of the cyclic loads is prudent. Given that the overall aim is to show that there is a time invariant plastic strain over the cycle of loading, it is only necessary to capture the local maxima and minima in the load cycle. By doing so the maximum and minimum in the plastic strain history will also be defined. Thus the load history is separated into m distinct points which describe the maximums and minimums in the plastic strain history.

3.2 Cyclic Solutions

3.2.1 Material Model

The cyclic solution relies on the assumption that if a stable cyclic solution exists it may be found by repeated cycling of the cyclic loads in a non-linear FEA. Thus Stage 1 may be done using standard FEA where the cyclic loads are cycled until the cyclic strains over the cycle converge. That is the strain at all points in the cycle are the same from one cycle to the corresponding point in the next cycle:

$$\varepsilon_{ij}^{T}(t) = \varepsilon_{ij}^{T}(t+\varphi) \quad \text{and} \quad \varepsilon_{ij}^{p}(t) = \varepsilon_{ij}^{p}(t+\varphi)$$

where ε_{ij}^{T} is the total strain.

If doing this using standard FEA it may be difficult to ascertain if the cycle has converged during the Stage 1 analysis and care is required in ensuring the loads are applied using appropriate amplitudes and that the finite element package solves for the extremes in the load cases. If using built-in material models the analysis must be post-processed to obtain the residual stress and any varying residual strains before the ratchet analysis can start. The input and output tasks required for post processing can be costly in both computational effort and time. It would also be possible to use the direct cyclic procedure which is incorporated into the ABAQUS package, however this process must also be post processed before its results may be read into the ratchet analysis.

Given the potential difficulties and added cost in post processing Stage 1 it would be

beneficial if an alternative method, which does not require the use of post processing, could be developed. Assuming the cyclic loads at the m critical points may be described by fully elastic stresses, $\widehat{\sigma}_{ij}^{m}$, it is possible to use the residual condition and these superimposed elastic stresses to define the load cycle.

The residual stresses and strains at point l in the load cycle are given by:

$$\overline{\rho}_{ij} + \sum_{\theta=1}^{\theta=l} \rho_{ij}^{\Delta,\theta} = C_{ijkq}\left(\varepsilon_{kq}^{Tr,l} - \varepsilon_{kq}^{p,l}\right)$$

where $\varepsilon_{kq}^{Tr,l}$ is the total residual strain at point l and $\rho_{ij}^{\Delta,\theta}$ is the varying residual stress at load point θ

$$\rho_{ij}^{\Delta,1} = 0 \;\; and \;\; \rho_{ij}^{\Delta,\theta} = \rho_{ij}^{r,\theta} - \rho_{ij}^{r,\theta-1} \; for \; 1 < \theta \leq m$$

and

$$C_{ijkq} = \lambda\delta_{ij}\delta_{kq} + \mu(\delta_{ik}\delta_{jq} + \delta_{iq}\delta_{jk}) \tag{3}$$

with:

$$\lambda = \frac{vE}{(1+v)(1-2v)} \;\text{ and }\; \mu = \frac{E}{2(1+v)}$$

The loaded points are given by the superposition of the elastic stress in equilibrium with the cyclic loads:

$$\sigma_{ij}^{l} = \overline{\rho}_{ij} + \hat{\sigma}_{ij}^{l} + \sum_{\theta=1}^{\theta=l} \rho_{ij}^{\Delta,\theta}$$

Here attention is restricted to von Mises plasticity, giving the yield conditions:

$$f^{l} = \left|\overline{\rho}_{ij} + \widehat{\sigma}_{ij}^{l} + \sum_{\theta=1}^{\theta=l} \rho_{ij}^{\Delta,\theta}\right| - \sigma^{y} \leq 0 \;\text{ for }\; 1 \leq l \leq m$$

with:

$$\left|\overline{\rho}_{ij} + \widehat{\sigma}_{ij}^{l} + \sum_{\theta=1}^{\theta=l} \rho_{ij}^{\Delta,\theta}\right| = \sqrt{\frac{3}{2}\left(\overline{\rho}'_{ij} + \widehat{\sigma}'^{l}_{ij} + \sum_{\theta=1}^{\theta=l} \rho_{ij}'^{\Delta,\theta}\right)\left(\overline{\rho}'_{ij} + \widehat{\sigma}'^{l}_{ij} + \sum_{\theta=1}^{\theta=l} \rho_{ij}'^{\Delta,\theta}\right)} \tag{4}$$

where the superscript $'$ denotes the deviatoric part of the stress.

The plastic strain rate at a point l is given by, for Mises plasticity:

$$\dot{\varepsilon}_{ij}^{p,l} = \dot{\gamma}^l r_{ij}^l = \gamma^l \frac{\overline{\rho}'_{ij} + \widehat{\sigma}'^l_{ij} + \sum_{\theta=1}^{\theta=l} \rho'^{\Delta,\theta}_{ij}}{\left| \overline{\rho}_{ij} + \widehat{\sigma}^l_{ij} + \sum_{\theta=1}^{\theta=l} \rho_{ij}^{\Delta,\theta} \right|}$$

where $\dot{\gamma}^l$ is the rate of change of the plastic consistency parameter

3.2.2 Solution Algorithms

In the algorithms that follow, the superscript ^{n} is the value of the variable at the last converged solution at time $t - \Delta t$, and the superscript $^{n+1}$ is the value of the variable at the current time t, the superscript ^{trial} is used for the trial values of the variables before the application of the plasticity algorithms. The algorithm is defined for the solution at the m extreme cyclic load points. If a solution is required between these points, interpolation of the superimposed elastic stresses is required. The algorithm starts at $l = 1$ and cycles through the critical load cases with $l = m$ being the final load case. The Stage 1 algorithms continue to loop until the residual stress and strain remain constant over a number of cycles.

The stress at point l in the load cycle is given by:

$$\overline{\rho}_{ij} + \rho_{ij}^{\nabla,trial} = C_{ijkq} \left(\varepsilon_{kq}^{Tr,l^{n+1}} - \varepsilon_{kq}^{p,l^n} \right)$$

where

$$\rho_{ij}^{\nabla,trial} = \begin{cases} \rho_{ij}^{\Delta,l,trial} & l = 1 \\ \sum_{\theta=1}^{\theta=l-1} \rho_{ij}^{\Delta,\theta} + \rho_{ij}^{\Delta,l,trial} & 1 < l \leq m \end{cases}$$

$$f^{trial} = \sqrt{\frac{3}{2} \left(\overline{\rho}'_{ij} + \rho_{ij}^{\prime\nabla,trial} + \hat{\sigma}'_{ij}{}^l \right) \left(\overline{\rho}'_{ij} + \rho_{ij}^{\prime\nabla,trial} + \hat{\sigma}'_{ij}{}^l \right)} - \sigma^y$$

If $f^{trial} \leq 0$ then: (elastic)

$$\varepsilon_{ij}^{p^{n+1}} = \varepsilon_{ij}^{p^n}$$

$$\overline{\rho}_{ij} + \rho_{ij}^{\nabla,n+1} = \overline{\rho}_{ij} + \rho_{ij}^{\nabla,trial}$$

and

$$\rho_{ij}^{\nabla,n+1} = \begin{cases} \rho_{ij}^{\Delta,l,n+1} & l = 1 \\ \sum_{\theta=1}^{\theta=l-1} \rho_{ij}^{\Delta,\theta} + \rho_{ij}^{\Delta,l,n+1} & 1 < l \leq m \end{cases}$$

Else: (plastic)

$$r_{ij}^{n+1} = \frac{3}{2} \frac{\left(\overline{\rho}'_{ij} + \rho_{ij}^{\prime\nabla,trial} + \hat{\sigma}'_{ij}{}^{l} \right)}{f^{trial}}$$

$$\Delta\gamma^{n+1} = \frac{f^{trial}}{3\mu}$$

where $\Delta\gamma$ is the increment in the plastic consistency parameter

$$\varepsilon_{ij}^{p,n+1} = \varepsilon_{ij}^{p,n} + \Delta\gamma^{n+1} r_{ij}^{n+1}$$

$$\overline{\rho}_{ij} + \rho_{ij}^{\nabla,n+1} = \overline{\rho}_{ij} + \rho_{ij}^{\nabla,trial} - 2\mu\Delta\gamma^{n+1} r_{ij}^{n+1}$$

and

$$\rho_{ij}^{\nabla,n+1} = \begin{cases} \rho_{ij}^{\Delta,l,n+1} & l = 1 \\ \sum_{\theta=1}^{\theta=l-1} \rho_{ij}^{\Delta,\theta} + \rho_{ij}^{\Delta,l,n+1} & 1 < l \leq m \end{cases}$$

The consistent Tangent modulus is then:

$$C_{ijkq}^{con} = \kappa\delta_{ij}\delta_{kq} + 2\theta\mu \left(I_{ijkq} - \frac{1}{3} 1_{ij} 1_{kq} \right) - \frac{4}{3}\mu\phi r_{ij}^{n+1} r_{kq}^{n+1}$$

where:

$$\mu = \frac{E}{2\left(1+v\right)} \ , \ \kappa = \frac{E}{3\left(1-2v\right)} \ , \ \theta = \frac{\sigma^{y}}{\left| \bar{\rho}'_{ij} + \rho_{ij}^{\prime\nabla,trial} + \hat{\sigma}_{ij}{}^{\prime l} \right|} \ and \ \phi = \theta$$

Endif

If $(l = m)$ then check convergence on $\overline{\rho}'_{ij}$

If $\left(\rho_{ij}^{\Delta\prime,0} \leq tolerance \right)$ then: Converged Goto Stage 2

Else $\overline{\rho}_{ij} = \overline{\rho}_{ij} + \rho_{ij}^{\prime\Delta,0}$

Endif

endif

3.3 Potential Difficulties in Implementation

Given the non-linear nature of the algorithms used to solve for the plastic strain increment during the cyclic solutions, it is not guaranteed that the solver will converge during every increment. It is then necessary to allow for cut backs in the solution process. This potentially requires solutions at points between the m critical loaded cases, at a point l, for which the elastic stresses are unknown. However, the elastic stress at l between points θ and $\theta + 1$ may be found by interpolation of the elastic stress at points θ and $\theta + 1$. To do so it is necessary to know the relative "distance" between point l and points θ and $\theta + 1$. To help with this, 1 unit of time during the Stage 1 cyclic solutions is made equal to the difference between θ and $\theta + 1$: i.e for a 2 extreme load cycle time, t=1 is at the first critical load case, t=2 is the second critical load case and t=3 is back to the first critical load case. By knowing the number of points in the load cycle and the current solution time, it is possible to use interpolation to find the superimposed elastic stress required by the solution at any value of solution time.

The use of time as a place holder for the solution process allows for the use of automatic time stepping and cut backs during the Stage 1 cyclic solutions. Thus if a stable stress configuration exists for the given loads, the solver should be capable of finding the corresponding strain state. However care must be taken in ensuring the solver solves for time= *integer*, as these points in time represent the critical load cases. If the solver does not solve for these times the load cycle will not be adequately described by the solution process. Therefore, when performing a Stage 1 analysis it is necessary to specify time points for field or history outputs in the ABAQUS job description to force the solver to solve for time= *integer*.

If the cyclic loads are large enough to cause the structure to reach a limit state then the Stage 1 solution will fail due to loss of equilibrium. In this case, all that can be determined from the solution is that the cyclic loads lie outside of the cyclic load limit boundary. To obtain a ratchet solution the analysis will have to be restarted at a lower value of cyclic load. It may also be possible for the cyclic loads to lie outwith the ratchet boundary, see (Abou-Hanna and McGreevy 2011) for an example load case where cyclic loads result in ratchet. If this is the case, the Stage 1 analysis will fail to converge from one load cycle to the next. All that can be determined from a solution in this case is that the cyclic loads lie between the ratchet and limit boundaries. For a ratchet solution to be found, the cyclic load will have to be reduced and the analysis started again.

3.4 Ratchet Solution

The ratchet solution uses a modified yield strength similar to the Hybrid Method, which adapted the process used in the Non-Cyclic Method from the method proposed by Gokhfeld (1980). In the Hybrid procedure the modified yield strength is calculated at the start of the ratchet solution, based on the original direction of the stress resulting from the addition of the constant load, and is not updated thereafter. However, if redistribution takes place in the structure, such that the normal directions of the stress resulting from the addition of the constant load changes during the analysis, this can result in stresses which do not satisfy Melan's theorem, see (Martin and Rice 2009).

To overcome the problems which result in using a constant modified yield strength, the proposed methods update the modified yield strength on a per iteration basis (Method 1) or on a per increment basis (Method 2). Assuming a set of cyclic plastic strains and stresses are found from the cyclic loads which result in a steady state residual stress giving a time invariant residual of, $\overline{\rho}_{ij}$, and a series of varying residual stresses of,$\rho_{ij}^{\Delta,l}$, which satisfy $\sum_{\theta=1}^{\theta=m} \rho_{ij}^{\Delta,\theta} = 0$, the additional constant load the structure can support may be found using the material model in Section 3.4.1.

3.4.1 Material Model

The Stage 2 ratchet analysis starts from an unstressed state, i.e. the strains present in the model after Stage 1 are removed before starting the ratchet analysis. The ratchet analysis may then be formulated as follows.

The constant residual resulting from the constant load only is given by:

$$\rho_{ij}^{c} = C_{ijkq}\left(\varepsilon_{kq}^{Tr} - \varepsilon_{kq}^{p}\right)$$

The constant loaded stress is given by:

$$\sigma_{ij}^{c} = \rho_{ij}^{c} + \hat{\sigma}_{ij}^{c}$$

The total stress at a given point, l, in the load cycle is given by:

$$\sigma_{ij}^{l} = \rho_{ij}^{c} + \hat{\sigma}_{ij}^{c} + \overline{\rho}_{ij} + \left(\sum_{\theta=1}^{\theta=l} \rho_{ij}^{\Delta,\theta}\right) + \hat{\sigma}_{ij}^{l}$$

The structure must satisfy the loading and unloading conditions:

$$\gamma^{l} \geq 0 \ , \ f^{l} \leq 0 \ , \ \gamma^{l} f^{l} = 0$$

and also on yielding the stresses must satisfy the consistency condition:

$$\dot{f}^l = 0$$

with the yield condition:

$$f\left(\sigma_{ij}^l\right) = \sqrt{\frac{3}{2}\sigma_{ij}'^l\sigma_{ij}'^l} - \sigma^y = f^l = \left|\rho_{ij}^c + \hat{\sigma}_{ij}'^c + \overline{\rho}_{ij} + \widehat{\sigma}_{ij}^l + \sum_{\theta=1}^{\theta=l}\rho_{ij}^{\Delta,\theta}\right| - \sigma^y \leq 0 \text{ for } 1 \leq l \leq m \tag{5}$$

Thus the problem reduces to finding a constant stress which satisfies all of the yield criteria. However the direction of plastic strain will be different for the m load cases, requiring the constant stress to redistribute in different ways for the m different load cases. This makes identifying a limiting case difficult as the resulting constant stresses cannot be directly compared, due to their different directions.

3.4.2 Simplifying the yielding behaviour

The material model in section 3.4.1 is difficult to implement using standard plasticity models as the direction of plastic straining for each load point differs. This makes identifying the limiting point on the cycle difficult because the allowable constant stress at each load point cannot be directly compared due to the differences in direction. In order to identify a limiting case it is assumed that the plastic strain that occurs during the Stage 2 analysis is based on the direction of the constant stress only, i.e.

$$r_{ij} = \frac{3}{2}\frac{\sigma_{ij}'^c}{\sqrt{\frac{3}{2}\sigma_{kq}'^c\sigma_{kq}'^c}} = \frac{3}{2}\frac{\rho_{ij}'^c + \hat{\sigma}_{ij}'^c}{\sqrt{\frac{3}{2}\sigma_{kq}'^c\sigma_{kq}'^c}}$$

This allows the constant stress to be scaled by a factor X for each load case, to find the maximum equivalent constant stress that can be supported by the material point whilst satisfying Melan's theorem 5, i.e.:

$$\left|X^l\left(\rho_{ij}^c + \hat{\sigma}_{ij}'^c\right) + \overline{\rho}_{ij} + \widehat{\sigma}_{ij}^l + \sum_{\theta=1}^{\theta=l}\rho_{ij}^{\Delta,\theta}\right| - \sigma^y = 0 \text{ for } 1 \leq l \leq m$$

where

$$X^l = \frac{-b^l + \sqrt{\left(b^l\right)^2 - 4ac^l}}{2a}$$

with:

$$a = \frac{3}{2}\sigma_{ij}'^c\sigma_{ij}'^c \ , \ b^l = 3\sigma_{ij}'^c\left(\overline{\rho}_{ij}' + \left(\sum_{\theta=1}^{\theta=l}\rho_{ij}'^{\Delta,\theta}\right) + \hat{\sigma}_{ij}'^l\right) \text{ and}$$

$$c^l = \frac{3}{2}\left(\overline{\rho}'_{ij} + \left(\sum_{\theta=1}^{\theta=l} \rho'^{\Delta,\theta}_{ij}\right) + \hat{\sigma}'^{l}_{ij}\right)\left(\overline{\rho}'_{ij} + \left(\sum_{\theta=1}^{\theta=l} \rho'^{\Delta,\theta}_{ij}\right) + \hat{\sigma}'^{l}_{ij}\right) - \sigma^{y^2}$$

The constant stress must therefore satisfy the the yield condition:

$$f = \sqrt{\frac{3}{2}\sigma'^{c}_{ij}\sigma'^{c}_{ij}} - \sigma^{y,mod} \leq 0$$

with

$$\sigma^{y,mod} = min\left(\sqrt{\tfrac{3}{2}\left(X^l\left(\rho^c_{ij} + \hat{\sigma}'^{c}_{ij}\right)\right)\left(X^l\left(\rho^c_{ij} + \hat{\sigma}'^{c}_{ij}\right)\right)}\right)$$

$$= min\left(X^l\right)\sqrt{\tfrac{3}{2}\left(\rho^c_{ij} + \hat{\sigma}'^{c}_{ij}\right)\left(\rho^c_{ij} + \hat{\sigma}'^{c}_{ij}\right)}$$

Therefore if $X < 1$, the total equivalent stress violates the yield condition and stress must redistributed to satisfy Melan's theorem: i.e. redistribute such that $X = 1$. Figure 4 gives a pictorial description of the simplified yielding behaviour.

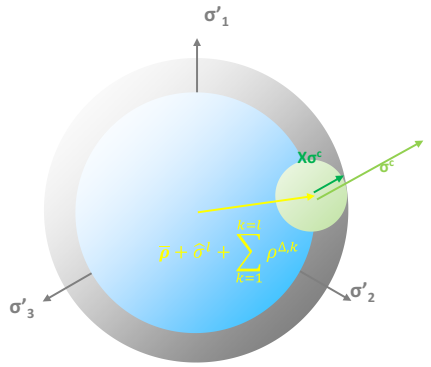

(a) Interaction of yield surfaces between stage 1 and stage 2.

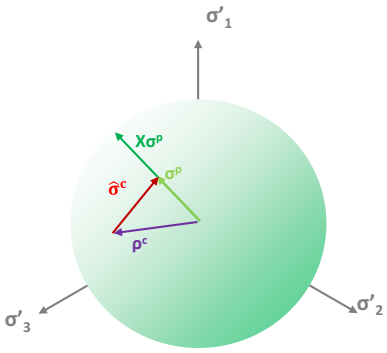

(b) Stage two yielding calculation where X≥1, i.e. yield function satisfied

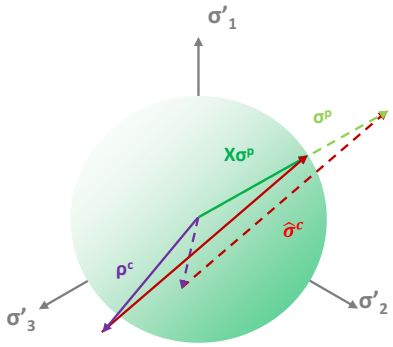

(c) Stage two yielding behaviour X≤1 i.e. where redistribution is necessary to satisfy Melan's theorem

Figure 4: Pictorial description of simplified yielding behaviour during methods 1 and 2. Gray circle represents the von Mises yield surface of the mateiral

3.4.3 Solution Algorithms

The following solution algorithms update the value of X during the solution process to avoid the possibility of non-conservative results, as can occur in the Hybrid Method. It is possible to do this every iteration or every increment.

Method 1 updates the value of X every iteration:

$$\rho_{ij}^{c,trial^n} = C_{ijkq}\left(\varepsilon_{kq}^{Tr^{n+1}} - \varepsilon_{kq}^{p^n}\right)$$

X is the smallest of:

$$X^l = \frac{-b^l + \sqrt{(b^l)^2 - 4ac^l}}{2a}$$

where:

$$a = \frac{3}{2}\left(\rho_{ij}^{\prime c,l} + \hat{\sigma}_{ij}^{\prime c,n+1}\right)\left(\rho_{ij}^{\prime c,l} + \hat{\sigma}_{ij}^{\prime c,n+1}\right)$$

and

$$b^l = 3\left(\rho_{ij}^{\prime c,l} + \hat{\sigma}_{ij}^{\prime c,n+1}\right)\left(\overline{\rho}_{ij}^{\prime} + \left(\sum_{\theta=1}^{\theta=l}\rho_{ij}^{\prime\Delta,\theta}\right) + \hat{\sigma}_{ij}^{\prime l}\right)$$

and

$$c^l = \frac{3}{2}\left(\overline{\rho}_{ij}^{\prime} + \left(\sum_{\theta=1}^{\theta=l}\rho_{ij}^{\prime\Delta,\theta}\right) + \hat{\sigma}_{ij}^{\prime l}\right)\left(\overline{\rho}_{ij}^{\prime} + \left(\sum_{\theta=1}^{\theta=l}\rho_{ij}^{\prime\Delta,\theta}\right) + \hat{\sigma}_{ij}^{\prime l}\right) - (\sigma^y)^2$$

Then

$$X = min\left(X^l\right)$$

$$\sigma^{y,mod} = \sqrt{\frac{3}{2}X\left(\rho_{ij}^{\prime c,trial} + \hat{\sigma}_{ij}^{\prime c,n+1}\right)X\left(\rho_{ij}^{\prime c,trial} + \hat{\sigma}_{ij}^{\prime c,n+1}\right)} =$$

$$X\sqrt{\frac{3}{2}\left(\rho_{ij}^{\prime c,trial} + \hat{\sigma}_{ij}^{\prime c,n+1}\right)\left(\rho_{ij}^{\prime c,trial} + \hat{\sigma}_{ij}^{\prime c,n+1}\right)}$$

$$f^{trial} = \sqrt{\frac{3}{2}\left(\rho_{ij}^{\prime c,trial} + \hat{\sigma}_{ij}^{\prime c,n+1}\right)\left(\rho_{ij}^{\prime c,trial} + \hat{\sigma}_{ij}^{\prime c,n+1}\right)} - \sigma^{y,mod}$$

If $f^{trial} \leq 0$ then (elastic:

$$\varepsilon_{ij}^{er^{n+1}} = \varepsilon_{ij}^{er,trial}$$

$$\varepsilon_{ij}^{p^{n+1}} = \varepsilon_{ij}^{p^n}$$

$$\rho_{ij}^{\prime c,n+1} = \rho_{ij}^{\prime c,trial} + \hat{\sigma}_{ij}^{\prime c,n+1}$$

$$\rho_{ij}^{c,n+1} = \frac{1}{3} tr\left(\rho_{ij}^{c,trial}\right) + \left(\rho_{ij}^{\prime c,n+1}\right)$$

Else: (plastic)

$$r_{ij}^{n+1} = \frac{3}{2} \frac{\left(\rho_{ij}^{\prime c,trial} + \hat{\sigma}_{ij}^{\prime c,n+1}\right)}{f^{trial}}$$

$$\Delta\gamma^{n+1} = \frac{f^{trial}}{3\mu}$$

$$\varepsilon_{ij}^{p^{n+1}} = \varepsilon_{ij}^{p^n} + \Delta\gamma^{n+1} r_{ij}^{n+1}$$

$$\rho_{ij}^{\prime c,n+1} = \rho_{ij}^{\prime c,trial} - 2\mu\Delta\gamma^{n+1} r_{ij}^{n+1}$$

$$\rho_{ij}^{c,n+1} = \frac{1}{3} tr\left(\rho_{ij}^{c,trial}\right) + \left(\rho_{ij}^{\prime c,n+1}\right)$$

Endif

The consistent tangent modulus is then given by:

$$C_{ijkq}^{con} = \kappa\delta_{ij}\delta_{kq} + 2\theta\mu\left(I_{ijkq} - \frac{1}{3}\delta_{ij}\delta_{kq}\right) - \frac{4}{3}\mu\left(2X + 2\frac{c}{\sqrt{(b^{\varrho})^2 - 4ac^{\varrho}}}\right) r_{ij} r_{kq} -$$

$$4\mu\frac{X\left|\rho_{rs}^{\prime c,trial}\right|}{\sqrt{(b^{\varrho})^2 - 4ac^{\varrho}}} r_{ij}\left(\bar{\rho}_{kq}^{\prime} + \left(\sum_{\theta=1}^{\theta=\varrho} \rho_{kq}^{\prime\Delta,\theta}\right) + \hat{\sigma}_{kq}^{\prime\varrho}\right)$$

where $^{\varrho}$ is the load case which gave the smallest X:

$$\mu = \frac{E}{2\left(1+v\right)}\ ,\ \kappa = \frac{E}{3\left(1-2v\right)}\ ,\ \theta = \frac{\sigma^y}{\left|\rho_{ij}^{\prime c,trial} + \hat{\sigma}_{ij}^{\prime c,n+1}\right|}\ and\ \varphi = \theta$$

Method 2 updates the value of modified yield strength at the start of every increment using the value of constant load from the last increment:

$$\rho_{ij}^{c,trial} = C_{ijkq}\left(\varepsilon_{kq}^{Tr^{n+1}} - \varepsilon_{kq}^{p^n}\right)$$

X is the smallest of:

$$X^l = \frac{-b^l + \sqrt{(b^l)^2 - 4ac^l}}{2a}$$

where:

$$a = \frac{3}{2}\left(\rho_{ij}^{\prime c,n} + \hat{\sigma}_{ij}^{\prime c,n}\right)\left(\rho_{ij}^{\prime c,l} + \hat{\sigma}_{ij}^{\prime c,n}\right)$$

and

$$b^l = 3\left(\rho_{ij}^{\prime c,l} + \hat{\sigma}_{ij}^{\prime c,n+1}\right)\left(\overline{\rho}_{ij}^{\prime} + \left(\sum_{\theta=1}^{\theta=l}\rho_{ij}^{\prime\Delta,\theta}\right) + \hat{\sigma}_{ij}^{\prime l}\right)$$

and

$$c^l = \frac{3}{2}\left(\overline{\rho}_{ij}^{\prime} + \left(\sum_{\theta=1}^{\theta=l}\rho_{ij}^{\prime\Delta,\theta}\right) + \hat{\sigma}_{ij}^{\prime l}\right)\left(\overline{\rho}_{ij}^{\prime} + \left(\sum_{\theta=1}^{\theta=l}\rho_{ij}^{\prime\Delta,\theta}\right) + \hat{\sigma}_{ij}^{\prime l}\right) - (\sigma^y)^2$$

Then

$$X = min\left(X^l\right)$$

$$\sigma^{y,mod} = \sqrt{\frac{3}{2}X\left(\rho_{ij}^{\prime c,n} + \hat{\sigma}_{ij}^{\prime c,l}\right)X\left(\rho_{ij}^{\prime c,n} + \hat{\sigma}_{ij}^{\prime c,l}\right)} =$$

$$X\sqrt{\frac{3}{2}\left(\rho_{ij}^{\prime c,n} + \hat{\sigma}_{ij}^{\prime c,l}\right)\left(\rho_{ij}^{\prime c,n} + \hat{\sigma}_{ij}^{\prime c,l}\right)}$$

$$f^{trial} = \sqrt{\frac{3}{2}\left(\rho_{ij}^{\prime c,trial} + \hat{\sigma}_{ij}^{\prime c,n+1}\right)\left(\rho_{ij}^{\prime c,trial} + \hat{\sigma}_{ij}^{\prime c,n+1}\right)} - \sigma^{y,mod}$$

If $f^{trial} \leq 0$ then (elastic):

$$\varepsilon_{ij}^{er^{n+1}} = \varepsilon_{ij}^{er,trial}$$

$$\varepsilon_{ij}^{p^{n+1}} = \varepsilon_{ij}^{p^n}$$

$$\rho_{ij}^{\prime c,n+1} = \rho_{ij}^{\prime c,trial} + \hat{\sigma}_{ij}^{\prime c,n+1}$$

$$\rho_{ij}^{c,n+1} = \frac{1}{3} tr\left(\rho_{ij}^{c,trial}\right) + \left(\rho_{ij}^{\prime c,n+1}\right)$$

Else: (plastic)

$$r_{ij}^{n+1} = \frac{3}{2} \frac{\left(\rho_{ij}^{\prime c,trial} + \hat{\sigma}_{ij}^{\prime c,n+1}\right)}{f^{trial}}$$

$$\Delta\gamma^{n+1} = \frac{f^{trial}}{3\mu}$$

$$\varepsilon_{ij}^{p^{n+1}} = \varepsilon_{ij}^{p^n} + \Delta\gamma^{n+1} r_{ij}^{n+1}$$

$$\rho_{ij}^{\prime c,n+1} = \rho_{ij}^{\prime c,trial} - 2\mu\Delta\gamma^{n+1} r_{ij}^{n+1}$$

$$\rho_{ij}^{c,n+1} = \frac{1}{3} tr\left(\rho_{ij}^{c,trial}\right) + \left(\rho_{ij}^{\prime c,n+1}\right)$$

Endif

The consistent tangent modulus is then:

$$C_{ijkq}^{con} = \kappa\delta_{ij}\delta_{kq} + 2\theta\mu\left(I_{ijkq} - \frac{1}{3}\delta_{ij}\delta_{kq}\right) - \frac{4}{3}\mu\varphi r_{ij}^{n+1} r_{kq}^{n+1}$$

where:

$$\mu = \frac{E}{2\left(1+v\right)}\ ,\ \kappa = \frac{E}{3\left(1-2v\right)}\ ,\ \theta = \frac{\sigma^y}{\left|\rho_{ij}^{\prime c,trial} + \hat{\sigma}_{ij}^{\prime c,n+1}\right|}\ and\ \varphi = \theta$$

3.5 Applications

3.5.1 Implementation

The algorithms were implemented in the finite element software ABAQUS using the user-subroutine UMAT. Other finite element software may also be used in a similar manner. The job is submitted using m+5 steps, i.e:

Step 1 Apply constant load and solve for elastic stresses. Write stresses to statev array.

Step 2 to m+1 Apply l^{th} cyclic load and solve for elastic stresses. Write stresses to STATEV array.

Step m+2 Return geometry to unstressed state

Step *m*+3 Perform Stage 1 analysis. Write varying cyclic stresses to statev array.

Step *m*+4 Return model to unstressed state

Step *m*+5 Perform Stage 2 analysis

The constant load at the ratchet boundary is the largest load for which the Stage 2 analysis can find a stable solution.

3.5.2 Axi-symmetric Bree Cylinder

The axi-symmetric Bree problem analysed in (Martin and Rice 2009) is used to verify the proposed method. The Hybrid Method solutions have been found using a variation of the model proposed here and show good agreement with the original solutions in (Martin and Rice 2009), verifying the use of the residual stress state during the analysis. Note that little redistribution of stress occurs in the Bree cylinder, so little difference is expected between the proposed method and the Hybrid Method. The LMM result have been given as they have been previously verified and thus can be taken as an accurate solution. A model was defined with the dimensions given in figure 5 using second order reduced integration axi-symmetric elements. The mesh consisted of 10 elements through thickness with the element height chosen to keep the elements square. The material properties used were Young's modulus 184GPa, Poisson's ratio 0.3 and yield strength 402.7MPa. The cylinder is subject to a constant mechanical load which consists of an internal pressure, P, and corresponding axial thrust, F, to simulate end cap pressure. The cyclic load is applied through a cyclic internal temperature; the external temperature is fixed at all times to 20 $^\circ$C. The temperature gradient is found by thermal analysis, thermal conductivity 0.035W/mm, and the resultant cyclic stress is found assuming a thermal expansion coefficient of 1.335x10^{-5} $^\circ$C^{-1}. The end of the cylinder that has the end cap thrust applied is constrained to remain in plane section.

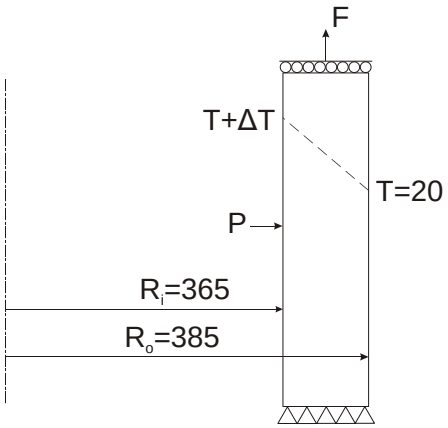

Figure 5: Axi-symmetric Bree Problem

The results given in figure 6 show that both of the proposed methods produce nominally the same results as the Hybrid Method due to the limited amount of redistribution

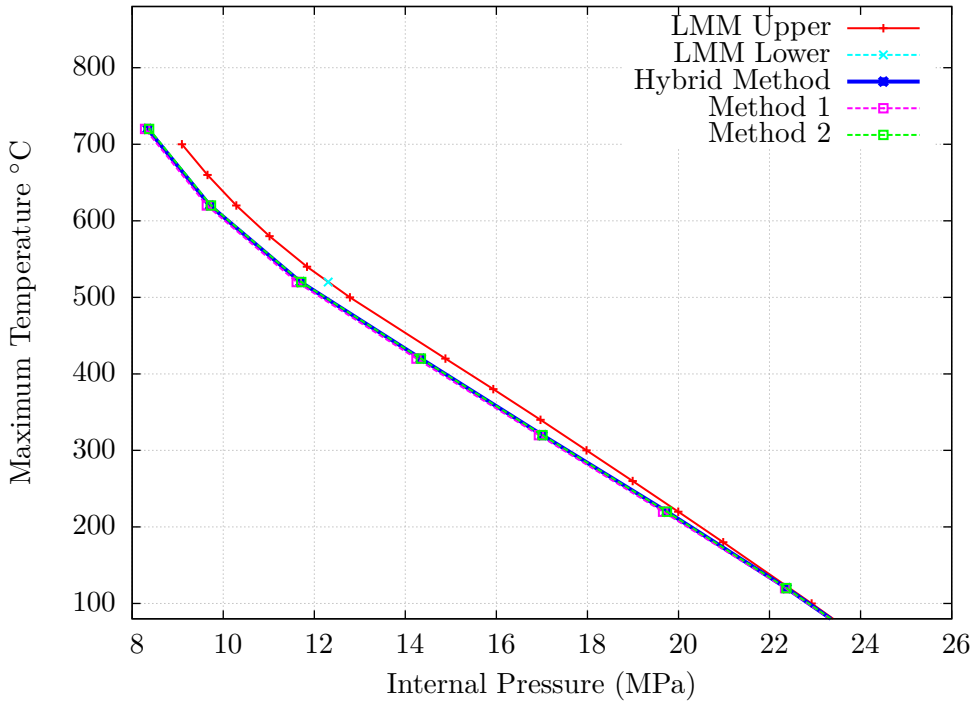

Figure 6: Bree Cylinder Ratchet Boundaries From Various Methods

in the stress field. The results also show that the proposed methods do not overcome the deviation of the calculated boundary from the LMM. It might at first be tempting to say this is due to the method being a lower bound; however it is shown in figure 6 that the lower bound extension to the LMM is capable of producing a lower bound closer to that given by the upper bound LMM.

This is an indication that there is a fundamental limitation to the vector summation type of direct ratchet methods such as the Hybrid Method, the UMY and LDYM methods, and the methods presented in this section. In the Bree cylinder analysis all of the methods were able to find the ratchet condition. The ratchet condition in this case is the stress throughout the section reaches yield at some point in the load cycle. This is shown in figure 7, which gives the equivalent stress in the structure for ΔT=500 at the T=20 and T=520 points on the load cycle. It can be seen that the inner portion of the cylinder is limited by the T=20 load case and the outer portion of the cylinder is limited by the T=520 load case. This indicates that with the current vector type lower bound methods no further improvement can be achieved on the ratchet boundary, thus the method must be fundamentally altered if greater agreement with the LMM is to be achieved.

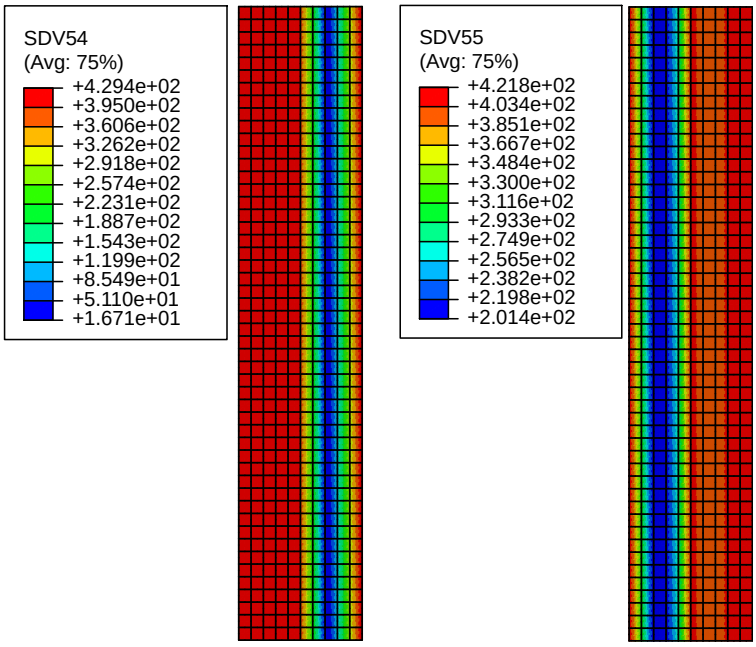

Figure 7: Total Equivalent Stress ΔT=500 $^\circ$C:
Left: 20 $^\circ$C, Right 520 $^\circ$C

3.5.3 Pressurised two bar

The pressurized two bar structure is shown in figure 8. Bar 1 has an internal radius of 2.00mm and an external radius of 2.68mm. Bar 2 has an internal radius of 2.00mm and an external radius of 3.22mm. Bar 2 is twice the length of bar 1 and both have the same material properties: Young's modulus 210GPa, Poisson's ratio 0.3, yield strength 200MPa and thermal expansion coefficient 1.17x10-5 $^\circ$C^{-1}. The ends of the cylinders are constrained to remain in plane section at all times. The model was defined in 3D using second order reduced integration elements, with six elements through the thickness of bar 2, and 3 through the thickness of bar 1.

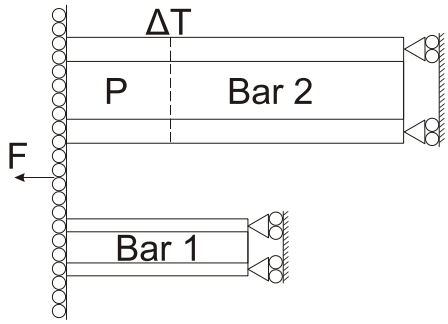

Figure 8: Pressurised Two Bar Problem

The load cycle is described by a constant load which consists of internal pressure, P, applied to bar 2 and axial force, F, distributed between both bars by a plane section constraint. The cyclic load is applied as a varying temperature, above the reference temperature, in bar 2, with the temperature uniform throughout the bar. Bar 1 remains at all times at the reference temperature. The pressure and axial force are considered for three separate conditions, where the force in Newtons divided by the pressure in MPa equals 10, 15 and 20. This is done to test the proposed methods under varying

extents of multi-axial stress conditions. The ratchet boundaries, as determined by the proposed methods, the Hybrid Method and the LMM, are given in figure 9 to figure 11. The LMM solutions are presented as they agree closely with the verified DCA results given in (Martin and Rice 2009).

The results show that the proposed methods give different results to the Hybrid Method for the varying degrees of multi-axial stress condition. In most of the points considered the proposed Method 1 produces results below that of the Hybrid Method. This can be attributed to the consistent tangent modulus becoming ill conditioned in the complex stress fields, resulting in a premature failure of the Stage 2 limit analysis. The proposed Method 2 produces a boundary more consistent with the upper bound LMM than the Hybrid Method in all of the conditions analysed. Note that both of the proposed methods avoid the possibility of the non-conservative results seen in the Hybrid Method for F/P=20, figure 11, at a cyclic temperature above approximately 140 $^\circ$C. This is attributed to the Hybrid Method not accounting for redistribution in the stress and as suchnot representing the effective weakening of the structure caused by the redistribution in the stress field .

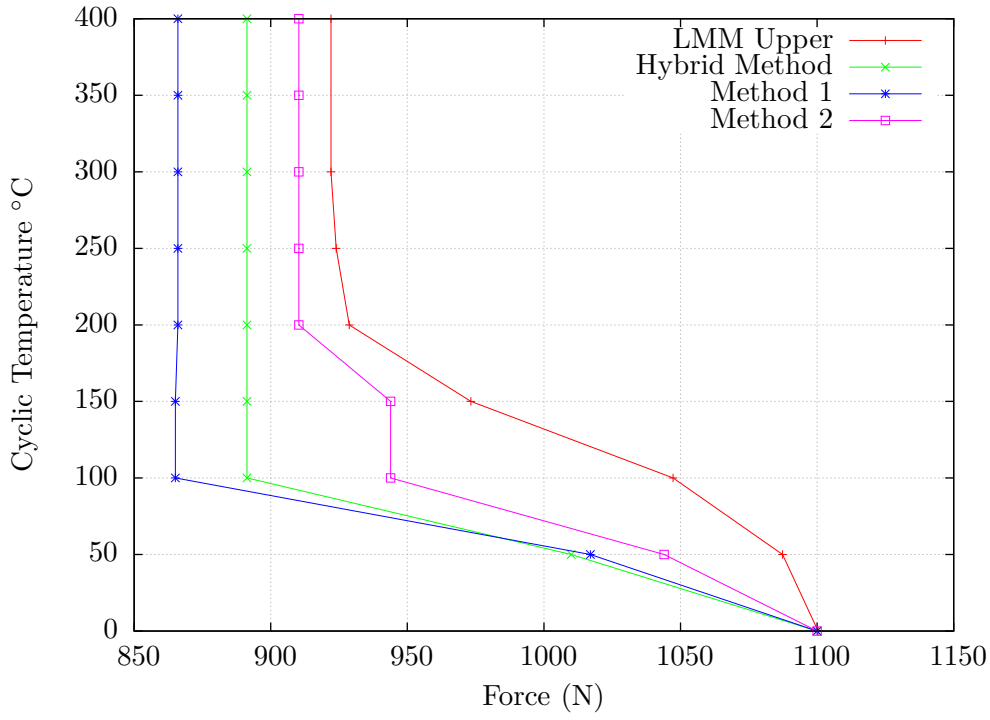

Figure 9: Pressurised Two Bar Ratchet Boundaries by Various Methods with F/P=10

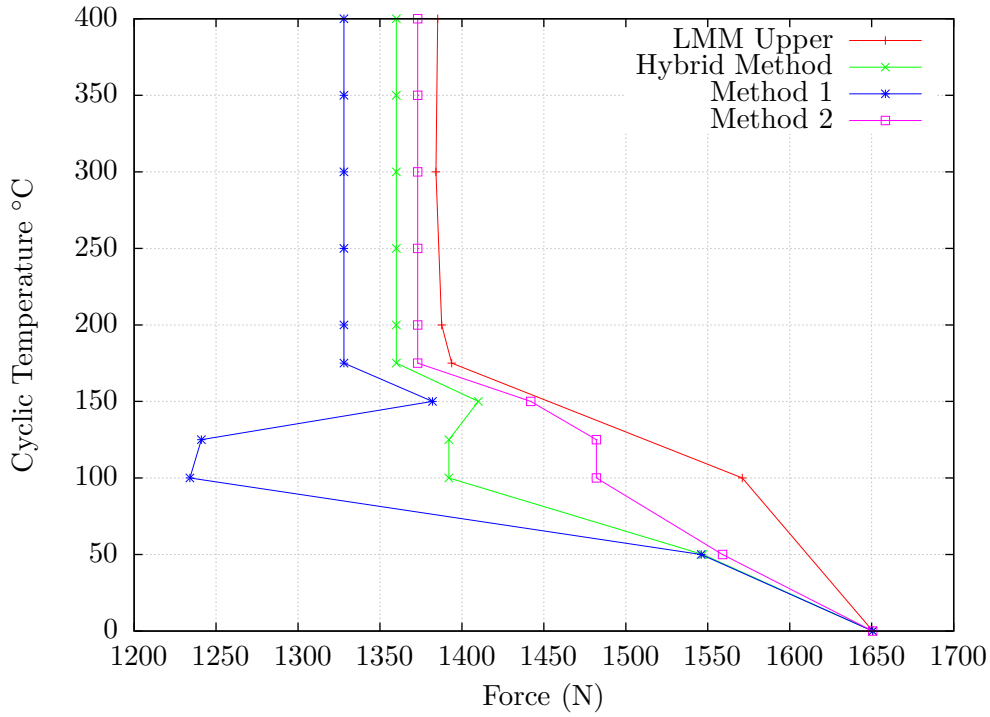

Figure 10: Pressurised Two Bar Ratchet Boundaries by Various Methods with F/P=15

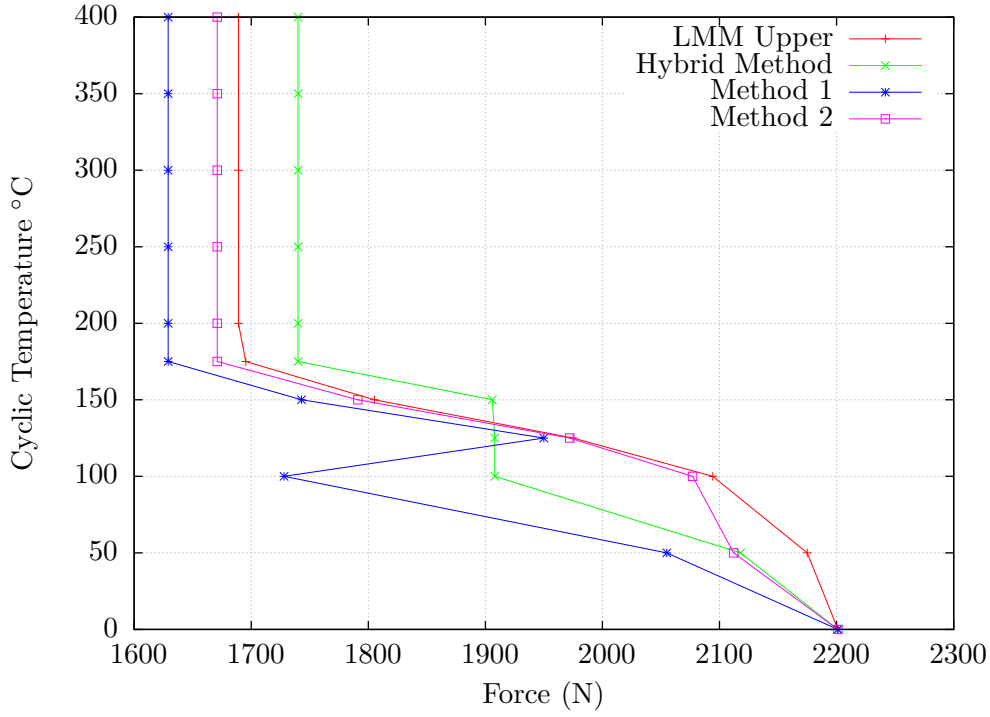

Figure 11: Pressurised Two Bar Ratchet Boundaries by Various Methods with F/P=20

3.5.4 Plate with Hole

The plate with hole is square with edge length L. The hole is centrally located with a radius a, such that a/L=0.1. The depth d of the plate is such that d/L= 0.005, see figure 12 for a schematic of the geometry. Symmetry is used to model only one eighth of the plate. The load case analysed is constant pressure P applied on one set of the free ends plus temperature cycled throughout the structure from to θ_0 to $\theta(r,t)$, see equation 6, where θ_0 is assumed to be $0\,^{\circ}$C. At all times the free ends of the plate are constrained to remain plane.

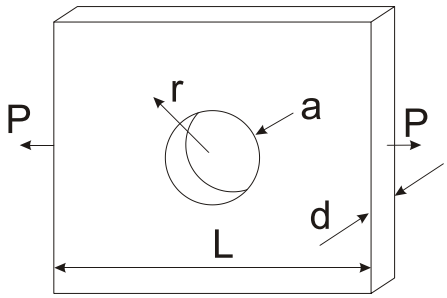

Figure 12: Plate with Hole Problem

$$\theta(r,t) = \theta_0 + (\Delta\theta(t) - \theta_0)\frac{ln\left(\frac{5a}{r}\right)}{ln(5)} \tag{6}$$

The plate material properties are assumed to be temperature independent and isotropic. The elastic modulus E= 208GPa, Poisson's ratio, $v = 0.3$, coefficient of thermal expansion, $\alpha = 5\text{x}10^{-5\circ}\text{C}^{-1}$ and yield strength, σ^y=360MPa .

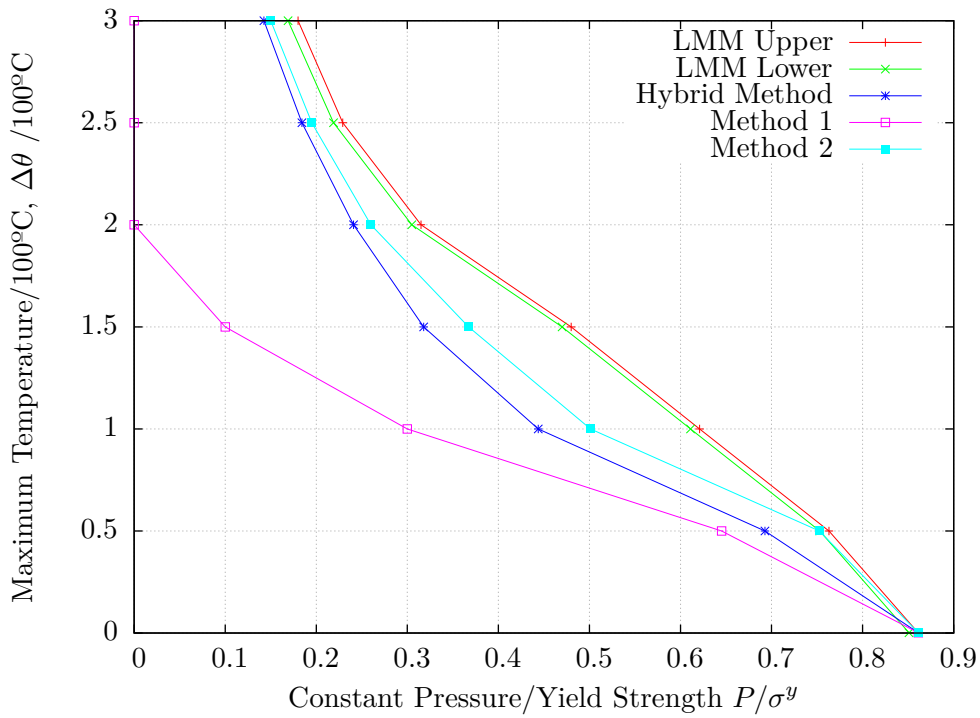

Figure 13: Plate with Hole Ratchet Boundary by Various Methods

The ratchet boundaries obtained from several methods are shown in figure 13. The LMM result have been previously verified by elastic plastic FEA (see Ure et.

al. 2011) and may be taken as accurate. Figure 13 shows that the proposed Method 1 becomes unstable at relatively low cyclic loads. A number of possible reasons for this are discussed in 3.6. The proposed Method 2, however, shows a more stable solution, similar to the lower bound LMM with a cyclic temperature ratio of 0.5. In general Method 2 finds a ratchet boundary more consistent with the upper bound LMM than the Hybrid Method. This is attributed to the increase in modified yield strength in the majority of the structure that occurs on redistribution of the constant load, as illustrated in figures 14a and 14b.

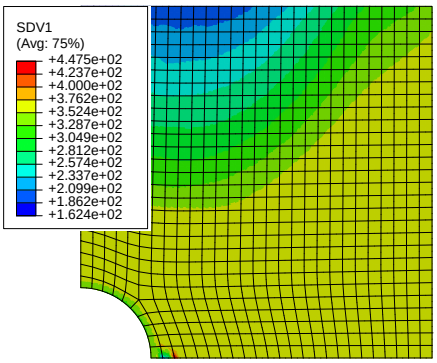

(a) Modified von Mises yield strength (MPa) Method 2

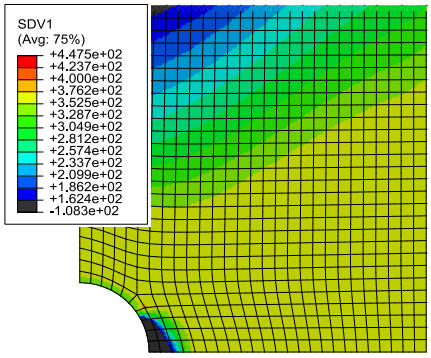

(b) Modified von Mises yield strength (MPa) Hybrid Method

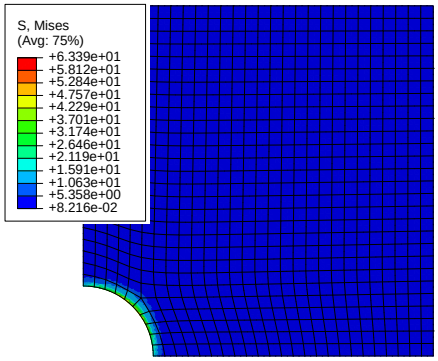

(c) Constant equivalent residual stress due to cyclic loading,$|\overline{\rho}|$ (MPa), for $\frac{\Delta\theta}{100}$=0.5

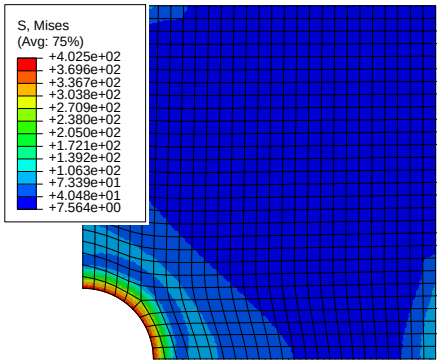

(d) Constant equivalent residual stress,$|\overline{\rho}|$ (MPa), for $\frac{\Delta\theta}{100}$=1.0

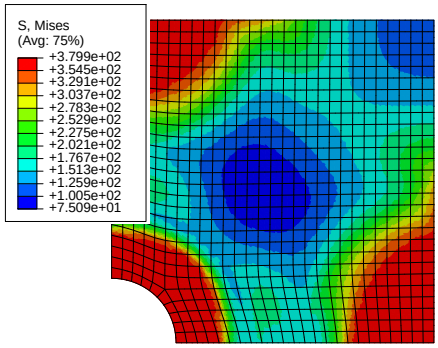

(e) Constant equivalent residual stress,$|\overline{\rho}|$ (MPa), for $\frac{\Delta\theta}{100}$=2.5

Figure 14: Plate with Hole Stresses

It can be seen that Method 2, whilst accounting for redistribution, starts to deviate significantly from the LMM results for temperature ratios above 0.5 but then tends toward the LMM results beyond a temperature ratio of approximately 1.5. The cyclic stress solutions from Stage 1 with a temperature ratio of 0.5 indicate that the region of residual stress from Stage 1 is highly localized around the bore of the hole, with the residual stress elsewhere being relatively low, as shown in figure 14c. The results at temperature ratio 1 show that regions of residual stress are starting to form at the edge of the plate, as shown in figure 14d. When the cyclic temperature ratio is 2.5, the residual stress zones at the centre of the plate and also at the edges of the plate result in full reverse yielding at the residual state: i.e. cause reverse plasticity as shown in figure 14e. This suggests that when the residual stress is small, as in figure 14c, the effect of the cyclic solution on the Stage 2 ratchet analysis is negligible. As the cyclic temperature increases, the residual stress increases at the points where the constant load is applied. This appears to have a larger impact on Stage 2. As the residual stress at the loaded faces becomes large and causes reverse plasticity, the effect this has on the ratchet analysis is reduced. This suggests that the regions of residual stress which result in plastic strains that are not carried over to the Stage 2 impact on the application of the constant load. By removing the plastic strains from the analysis before performing the limit analysis, the compatibility of the problem is not fully accounted for. Whilst compatibility is not a necessary condition required for Melan's theorem, it is enforced in the FEA. This indicates that not preserving the compatibility between Stage 1 and Stage 2 could be a source of the discrepancy between the proposed methods and the LMM results.

3.6 Discussion

From the results presented in figures 9 to 11 and figures 14c to 14e, it is clear that Method 1 is highly unstable. This is accredited to the per iteration update of X which can result in a rapidly changing consistent tangent modulus. The results from Method 2 are generally in better agreement with the LMM than the Hybrid Method. Also the non-conservative results present in the Hybrid Method, as shown in figure 11, are not seen in the Method 2. This can be attributed to updating the modified yield strength, or X, and thus ensuring the constant stress consistently satisfies the extended Melan's theorem. However in general the results from Method 2 are still unreliable and potentially overly conservative.

It has been demonstrated by the lower bound approximation of the LMM that it should be possible to find residual stress fields which satisfy Melan's theorem closer to

the upper bound solutions. The results for the pressurized bar, F/P=20, show that the stress condition for this particular stress field is predominantly uniaxial. Under these conditions the results show reasonable agreement with the upper bound LMM, an exception is the point at 50°C. Yielding first occurs in bar 1 at a cyclic temperature of approximately 84°C and reverse plasticity at 168°C. Beyond 168°C bar 1 becomes perfectly flexible to additional strain caused by the thermal load in bar 2. After 168°C the stress cycle in bar 1 is the same for all cyclic temperatures. Thus the cyclic stress contribution during the Stage 2 analysis remains constant, and the Stage 2 results for constant pressure are the same for cyclic temperature greater than 168°C. In general, for all of the load cases these points show better agreement with the LMM. Due to the reverse plasticity mechanism in bar 1 it becomes perfectly flexible to additional constant load. It is then reasonable to assume that below this temperature a possible source of the difference to the LMM is an error in the compatibility internally in each bar and between the two bars.

The result for the Bree cylinder show differences to the LMM for cyclic temperatures considerably below the first yield and reverse plasticity loads. At these points compatibility issues caused by cyclic solutions should not occur, as no plastic strains result from the cyclic loads. However the plane section constraint on the free end of the cylinder could have an impact on the stress state and normal directions that results from a given plastic strain direction. In the actual structure the direction of the plastic strains would be given by the combination of constant plus cyclic load, thus the normal directions would be $r_{ij} = \frac{3}{2}\frac{\sigma'_{ij}}{\sqrt{\frac{3}{2}\sigma'_{kq}\sigma'_{kq}}}$. The normal directions used in the Stage 2 analysis are for the constant load only, i.e $r_{ij} = \frac{3}{2}\frac{\sigma'^{c}{}_{ij}}{\sqrt{\frac{3}{2}\sigma'^{c}_{kq}\sigma'^{c}_{kq}}}$. The difference in normal directions could have an impact on the axial strain in the parts of the structure that yield. This would affect the plane section constraint and the resulting redistribution of stress. The same argument could also be applied to the stresses in bar 2 in the pressurized two bar structure, giving a possible reason for the greater deviation of the results below the alternating plasticity boundary for F/P=10 and F/P=15.

Therefore two problems with the proposed methods are identified:

Problem 1 An error in the plastic strain direction during Stage 2 due to the separation of constant and cyclic stresses during the Stage 2 analysis. This was necessary to identify a single limiting value for X.

Problem 2 Compatibility problems which result from removing the plastic strains from Stage 1 before starting Stage 2. This would further contribute to the extent of problem 1.

Whilst maintaining the plastic strains from Stage 1 to solve problem 2 would be relatively easy, using the actual plastic strain direction would make identifying a limiting case for X more difficult, as the direction of plastic strain would be different for the different cyclic loads. The results from Methods 1 and 2 therefore suggest it is necessary to consider the actual plastic strain directions when finding a constant stress which satisfies the yield condition given in equation 5.

4 Melan's Theorem as a Class of Material Model

In Section 3 it was shown that the Hybrid method and Methods 1 and 2 were limited in accuracy by their formulation. It was discussed that whilst Method 1 and Method 2 were able to find stress fields which satisfied Melan's theorem, several other problems limited their accuracy.

Loss of Compatibility: Whilst compatibility is not strictly necessary for Melan's theorem it is of utmost importance when considering a FEA. When Stage 1 of the Hybrid Method, Method 1 and 2 is completed, the strains are set back to an un-strained state. Doing so causes the reloading of the structure to take a different load path than it would if the strain from Stage 1 were to be used as the starting point of Stage 2.

Error in Plastic strain Direction: The plastic strain direction used in the Stage 2 analysis is given by the constant load only i.e.:

$$r_{ij} = \frac{3}{2}\frac{\rho'^{c}_{ij} + \hat{\sigma}'^{c}_{ij}}{\sqrt{\frac{3}{2}\sigma'^{c}_{kq}\sigma'^{c}_{kq}}}$$

However the "actual" plastic strain direction which would occur due to the application of both the cyclic and constant load is:

$$r_{ij} = \frac{3}{2}\frac{\sigma'_{ij}}{\sqrt{\frac{3}{2}\sigma'_{kq}\sigma'_{kq}}}$$

therefore the redistribution stress field results in plastic strains which do not accurately model the "actual" redistribution.

The result of these 2 problems is a limiting effect on the amount of redistribution which can take place in the constant stress field, which can result in premature failure of the Stage 2 limit analysis. This results in the excessively conservative results of Methods 1 and 2. The compatibility problem may be easily overcome by retaining the strains from the end of Stage 1. However doing so will not fully resolve the problem and premature failure due to limited redistribution could still occur.

When multiple load cases must be considered simultaneously, as in Melan's Theorem, it is necessary to apply assumptions to allow the application of standard material models. To allow the multiple load cases to be compared simultaneously to identify a limiting case, it is necessary to assume a common plastic strain direction for all load cases. Thus the plastic strain direction during Stage 2 is assumed to be given

by the constant load only. To improve the final solution given by the ratchet method, it is necessary to find a way of considering numerous load cases simultaneously whilst maintaining an accurate description of plastic strain with respect to all of the load cases. In this chapter Melan's Theorem and the Extended Melan's Theorem is reinterpreted in such a way to allow this.

4.1 Melan's Theorem and Plasticity Theory

Melan's Theorem can be formally expressed as:

Consider a structure is subject to an arbitrary set of time varying loads $P(t)$, which can be described by fully elastic stresses $\hat{\sigma}_{ij}(t)$, and these loads result in a constant, self-equilibrating, residual stress, ρ_{ij}. Shakedown will occur if, under the combined action of the residual, ρ_{ij} plus elastic $\hat{\sigma}_{ij}(t)$ stresses, the yield condition is not violated anywhere in the structure at all times in the load cycle i.e.:

$$|\rho_{ij} + \hat{\sigma}_{ij}(t)| \leq \sigma^y \text{ for all t} \tag{7}$$

Assuming the load cycle can be adequately modelled by two load extremes P^1 and P^2, which result in fully elastic stress fields of $\hat{\sigma}^1_{ij}$ and $\hat{\sigma}^2_{ij}$, then Melan's Theorem may be defined as:

$$\left|\rho_{ij} + \hat{\sigma}^1_{ij}\right| \leq \sigma^y \tag{8}$$

and

$$\left|\rho_{ij} + \hat{\sigma}^2_{ij}\right| \leq \sigma^y \tag{9}$$

The problem then reduces to finding a residual stress field which satisfies both of the yield criteria in equations 8 and 9. However from the results of the Hybrid Method and Methods 1 and 2 it is also necessary to maintain correct descriptions of the plastic strains in the structure to prevent premature failure of the analysis and overly conservative results. If the loading on the structure is such that the first point on the load cycle, P^1, is the only point in the load cycle which violates yield for a particular material point, then the response of that material point, assuming perfect plasticity, may be defined as:

$$\sigma^1_{ij} = C_{ijkq}\left(\varepsilon^{T,1}_{kq} - \varepsilon^p_{kq}\right) \tag{10}$$

where σ^1_{ij} is the stress at load point 1.

Any plasticity must obey the Kuhn-Tucker loading and unloading conditions i.e.

$$\gamma \geq 0 \ , \ f \leq 0 \ , \ \gamma f = 0$$

and also on yielding the stresses must satisfy the consistency condition:

$$\gamma \dot{f} = 0$$

with the yield condition:

$$f\left(\sigma_{ij}^{1}\right) = \left|\sigma^{1}\right| - \sigma^{y}$$

The plastic strain rate is assumed to be:

$$\dot{\varepsilon}_{ij}^{p} = \dot{\gamma} \frac{\delta f^{1}}{\delta \sigma_{ij}^{1}} \tag{11}$$

If the loading on the structure is such that the second point on the load cycle, P^2, is the only point in the load cycle which violates yield for a particular material point, then the response of that material point, assuming perfect plasticity, may be defined as:

$$\sigma_{ij}^{2} = C_{ijkq}\left(\varepsilon_{kq}^{T,2} - \varepsilon_{kq}^{p}\right) \tag{12}$$

Any plasticity must obey the Kuhn-Tucker loading and unloading conditions i.e.

$$\gamma \geq 0 \ , \ f \leq 0 \ , \ \gamma f = 0$$

and also on yielding the stresses must satisfy the consistency condition:

$$\gamma \dot{f} = 0$$

with the yield condition:

$$f\left(\sigma_{ij}^{2}\right) = \left|\sigma^{2}\right| - \sigma^{y}$$

The plastic strain rate is assumed to be:

$$\dot{\varepsilon}_{ij}^{p} = \dot{\gamma} \frac{\delta f^{2}}{\delta \sigma_{ij}^{2}} \tag{13}$$

Therefore if only one point in the load cycle violates Melan's theorem at each material point the problem may be accurately solved using standard material models with the appropriate cyclic stress used to define σ_{ij}^{m}. However consider the case when

both load points violate Melan's theorem for a particular material point. The loaded stress and strain conditions are given by:

$$\sigma_{ij}^{1} = C_{ijkq}\left(\varepsilon_{kq}^{T,1} - \varepsilon_{kq}^{p}\right) \quad \text{and} \quad \sigma_{ij}^{2} = C_{ijkq}\left(\varepsilon_{kq}^{T,2} - \varepsilon_{kq}^{p}\right) \tag{14}$$

Any plasticity must obey the Kuhn-Tucker loading and unloading conditions i.e.

$$\gamma^{l} \geq 0 \ , \ f^{l} \leq 0 \ , \ \gamma^{l} f^{l} = 0 \ \text{ for } \ l = 1, 2$$

and also on yielding the stresses must satisfy the consistency condition:

$$\gamma^{l} \dot{f}^{l} = 0 \ \text{ for } \ l = 1, 2$$

with the yield condition:

$$f\left(\sigma_{ij}^{l}\right) = \left|\sigma_{ij}^{l}\right| - \sigma^{y} \ \text{ for } \ l = 1, 2$$

The net plastic strain rate is assumed to be the combined total for both load conditions and is given by Koiter's rule:

$$\dot{\varepsilon}_{ij}^{p} = \sum_{\theta=1}^{\theta=2} \dot{\gamma}^{\theta} \frac{\delta f^{\theta}}{\delta \sigma_{ij}^{\theta}} \tag{15}$$

Therefore Melan's theorem may be thought of as a special case of plasticity model where numerous load cases contribute to the net plastic strain rate. To solve for the material response described by equations 14 to 15 it is necessary to implement a plasticity model which deviates from the traditional single yield surface plasticity models commonly available in finite element software.

4.2 The Extended Melan's Theorem and Plasticity Theory

The extended Melan's Theorem was formally expressed in Section 2.4 and is summarised as:

$$\left|\rho_{ij}^{c} + \overline{\rho}_{ij} + \rho_{ij}^{\Delta}(t) + \hat{\sigma}_{ij}^{c} + \hat{\sigma}_{ij}(t)\right| \leq \sigma^{y} \tag{16}$$

with

$$\rho_{ij}^{\Delta}(t) = \rho_{ij}^{\Delta}(t + \varphi) \tag{17}$$

in regions of the structure where the cyclic stresses are sufficient to cause reverse plasticity.

Consider a structure subject to a constant load P^{c} and is also subject to a cyclic

load $P(t)$ which can be considered as having two load extremes P^1 and P^2. If reverse plasticity is present then both load conditions violate the the yield functions given by the extended Melan's theorem and the strains and stresses at the extreme points in the load cycle may be expressed as:

$$\sigma_{ij}^1 = C_{ijkq}\left(\varepsilon_{kq}^{T,1} - \varepsilon_{kq}^{p,1}\right) \quad \text{and} \quad \sigma_{ij}^2 = C_{ijkq}\left(\varepsilon_{kq}^{T,2} - \varepsilon_{kq}^{p,2}\right) \tag{18}$$

where $\varepsilon_{ij}^{p,1} \neq \varepsilon_{ij}^{p,2}$ in some part of the structure due to the alternating plasticity mechanism.

Any plasticity must obey the Kuhn-Tucker loading and unloading conditions i.e.

$$\gamma^l \geq 0 \ , \ f^l \leq 0 \ , \ \gamma^l f^l = 0 \ \text{ for } \ l = 1, 2$$

and also on yielding the stresses must satisfy the consistency condition:

$$\gamma \dot{f}^l = 0 \ \text{ for } \ l = 1, 2$$

with the yield condition:

$$f\left(\sigma_{ij}^l\right) = \left|\sigma_{ij}^l\right| - \sigma^y \ \text{ for } \ l = 1, 2$$

The net plastic strain at the constant residual state, i.e. cyclically unloaded, is assumed to be the combined total for both load conditions, i.e. the net plastic strain rate from loading and unloading which results at the shakedown condition, and is given by Koiter's rule:

$$\dot{\varepsilon}_{ij}^p = \sum_{\theta=1}^{\theta=2} \dot{\gamma}^\theta \frac{\delta f^\theta}{\delta \sigma_{ij}^\theta} \tag{19}$$

Therefore the extended Melan's theorem may also be thought of as a special case of a plasticity model where numerous load cases contribute to the net plastic strain increment. Here, however, there is an added complication of the plastic strain being different from one load case to another.

4.3 The Residual Stress as a Shared State for all Load Cases

In Sections 4.1 and 4.2 it was shown that both Melan's theorem and the extended Melan's theorem may be taken as a plastic material model in which numerous load cases contribute to the net plastic strain. However to solve the model with two different stress conditions would require a special finite element which could calculate both stress conditions at the same time. In this Section the residual stress is proposed as a

common material state to all load cases, thus allowing the problem to be solved using conventional finite elements.

4.3.1 Shakedown

First consider the pure shakedown problem. If the cyclic load case may be expressed as m extreme points in the load cycle, which may be described by fully elastic stresses $\widehat{\sigma}_{ij}^{l}$ with $l = 1, 2..m$, the total loaded stress at point l in the load cycle may be expressed as:

$$\sigma_{ij}^{l} = \rho_{ij} + \widehat{\sigma}_{ij}^{l} \tag{20}$$

The solution may then be carried out by converging on the residual stresses and strains with the loaded conditions calculated by superposition of the fully elastic cyclic stresses. The problem may then be defined as:

$$\rho_{ij} = C_{ijkq}\left(\varepsilon_{kq}^{Tr} - \varepsilon_{kq}^{p}\right) \tag{21}$$

The loaded conditions are then given by:

$$\sigma_{ij}^{l} = \rho_{ij} + \widehat{\sigma}_{ij}^{l} \tag{22}$$

Any plasticity must obey the Kuhn-Tucker loading and unloading conditions i.e.

$$\gamma^{l} \geq 0 \ , \ f^{l} \leq 0 \ , \ \gamma^{l} f^{l} = 0 \ \text{ for all } l$$

and also on yielding the stresses must satisfy the consistency condition:

$$\gamma^{l} \dot{f}^{l} = 0 \ \text{ for all } l$$

with the yield condition:

$$f\left(\sigma_{ij}^{l}\right) = f\left(\rho_{ij} + \widehat{\sigma}_{ij}^{l}\right) = \left|\rho_{ij} + \widehat{\sigma}_{ij}^{l}\right| - \sigma^{y} \ \text{ for all } l$$

and the net plastic strain rate is assumed to be due to all load cases and given by Koiter's Rule:

$$\dot{\varepsilon}_{ij}^{p} = \sum_{\theta=1}^{\theta=m} \dot{\gamma}^{\theta} \frac{\delta f^{\theta}}{\delta \sigma_{ij}^{\theta}} \tag{23}$$

To implement the material model given in equations 21 to 23 in a FEA, it is necessary to integrate the model to give γ^{l} and define the consistent tangent modulus

to preserve the quadratic rate of convergence of the global Newton-Raphson solution procedure. This will be done for Mises plasticity in 5.2.

4.3.2 Reverse Plasticity

If the load case is such that the structure goes beyond the alternating plasticity boundary the residual condition changes due to the alternating plasticity, inducing a varying residual stress. However the load cycle may still be described by the constant residual if the varying residual stresses and strains are known. Assume that the structure is subject to a constant load P^c which results in fully elastic stresses $\hat{\sigma}^c_{ij}$ and is also subject to a cyclic load $P(t)$ which may be described by two extremes in the load case given by P^1 and P^2, which result in fully elastic stresses $\hat{\sigma}^1_{ij}$ and $\hat{\sigma}^2_{ij}$ respectively.

The constant residual stress may be expressed as:

$$\rho^c_{ij} + \overline{\rho}_{ij} = C_{ijkq}\left(\varepsilon^{Tr}_{kq} - \varepsilon^p_{kq}\right) \tag{24}$$

where ε^p_{ij} is made up of a constant residual strain due to the cyclic loading and a constant residual strain due to the constant load.

The loaded conditions are then given by:

$$\sigma^l_{ij} = \rho^c_{ij} + \overline{\rho}_{ij} + \sum_{\theta=1}^{\theta=l} \rho^{\Delta,\theta}_{ij} + \hat{\sigma}^c_{ij} + \widehat{\sigma}^l_{ij} \ \text{ for } \ l = 1, 2 \tag{25}$$

Any plasticity must obey the Kuhn-Tucker loading and unloading conditions i.e.

$$\gamma^l \geq 0 \ , \ f^l \leq 0 \ , \ \gamma^l f^l = 0 \ \text{ for l=1,2}$$

and also on yielding the stresses must satisfy the consistency condition:

$$\gamma \dot{f}^l = 0 \ \text{ for } \ l = 1, 2$$

with the yield condition:

$$f\left(\sigma^l_{ij}\right) = f\left(\rho^c_{ij} + \overline{\rho}_{ij} + \textstyle\sum_{\theta=1}^{\theta=l} \rho^{\Delta,\theta}_{ij} + \hat{\sigma}^c_{ij} + \widehat{\sigma}^l_{ij}\right) =$$

$$\left|\rho^c_{ij} + \overline{\rho}_{ij} + \textstyle\sum_{\theta=1}^{\theta=l} \rho^{\Delta,\theta}_{ij} + \hat{\sigma}^c_{ij} + \widehat{\sigma}^l_{ij}\right| - \sigma^y \ \text{ for all } l$$

and the net plastic strain rate is assumed to be due to all load cases and given by

Koiter's Rule:

$$\dot{\varepsilon}_{ij}^{p} = \sum_{\theta=1}^{\theta=m} \dot{\gamma}^{\theta} \frac{\delta f^{\theta}}{\delta \sigma_{ij}^{\theta}} \tag{26}$$

Note also that for alternating plasticity and the assumed two point load cycle:

$$\rho_{ij}^{\triangle,1} + \rho_{ij}^{\Delta,2} = 0 \tag{27}$$

with

$$\sum_{\theta=1}^{\theta=m} \varepsilon_{ij}^{\triangle,\theta} = 0 \tag{28}$$

where $\varepsilon_{ij}^{\triangle,\theta}$ is the varying residual plastic strain at load point θ.

To implement the model in a FEA it must be integrated to give γ^{l}. However in this case a set of $\rho_{ij}^{\Delta,l}$ which gives $\sum_{\theta=1}^{\theta=m} \rho_{ij}^{\Delta,\theta}$=0 is also an unknown and it is difficult to find both simultaneously. It is therefore easier if the cyclic solution is found first and the results of that analysis are used to find the constant stress solutions.

Therefore, whether solving the shakedown or ratchet problem, Melan's theorem can be thought of as a special type of plasticity model in which multiple load cases may contribute to the net plastic strain at the shakedown state. To solve for the plastic strains with conventional finite elements it is necessary to identify a stress and strain condition common to all load cases. The common stress and strain condition proposed is the constant residual strain and corresponding stress the material models proposed in 4.3.1 and 4.3.2 are integrated into suitable forms for implementation within conventional FEA methods.

5 Non-smooth Multi Yield Surface Plasticity for Shakedown: The EMSP Method

5.1 The Material Model

In this section attention is limited to Mises plasticity: plastic flow which is incompressible and associative in nature, also referred to as J2 plasticity. In this Section a number of other assumptions will be applied unless otherwise stated:

Assumption 7 Perfect plasticity is assumed throughout

Assumption 8 All material properties are temperature independent

Assumption 9 The cyclic loads may be described by superimposed elastic stresses from an unstrained state, i.e non-linear geometry effects may be ignored

Consider a structure subject to an arbitrary load case which can be described by m load extremes. The material response for Mises plasticity may be described by:

$$\dot{\rho}_{ij} = C_{ijkq}\left(\dot{\varepsilon}^{Tr}_{kq} - \dot{\varepsilon}^{p}_{kq}\right) \tag{29}$$

where $\dot{\varepsilon}^{p}_{ij}$ is made up of a constant residual strain rate due to the cyclic loading and a constant residual strain rate due to the constant load and:

$$C_{ijkq} = \lambda\delta_{ij}\delta_{kq} + \mu(\delta_{ik}\delta_{jq} + \delta_{iq}\delta_{jk}) \tag{30}$$

with:

$$\lambda = \frac{vE}{(1+v)(1-2v)} \text{ and } \mu = \frac{E}{2(1+v)}$$

The loaded stress rates are given by:

$$\dot{\sigma}^{l}_{ij} = \dot{\rho}_{ij} + \dot{\hat{\sigma}}^{l}_{ij} \text{ for } l = 1, 2..m \tag{31}$$

with the yield functions:

$$\left|\rho_{ij} + \hat{\sigma}^{l}_{ij}\right| - \sigma^{y} \leq 0 \text{ for all } l$$

where:

$$\left|\rho_{ij} + \hat{\sigma}^{l}_{ij}\right| = \sqrt{\frac{3}{2}\left(\rho'_{ij} + \hat{\sigma}'^{l}_{ij}\right)\left(\rho'_{ij} + \hat{\sigma}'^{l}_{ij}\right)} \tag{32}$$

and the net plastic strain rate is assumed to be due to all load cases and given by Koiter's Rule:

$$\dot{\varepsilon}_{ij}^{p} = \sum_{\theta=1}^{\theta=m} \dot{\gamma}^{\theta} \frac{\delta f^{\theta}}{\delta \sigma_{ij}^{\theta}} \tag{33}$$

For Mises plasticity:

$$\frac{\delta f^{l}}{\delta \sigma_{ij}^{l}} = r_{ij}^{l} = \frac{\delta \left(\left| \rho_{kq} + \widehat{\sigma}_{kq}^{l} \right| - \sigma^{y} \right)}{\delta \left(\rho_{ij} + \widehat{\sigma}_{ij}^{l} \right)} = \frac{3}{2} \frac{\rho'_{ij} + \widehat{\sigma}'^{l}_{ij}}{\left| \rho_{kq} + \widehat{\sigma}_{kq}^{l} \right|} \tag{34}$$

with

$$\gamma^{l} \geq 0 \quad , \quad f^{l} \leq 0 \quad , \quad \gamma^{l} f^{l} = 0 \quad and \quad \gamma^{l} \dot{f}^{l} = 0$$

Let the set of yield surfaces at which yielding occurs be defined as the set of active yield criteria:

$$Q_{act} \text{ where } f = 0 \text{ and } \gamma \geq 0 \tag{35}$$

A complete treatment of the solution to the above model with the incorporation of hardening effects will be given in Section 5.6.2. Here let:

$$[g]_{\alpha\beta} = \left[r_{ij}^{\alpha} C_{ijkq} r_{kq}^{\beta} \right] \tag{36}$$

where

$$\alpha \in Q_{act} \text{ and } \beta \in Q_{act} \tag{37}$$

which gives the tangent modulus as:

$$E_{ijks}^{ep} = E_{ijks} - \sum_{\alpha} \sum_{\beta} [G]_{\alpha\beta} \left(C_{ijop} r_{op}^{\alpha} \right) \left(C_{ksqr} r_{qr}^{\beta} \right) \tag{38}$$

where

$$\sum_{\alpha,\beta,\varsigma \in Q_{act}} [g]_{\alpha\beta} [G]_{\beta\varsigma} = \delta_{\alpha\varsigma} \tag{39}$$

It is possible to describe equation 32 pictorially, see figure 15. The set of m yield functions may be visualized as a series of von Mises yield surfaces off-set by the negative of the superimposed elastic stresses, i.e. $-\widehat{\sigma}_{ij}^{l}$. For the residual stress to satisfy Melan's theorem it must lie in the region where all of the yield criteria overlap, shown as the shaded region in figure 15. The shaded region is bounded by a yield surface which is piecewise described by the yield surfaces formed by Melan's theorem. The yield surface ABC is defined by the critical load case 1 and yield surface CDA is defined by the critical

load case 2. The shakedown problem then reduces to finding a residual stress which satisfies the piecewise yield surface ABCDA. However, this piecewise yield criteria is not smooth and there is the potential for corners to appear in the yield surface. At these corners the solution becomes singular, as there are numerous possible solutions for the direction of plastic flow depending on the stress conditions. Therefore to find the residual stress condition a robust iterative procedure is required.

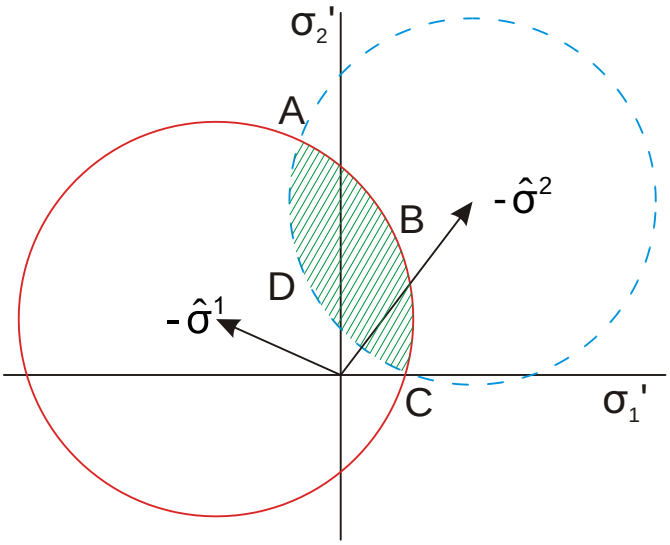

Figure 15: Melan's Theorem as Offset Yield Surfaces

5.2 Solution Scheme: The EMSP Method

The numerical method based on the material model given in Section 5.1 is given the name EMSP, were the "MSP" parts stands for multi surface plasticity and the "E" is elastic for elastic shakedown. The iterative solution procedure follows closely the works of Simo and Hughes (2000) in their Non-Smooth Multi yield surface plasticity model, with some alteration due to possible changes to the active yield surfaces not catered for in Simo and Hughes model, see Section 5.3. These changes are necessary when material points have behaviours close to the alternating plasticity boundary. Only the algorithms necessary to implement the shakedown solution method will be presented in this section. For a complete formulation of the integration scheme see Section 5.6.2, where the scheme is developed in full including the effects of hardening.

The algorithms are presented in the form of the material calculations required in a Finite Element procedure. Stress and internal variables are calculated, based on the displacements and total strains which have been updated based on the results of the previous iteration, to be provided back to the solver for the calculation of nodal

forces and equilibrium checks. The shakedown solution method requires fully elastic stresses which are in equilibrium with the m critical load cases. In order to obtain these solutions and use them in the shakedown solution, they are found during the first m steps of the solution procedure and written to an internal state variable array ready for use in the shakedown solution method which takes place in step $m+2$. The general procedure is:

Step 1 to m Load the model with the loads for critical load case m and solve for the elastic stresses. Write these stresses to the state variable array.

Step m+1 Return model back to unstressed state.

Step m+2 Perform Shakedown solution using results from steps 1 to m.

The lower bound solution method uses incrementally increasing loads until the solver cannot find a stable solution. This shakedown procedure incrementally increases the superimposed load based on a lower bound multiplier Y. The largest value of Y for which the solver can find a stable solution is taken as the lower bound multiplier at the shakedown boundary. In this case, the multiplier Y is made equal to the step time for step $m+2$, and thus the inbuilt solution controls in the Finite Element package may be used to set the convergence parameters on the lower bound multiplier.

The algorithms that follow have been obtained using a backward Euler integration scheme, the quantities at the end of the previous increment are given the superscript ^{n}, the quantities at the end of the current increment are given the superscript $^{n+1}$ and trial quantities (i.e. initial guesses based on initial strains) are given the superscript ^{trial}. For plastic cases a local iterative procedure is used to find ρ_{ij}^{n+1} and $\varepsilon_{ij}^{p,n+1}$, where the current iteration number is ζ.

1. Compute the trial elastic quantities

$$\rho_{ij}^{trial} = C_{ijkq}\left(\varepsilon_{kq}^{Tr,n+1} - \varepsilon_{kq}^{p,n}\right)$$

$$f^l = \left|\rho_{ij} + Y\widehat{\sigma}_{ij}^{l}\right| - \sigma^y = \sqrt{\frac{3}{2}\left(\rho'_{ij} + Y\widehat{\sigma}_{ij}^{\prime l}\right)\left(\rho'_{ij} + Y\widehat{\sigma}_{ij}^{\prime l}\right)} - \sigma^y \text{ for } l = 1, 2..m$$

2. Check yield conditions

$$\text{IF } \left|\rho_{ij}^{trial} + Y\widehat{\sigma}_{ij}^{l}\right| - \sigma^y \leq 0 \text{ for all } Q_{act}^{\zeta} \text{ THEN}$$

$$\rho_{ij}^{n+1} = \rho_{ij}^{trial}$$

$$\varepsilon_{ij}^{p,n+1} = \varepsilon_{ij}^{p,n}$$

ELSE :

$$k = 0$$

$$Q_{act}^{\zeta} = \left\{ \alpha \in l \,\text{where} \left| \rho_{ij}^{trial} + Y\widehat{\sigma}_{ij}^{\alpha} \right| - \sigma^{y} > 0 \right\}$$

$$\rho_{ij}^{n+1,\zeta} = \rho_{ij}^{trial}$$

$$\varepsilon_{ij}^{p,n+1,\zeta} = \varepsilon_{ij}^{p,n}$$

$$\triangle\gamma^{l,n,\zeta} = 0$$

goto 4

ENDIF

3. RETURN Values back to Solver

4. Evaluate Residuals

$$\rho_{ij}^{n+1,\zeta} = C_{ijkq}\left(\varepsilon_{kq}^{Tr,n+1} - \varepsilon_{kq}^{p,\zeta}\right)$$

$$R_{ij}^{\zeta} = -\varepsilon_{ij}^{p,\zeta} + \varepsilon_{ij}^{p,n} + \sum_{\alpha \in Q_{act}^{\zeta}} \triangle\gamma^{\alpha,\zeta} r_{ij}^{\alpha,\zeta}$$

$$r_{ij}^{l,n,\zeta} = \frac{3}{2} \frac{\rho_{ij}^{\prime\zeta} + Y\widehat{\sigma}_{ij}^{\prime l,\zeta}}{\left| \overline{\rho}_{kq} + Y\widehat{\sigma}_{kq}^{l,\zeta} \right|}$$

$$\alpha \in Q_{act}^{\zeta} \text{ and } \beta \in Q_{act}^{\zeta}$$

5. Check Convergence

$$f^{l,\zeta} = \sqrt{\frac{3}{2}\left(\rho_{ij}^{\prime} + Y\widehat{\sigma}_{ij}^{\prime l}\right)\left(\rho_{ij}^{\prime} + Y\widehat{\sigma}_{ij}^{\prime l}\right)} - \sigma^{y} \text{ for } l = 1, 2..m$$

IF $f^{\alpha,\zeta} \leq \text{TOL}_1, \; for\, \alpha \in Q_{act}^{\zeta}$

Check if any deactivated yield criteria require reactivating

IF $f^{l} \leq \text{TOL}_1 \, for\, all\, l$

Solution Converged

$$\rho_{ij}^{n+1} = \rho_{ij}^{\zeta}$$

$$\varepsilon_{ij}^{p,n+1} = \varepsilon_{ij}^{p,\zeta}$$

RETURN values to solver

ELSE

$$Q_{act}^{\zeta+1} = \left\{ \alpha \in m \text{ where } \left| \rho_{ij}^{trial} + Y\widehat{\sigma}_{ij}^{l} \right| - \sigma^{y} > 0 \right\}$$

Continue

ENDIF

ELSE

Continue

ENDIF

6. Compute Elastic and Tangent Moduli

$$[g_{\alpha\beta}]^{\zeta} = r_{ij}^{\alpha,\zeta} A_{ijkq} r_{kq}^{\beta,\zeta}$$

$$\left[g^{\alpha\beta}\right]^{\zeta} = \left[g_{\alpha\beta}^{\zeta}\right]^{-1}$$

$$C_{ijkq} = E_{ijkq}^{-1}$$

$$A_{ijkq}^{\zeta} = C_{ijkq} + \sum_{\alpha} \triangle\gamma^{\alpha} \frac{\delta r_{ij}^{\alpha,\zeta}}{\delta\left(\rho_{kq}^{\zeta} + Y\widehat{\sigma}_{kq}^{\alpha}\right)}$$

$$\frac{\delta r_{ij}^{\alpha,\zeta}}{\delta\left(\rho_{kq}^{\zeta} + Y\widehat{\sigma}_{kq}^{\alpha}\right)} = \frac{3}{2} \frac{\left(1_{ijkq} - \frac{1}{3} 1_{ij} 1_{kq}\right)}{\left|\rho_{st}^{\zeta} + Y\widehat{\sigma}_{st}^{\alpha}\right|} - \frac{r_{ij}^{\alpha,\zeta} r_{kq}^{\alpha,\zeta}}{\left|\rho_{st}^{\zeta} + Y\widehat{\sigma}_{st}^{\alpha}\right|}$$

7. Calculate the increment to the plastic consistency parameters

$$\triangle^{2}\gamma^{\alpha,\zeta} = \sum_{\beta} \left[g^{\alpha\beta}\right]^{\zeta} \left(f^{\beta,k} - r_{ij}^{\beta,\zeta} A_{ijkq}^{\zeta} R_{kq}^{\zeta}\right)$$

$$\triangle\bar{\gamma}^{\alpha,\zeta+1} = \triangle\gamma^{\alpha,\zeta} + \triangle^{2}\gamma^{\alpha,\zeta}$$

IF $\triangle\overline{\gamma}^{\alpha,\zeta+1} < 0$

Remove α from Q_{act}

Goto 4

ENDIF

8. Calculate Increment to plastic strains

$$\triangle\varepsilon_{ij}^{p,\zeta+1} = E_{ijkq} A_{kqop}^{\zeta} \left(R_{op} + \sum \triangle^{2}\gamma^{\beta,\zeta} r_{op}^{\beta,\zeta}\right)$$

9. Update iterative quantities

$$\triangle\gamma^{\alpha,\zeta+1} = \triangle\gamma^{\alpha,\zeta} + \triangle^2\gamma^{\alpha,\zeta}$$

$$\triangle\varepsilon_{ij}^{p,n+1} = \varepsilon_{ij}^{p,n} + \triangle\varepsilon_{ij}^{p,\zeta+1}$$

$$\text{set } \zeta = \zeta + 1$$

Goto 3

When using the solution scheme outlined here (inside the finite element solution which is a global Newton-Raphson scheme), it is necessary to use a consistent tangent modulus to preserve a quadratic rate of convergence for the FEA. For a detailed discussion on the formulation of the consistent tangent modulus see Section 5.6.2. The consistent tangent modulus may be calculated as follows

$$\Xi_{ijkq} = \left(C_{ijkq} + \sum_{\alpha} \triangle\gamma^{\alpha} \frac{\delta r_{ij}^{\alpha,\zeta}}{\delta\left(\bar{\rho}_{kq}^{\zeta} + Y\widehat{\sigma}_{kq}^{\alpha}\right)} \right)^{-1}$$

$$\left[g^{\alpha\beta}\right]^{\zeta} = \left[g_{\alpha\beta}\right]^{\zeta\,-1} = \left[r_{ij}^{\alpha,\zeta}\Xi_{ijkq}r_{kq}^{\beta,\zeta}\right]^{-1}$$

$$\frac{\delta\rho_{ij}^{n+1}}{\delta\varepsilon_{kq}^{Tr}} = \Xi_{ijkq} - \sum_{\alpha}\sum_{\beta}\left[g^{\alpha\beta}\right]^{\zeta} N_{ij}^{\alpha}N_{kq}^{\beta}$$

$$N_{ij}^{\alpha} = \Xi_{ijkq}r_{kq}^{\alpha}$$

The solution schemes presented in steps 1-9 make use of a local Newton's method for calculation of the plastic consistency parameters. The resulting set of simultainious equations becomes indeterminate if there are more than six yield criteria actively returning the yield surface during a single iteration. This does not however limit the number of load points to six. The stresses may be filtered and if necessary applied in several groups to give a bounding result, making sure to check all yield criteria before passing the stresses back to the global equilibrium solution.

5.3 Pictorial Description of the Solution Scheme

The above solution scheme is designed to give residual stresses which consistently satisfy Melan's theorem whilst maintaining a constitutively accurate description of the plastic strain increment. It may be described geometrically as in figures 16a to 16d. In these

figures the load cycle is assumed to be described by two extremes and thus the piecewise yield surface for the residual stress is made up of small sections of two off-set von Mises yield criteria as discussed in section 6.1. Depending on the trial residual stress, there are 6 possible behaviours of the solution scheme. Only five of these are considered in the Simo and Hughes non-smooth multi yield surface plasticity model.

1. The trial residual stress lies inside the shaded region in figure 16a. The residual stress therefore satisfies all of the yield conditions. If this occurs for all locations in the structure the load case lies inside the shakedown boundary and no plasticity calculation is necessary.

2. The trial residual stress is given by point B in figure 16b. In this case the trial residual stress violates the yield condition for yield surface 1 (red solid line). In this case the residual stress must be returned to the shaded portion of the yield surface along a stress path consistent with the assumed material response as shown in figure 16b by the dashed arrow starting at B.

3. The trial residual stress is given by point C in figure 16b. In this case the trial residual stress violates yield function 2 (blue dashed line) and the stress must be returned to the shaded portion of the yield surface. The residual stress is returned along a stress path consistent with the assumed material response, as shown in figure 16b, as the dashed arrow starting from C.

4. The trial residual stress is given by point D in figure 16c. This point lies in the region bounded by the surfaces created by sweeping the vectors $C_{ijkq}r^1_{kq}$ and $C_{ijkq}r^2_{kq}$ around the intersection of the two yield surfaces. In this case the trial residual stress violates the yield function for both yield surfaces 1 and 2. The residual stress must be returned to the singular point where the yield surfaces meet. This must be done whilst maintaining the assumed material response with respect to both of the yield surfaces.

5. In addition to the four basic trial conditions, given in items 1-4, it is possible to change the condition of the stress during the process to return the stress to the shaded region of the material. For instance, consider the trial residual stress given by point E in figure 16c. At the trial condition the residual stress violates the yield condition for both yield surfaces. However the path that the stress will follow is dominated by yield surface 2 (blue dashed line) and the stress will return along a path similar to that shown by the dashed arrow starting at E. Similarly if the trial stress is described by point F the stress will return along a path similar

to the dashed arrow starting at F, as the yielding is dominated by yield surface 1 (red solid line).

6. If the yield surfaces and trial stress condition is given by point G in figure 16d the trial stress condition violates yield surface 1 (red solid line). When the stress is returned to yield surface 1, it in turn creates a stress condition which violates yield surface 2 (blue dashed line). The stress conditions must therefore lie on the intersection between the two yield surfaces and returns along a path depicted by the dashed arrows starting at G. A similar but opposite scenario applies if the trial residual stress condition is given by point H. This particular response would not be captured in the multi yield surface plasticity model presented in (Simo and Hughes 2000). To solve for this behaviour a change to the algorithms presented in section 5.2 is required. In part 5 of the algorithms presented here all yield functions are checked to ensure they are ≤ 0 and that those which are currently active are $\backsimeq 0$.

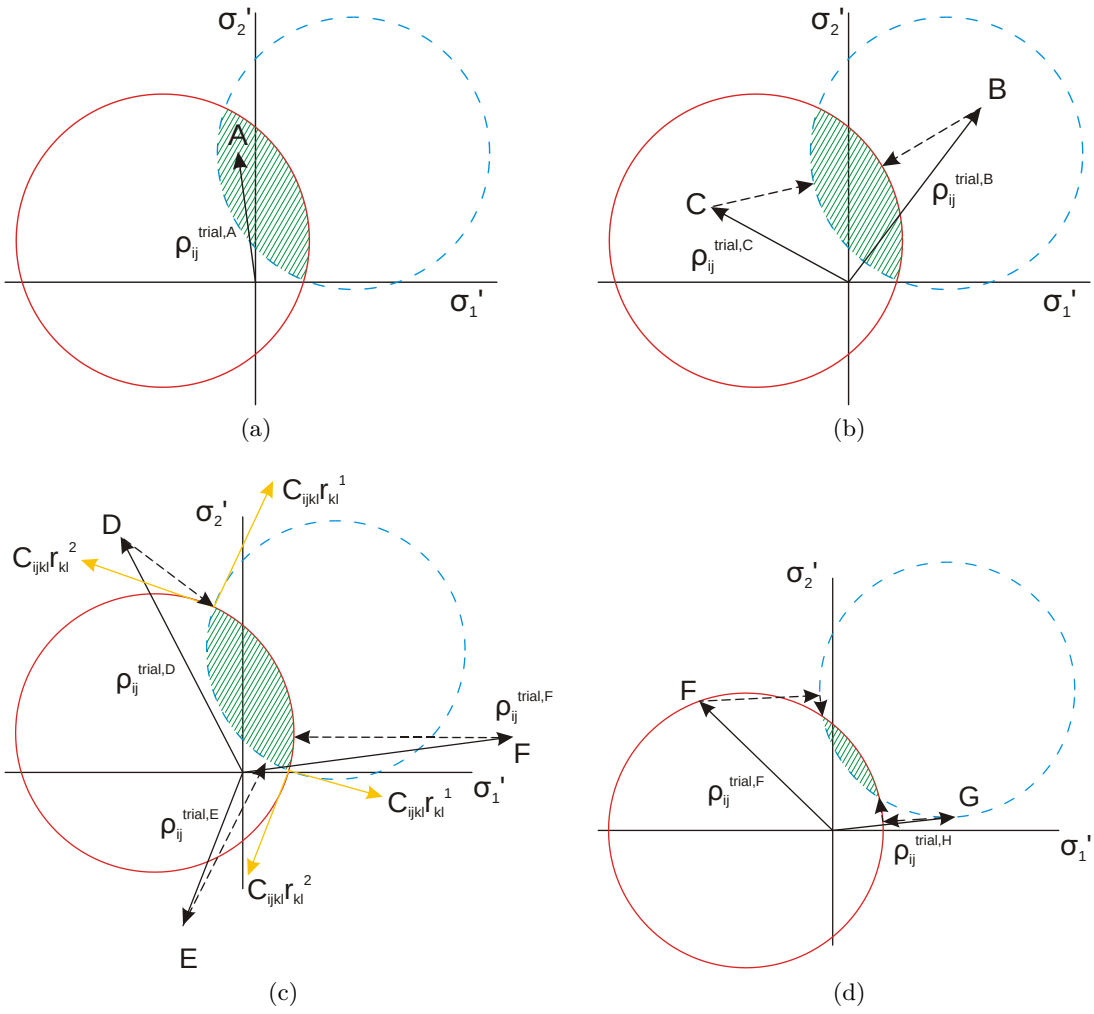

Figure 16: Possible Behaviours of the shakedown solution procedure

5.4 Convergence

The solution scheme presented in Section 5.2 is highly non-linear. However the iterative scheme for finding the plastic strain increment given in steps 1-9 is theoretically unconditionally convergent (Simo and Hughes 2000), so long as the yield surfaces overlap, i.e. the cyclic stresses are within the alternating plasticity limit. In cases where this is not the case the local iterative scheme for the plastic strain increment will fail, as is expected of a lower bound shakedown method. In such cases the time increment is cut until the convergence criteria are met.

In general for the benchmark problems studies in this thesis, the number of iterations required for the local iterative scheme to converge was less than 10. Note however that matrix inversion is required and therefore this scheme can present a relatively large computational cost. Therefore, to speed up the solution, if only one yield surface was active the plastic strain increment necessary to satisfy Melan's theorem could be identified using a single yield surface model as discussed in Section 4.1. It would however be necessary to check that no other yield surfaces became active during the solution process.

The global convergence of the method is also, theoretically, unconditionally convergent. However in practice it is dependent on the time step (Simo and Hughes 2000). Note also that the assumption is made that the direction of the plastic strain increment is constant throughout the step. In most practical applications the structure is likely to exhibit some level of stress redistribution and thus the direction of plastic strain may change throughout the load increment. However with appropriately selected load increments the error is likely to be negligible compared to other sources of error in the finite element solution, and no bigger than the same source of error in a conventional FEA utilising plasticity models.

Convergence studies showing the number of iterations to solution, as is usually done with upper bound methods, are not presented here. This is because non-linear material models, such as the shakedown and ratchet solutions proposed here, are subject to non-linear solution controls. These solution controls may be selected to show relatively quick or slow convergence of the methods and thus do not provide a comparable assessment of the solution method.

If the global solution scheme fails to converge, the load increment must be cut back to a smaller value to try and find a stable equilibrium configuration. Cut back strategies may be chosen to be as simple or complex as the developer requires. For the development code used during this research, the cut back strategies were relatively

simple, with half the current time step being used if the iterative scheme given in steps 1-9 failed to converge. If the global Newton Raphson scheme failed, i.e. no equilibrium solution was found, the finite element program was allowed to use the default cut back strategies included with the program.

5.5 Applications

5.5.1 Implementation

The solution methods have been implemented in the commercial finite element program ABAQUS (other packages could also be suitable) using a number of the available subroutines, in particular the user subroutine UMAT. The solution procedures have been split into several subroutines which are called from UMAT to keep the code organised. The solution proceeds in a number of ABAQUS steps as discussed in Section 5.2.

5.5.2 Axi-symmetric Bree Cylinder

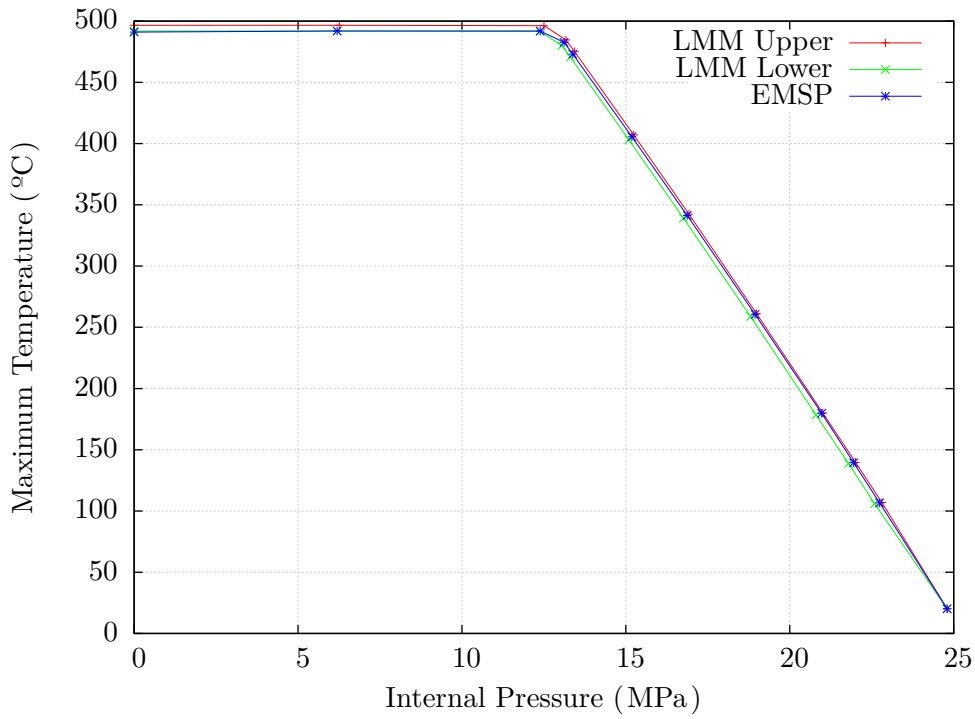

Figure 17: Bree Cylinder Elastic Shakedown Boundary by Various Methods

The EMSP method was applied to the Bree problem introduced in Section 3.5.2. The shakedown boundaries for the Bree problem given by the EMSP and the LMM are shown in figure 17. The LMM results were obtained using the method of (Ure 2013), using the same finite element mesh to allow direct comparison of the two methods. The convergence tolerance used in the LMM solution was 0.00001. The results show

that the MSP method gives good agreement with the LMM over the entire shakedown boundary. There is slightly more discrepancy at the boundary to alternating plasticity, however given that the alternating plasticity boundary is a localised stress effect it is likely that the EMSP method captures this in a more complete manner. Using the thermal stress in the cylinder at a cyclic temperature of 100°C it can be shown that the alternating plasticity boundary given by the EMSP method is in better agreement than the upper bound LMM, (see equations 40 to 42).

Cyclic stress at 100°C at maximum loaded integration point= 170.661MPa.

The total temperature at the alternating plasticity boundary may be calculated as follows:

$$\mathrm{T}+\Delta\mathrm{T} = 100 \times \frac{2 \times \sigma^{y}}{\text{elastic cyclic stress}} + 20 \tag{40}$$

thus

$$\mathrm{T}+\Delta\mathrm{T} = 100 \times \frac{2 \times 402.7}{170.661} + 20 \tag{41}$$

Therefore the total temperature at the alternating plasticity boundary is:

$$\mathrm{T}+\Delta\mathrm{T} = 100 \times 4.719 + 20 = 491.9^{\circ}\mathrm{C} \tag{42}$$

which is in better agreement with the MSP method's result of 491.12°C than the upper bound LMM result of 496.64°C.

5.5.3 Pressurised Two Bar Model

The EMSP method was applied to the pressurised two bar problem introduced in Section 3.5.3. The shakedown boundaries for the pressurised two bar problem are given for the EMSP method and the LMM in figures 18 to 20. The LMM results were obtained using (Ure 2013), using the same finite element mesh to allow direct comparison of the two methods. The convergence tolerance used in the LMM solution was 0.00001. From these results the EMSP gives excellent agreement with both the lower and upper bound LMM shakedown results. Note that the EMSP method removes the non-conservatism seen in the Hybrid Method shown in figure 11. In general the EMSP method shows significant improvement in the predicted elastic ratchet boundary (as defined in section 2.2) over the Hybrid Method and Methods 1 and 2.

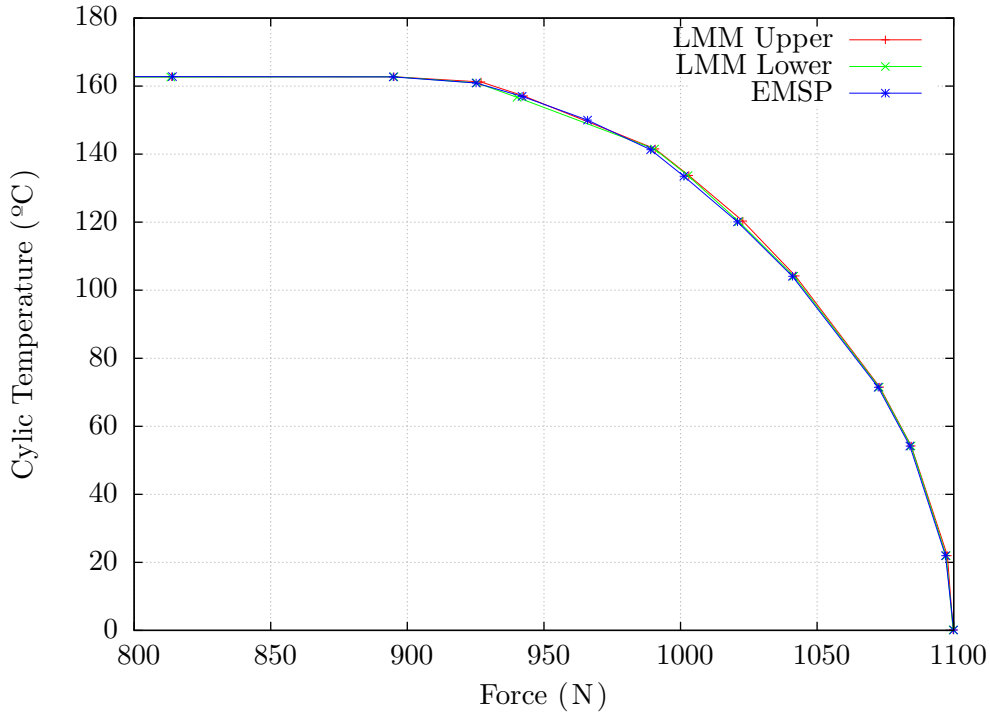

Figure 18: Pressurised Two Bar Elastic Shakedown Boundaries by Various Methods with F/P=10

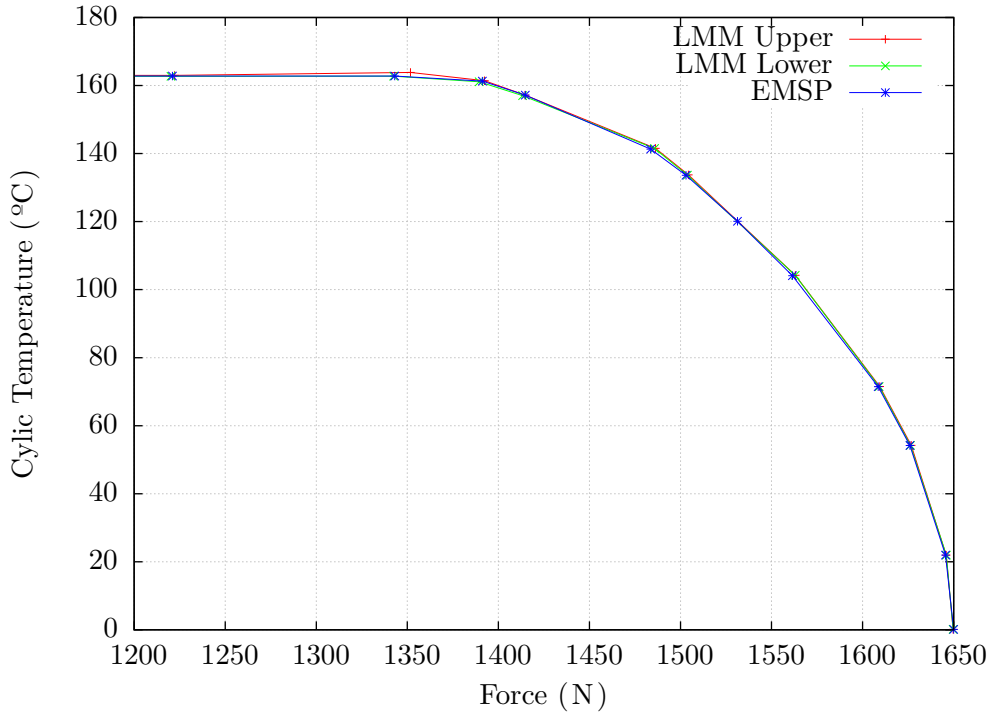

Figure 19: Pressurised Two Bar Elastic Shakedown Boundaries by Various Methods with F/P=15

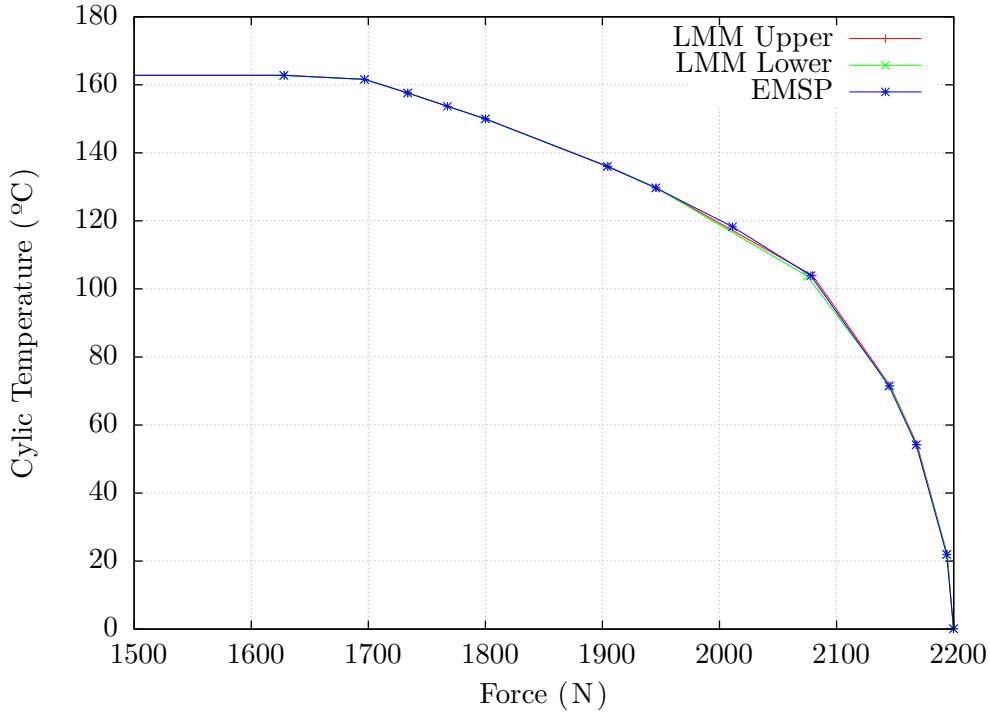

Figure 20: Pressurised Two Bar Elastic Shakedown Boundaries by Various Methods with F/P=20

5.5.4 Plate with Hole

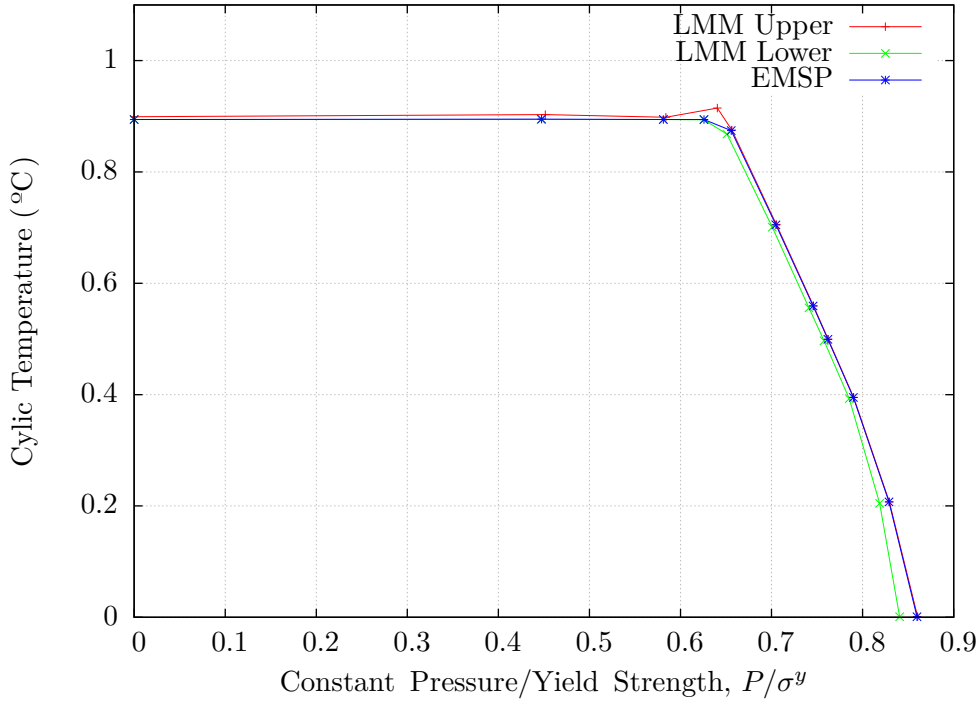

Figure 21: Plate with Hole Elastic Shakedown Boundaries by Various Methods

The EMSP method was applied to the plate with hole problem introduced in Section 3.5.4. Results from the EMSP method and the LMM are given in figure 21. The LMM results were obtained using (Ure 2013), using the same finite element mesh to allow direct comparison of the two methods. The convergence tolerance used in the LMM solution was 0.00001. From these results it can be seen that MSP gives excellent agreement with the both lower and upper bound LMM results.

5.5.5 Pipe Intersection

To demonstrate the capabilities of the method for a complex 3D component, the method is used to solve the pipe intersection model studied in (Ure et al. 2013). The problem consists of a pipe intersection joined by a dissimilar weld. A schematic of the problem is shown in figure 22. The main pipe is made from 316 stainless steel and has a diameter of 240mm, the small pipe is

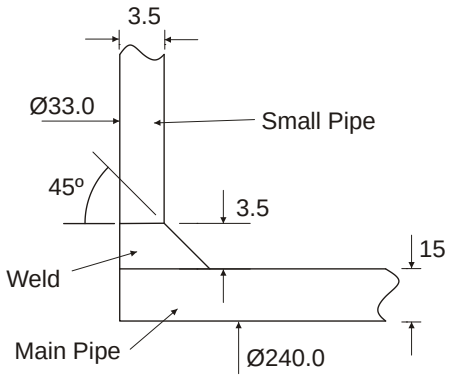

Figure 22: Pipe Intersection: Schematic

made from SA508 steel and has a diameter of 33mm. The weld is considered to have uniform material properties of inconel 82/182. All residual stresses and heat effects induced by the weld are ignored. The material properties assumed for this analysis are: 316 stainless steel, E=200000MPa, v=0.3, σ^y=220MPa and α=1.8x10^{-5}; SA508, E=200000MPa, v=0.3, σ^y =472MPa and α=1.4x10^{-5}; and inconel 82/182, E=200000MPa, v=0.3 σ^y =387.6MPa and α=1.5x10^{-5}.

The pipe intersection is subject to a constant internal pressure and cyclic temperature. The temperature is cycled from, being the reference temperature everywhere in the intersection, to the first loaded point in the load cycle with an internal temperature of 100 $^\circ$C and external temperature equal to the reference temperature, to the second loaded point in the load cycle where there is a uniform temperature of 100 $^\circ$C everywhere in the intersection. The 3D mesh used for the analysis is shown in figure 23.

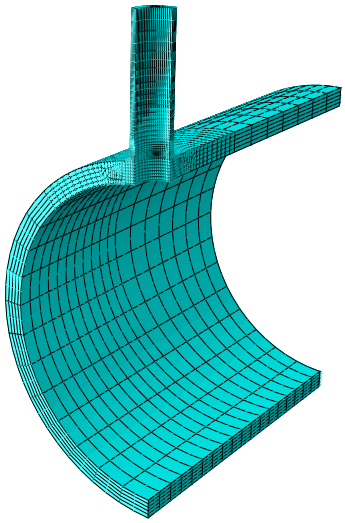

Figure 23: Pipe Intersection Mesh

Results for this problem obtained by both the EMSP and LMM are given in figure 24. The LMM results were obtained using (Ure 2013), using the same finite element mesh to allow direct comparison of the two methods. The convergence tolerance used in the LMM solution was 0.00001.

The results presented in figure 24 show that the EMSP method gives excellent agreement with the LMM. This demonstrates that the EMSP method can successfully consider more than two load points and multiple material definitions.

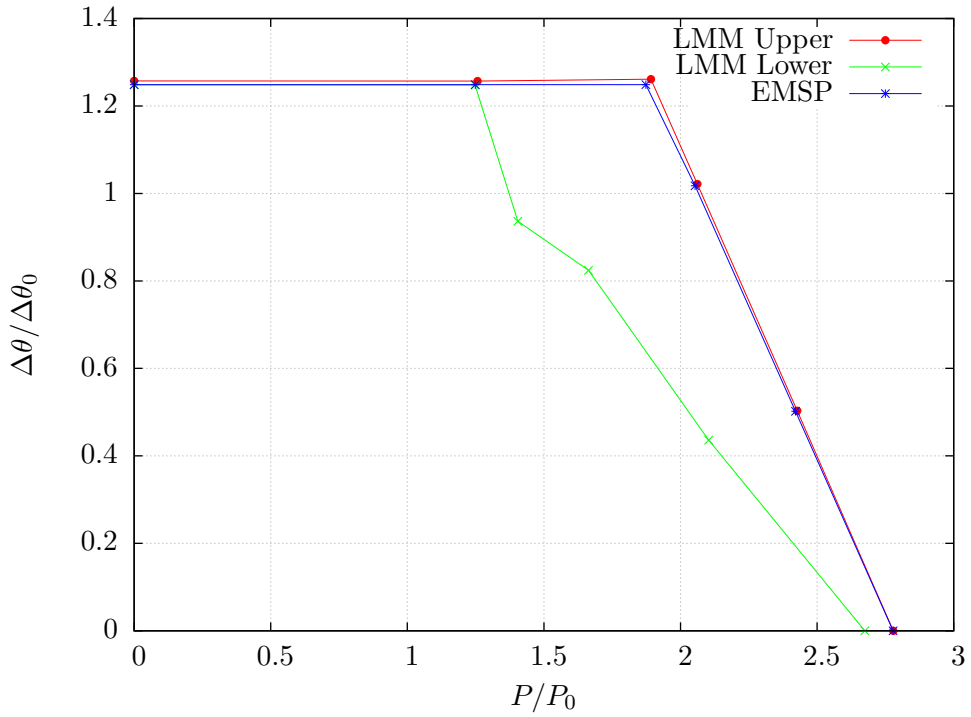

Figure 24: Pipe Intersection Elastic Shakedown Boundary by various methods

5.6 Extension of the Shakedown Method

The flexibility of this approach can be demonstrated by showing some of the possible extensions to the method that are currently difficult if not impossible to implement in other direct methods. Possible extensions include hardening and temperature dependent yield strength and simplified non-linear geometric effects. Other extensions of interest such as full non-linear geometry and/or temperature dependent material properties would require the simultaneous simulation of cyclic and constant loads along with consideration of the residual state at each deformed/temperature condition in the load cycle. This is currently not possible with the method, however it is theoretically possible to extend the method using element level formulations.

5.6.1 Temperature dependent yield

Whilst incorporating the effect of temperature dependent material properties on the residual stress, is not yet possible in current shakedown and ratchet methods, incorporation of temperature dependent yield strength is relatively simple. The temperature at a particular point on the load cycle may be passed to the material routines as a state variable. This may then be scaled as is done with any cyclic load. It

may also be set up to be adjusted by a constant temperature. The yield strength used at each cyclic point is then passed into the non-smooth multi-yield surface material model based on the temperature at that load point. This will not alter the convergence behaviour of the material model but will account for the reduction of yield strength at elevated temperatures.

Plate with Hole: Temperature Dependent Yield

The plate with hole is square with edge length L, the hole is centrally located with a radius a, such that a/L=0.1. The depth d of the plate is such that d/L= 0.005, see figure 25 for a schematic of the geometry. Symmetry is used to model only one eighth of the plate. The load case analysed is constant pressure P applied on one set of the free ends plus temperature cycled throughout the structure from to T_0 to $T(r,t)$, see equation 43, where T_0 is assumed to be 0ºC. At all times the free ends of the plate are constrained to remain plane.

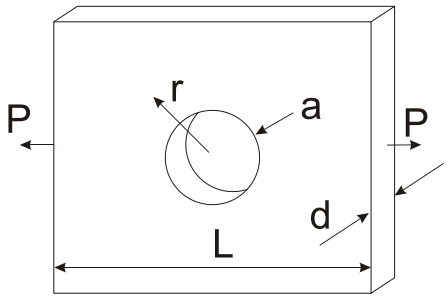

Figure 25: Plate with Hole

$$T(r,t) = T_0 + (\Delta T(t) - T)\frac{ln\left(\frac{5a}{r}\right)}{ln(5)} \tag{43}$$

The plate's elastic material properties are assumed to be temperature independent and isotropic. The elastic modulus = 208GPa, Poisson's ratio, $v = 0.3$, coefficient of thermal expansion, $\alpha = 5\text{x}10^{-5}\,^{\circ}\text{C}^{-1}$ the yield strength varies with temperature according to $\sigma^y(T) = \sigma^{y0} - 0.2 \times T$ where the units of the yield stress are MPa and $\sigma^{y0} = 360MPa$.

Results from the temperature dependent yield version of the EMSP and the LMM are given in figure 26. The LMM results were obtained using (Ure 2013), using the same finite element mesh to allow direct comparison of the two methods. The convergence tolerance used in the LMM solution was 0.0001. From the results in figure 26 it can be seen that the EMSP gives excellent agreement with the upper bound LMM results. In general the EMSP method is in better agreement with the upper bound LMM than the lower bound LMM.

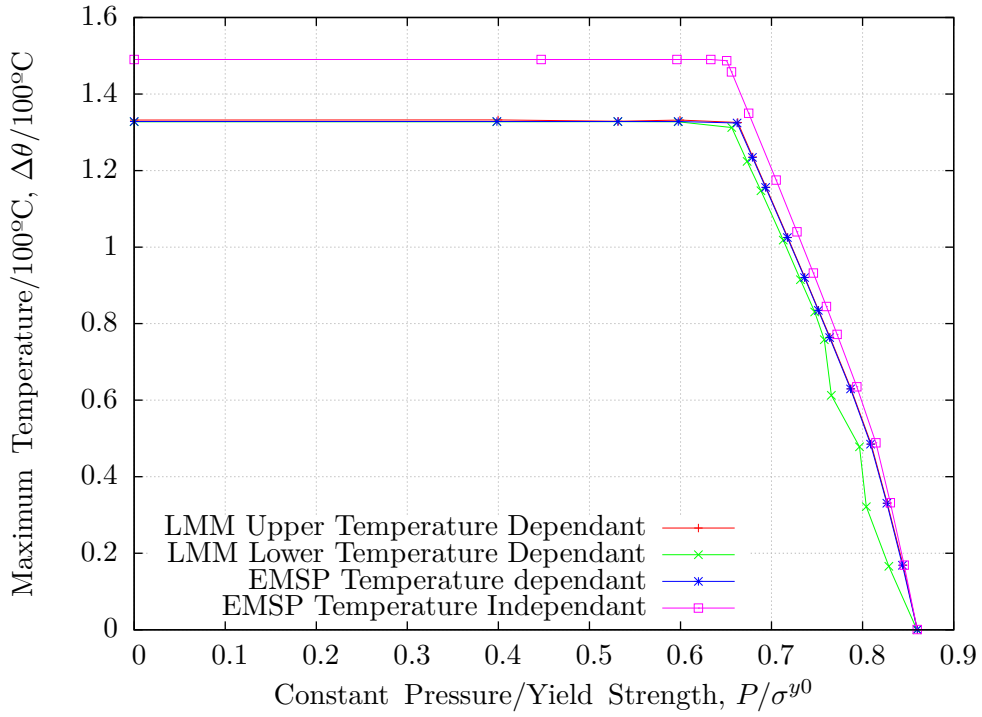

Figure 26: Plate with Hole Elastic Shakedown Boundaries by Various Methods with Temperature Dependent Yield

5.6.2 Hardening

It is possible to extend the shakedown method to incorporate hardening behaviour. When considering shakedown/ratchet it is important that the hardening behaviour saturates: i.e. the hardening modulus becomes zero at some γ. If this is not the case then the structure will never ratchet, which is an unrealistic model of the structural behaviour. Even with a hardening behavior which saturates, the simulation may allow large values of plastic strain to occur in the structure and this may not be the desired behaviour either: see (Indermohan and Reinhardt 2012). In such cases, limits can be placed on the total allowable plastic strain. The material model is extended here with attention restricted to linear and multi-linear kinematic hardening models and isotropic hardening. As the EMSP method is a lower bound method, shakedown is implied for any converged solution, therefore the same plastic strain results for all loaded points. Thus it is only necessary to consider the hardening variables at the residual condition.

The problem is assumed to be of the form:

$$\dot{\rho}_{ij} = C_{ijkq}\left(\dot{\varepsilon}^{Tr}_{kq} - \dot{\varepsilon}^{p}_{kq}\right)$$

$$\dot{\sigma}^{l}_{ij} = \dot{\rho}_{ij} + \dot{\hat{\sigma}}^{l}_{ij}$$

$$\dot{\varepsilon}^{p}_{ij} = \sum_{\alpha} \dot{\gamma}^{\alpha} \frac{\delta f^{\alpha}}{\delta \sigma^{\alpha}_{ij}}$$

$$\dot{\chi}_{ij} = -D_{ijkq} \dot{\eta}_{kq}$$

$$\dot{\eta} = \sum_{\alpha} \dot{\gamma}^{\alpha} \frac{\delta f^{\alpha}}{\delta \chi_{ij}}$$

with

$$\gamma^{\alpha} \geq 0 \quad , \quad f^{\alpha} \leq 0 \quad , \quad \gamma^{\alpha} f^{\alpha} = 0 \quad and \quad \gamma^{\alpha} \dot{f}^{\alpha} = 0$$

Integrating the model with the backward Euler scheme:

$$\rho^{n+1}_{ij} = C_{ijkq} \left(\varepsilon^{Tr,n+1}_{kq} - \varepsilon^{p,n+1}_{kq} \right)$$

$$\sigma^{l,n+1}_{ij} = \rho^{n+1}_{ij} + \widehat{\sigma}^{l,n+1}_{ij}$$

$$\varepsilon^{p,n+1}_{ij} = \varepsilon^{p,n}_{ij} + \sum_{\alpha} \Delta\gamma^{\alpha} \frac{\delta f^{\alpha,n+1}}{\delta \sigma^{\alpha,n+1}_{ij}}$$

$$\chi^{n+1}_{ij} = \chi^{n}_{ij} - D_{ijkq} \Delta\eta^{n+1}_{kq}$$

$$\Delta\eta^{n+1}_{ij} = \sum_{\alpha} \triangle\gamma^{\alpha} \frac{\delta f^{\alpha,n+1}}{\delta \chi^{n+1}_{ij}}$$

Defining the trial state as

$$\rho^{trial}_{ij} = C_{ijkq} \left(\varepsilon^{Tr,n+1}_{kq} - \varepsilon^{p,n}_{kq} \right)$$

$$\sigma^{n,trial}_{ij} = \rho^{trial}_{ij} + \widehat{\sigma}^{n,n+1}_{ij}$$

$$\varepsilon^{p,trial}_{ij} = \varepsilon^{p,n}_{ij}$$

$$\chi^{tiral}_{ij} = \chi^{n}_{ij}$$

$$\triangle\gamma^{n+1} = 0$$

$$\Delta\eta^{n+1} = 0$$

the system becomes

$$\rho_{ij}^{n+1} = \rho_{ij}^{trial} - 2\mu \sum_{\alpha} \Delta\gamma^{\alpha} \frac{\delta f^{\alpha,n+1}}{\delta \sigma_{ij}^{\alpha,n+1}} \tag{44}$$

$$\sigma_{ij}^{\alpha,n+1} = \sigma_{ij}^{\alpha,trial} - 2\mu \sum_{\alpha} \Delta\gamma^{\alpha} \frac{\delta f^{\alpha,n+1}}{\delta \sigma_{ij}^{\alpha,n+1}}$$

$$\varepsilon_{ij}^{p,n+1} = \varepsilon_{ij}^{p,n} + \sum_{\alpha} \Delta\gamma^{\alpha} \frac{\delta f^{\alpha,n+1}}{\delta \sigma_{ij}^{\alpha,n+1}}$$

$$\chi_{ij}^{n+1} = \chi_{ij}^{n} - D_{ijkq} \Delta\eta_{kq}^{n+1}$$

$$\Delta\eta_{kq}^{n+1} = \sum_{\alpha} \triangle\gamma^{\alpha} \frac{\delta f^{\alpha,n+1}}{\delta \chi_{ij}^{n+1}}$$

What remains is to define a method for calculating $\Delta\gamma^{\alpha}$.

Consider the change in strain energy that results on plastic straining of the structure:

$$\Gamma = \frac{1}{2}\left(\rho_{ij}^{trial} - \rho_{ij}\right) C_{ijkq} \left(\rho_{kq}^{trial} - \rho_{kq}\right) + \frac{1}{2}\left(\chi_{ij}^{n} - \chi_{ij}\right) D_{ijkq} \left(\chi_{kq}^{n} - \chi_{kq}\right)$$

The change in energy of the structure should be minimised to give the equilibrium condition. Thus:

$$\left(\rho_{ij}^{n+1}\,,\, \chi_{ij}^{n+1}\right) = ARG \left\{ \underset{(\tau_{kq}\,,\, \chi_{kq})}{Min} \left[\Gamma\left(\tau_{kq}\,,\, \chi_{kq}\right)\right] \right\}$$

The Lagrangian for the system is:

$$\mathcal{L} = \frac{1}{2}\left(\rho_{ij}^{trial} - \rho_{ij}\right) C_{ijkq} \left(\rho_{kq}^{trial} - \rho_{kq}\right) + \frac{1}{2}\left(\chi_{ij}^{n} - \chi_{ij}\right) D_{ijkq} \left(\chi_{kq}^{n} - \chi_{kq}\right) + \sum_{\alpha} \Delta\gamma^{\alpha} f^{\alpha}$$

The plastic consistency parameters $\Delta\gamma$ may then be found by utilising Newton's

method. The residuals are defined as:

$$\delta_{\rho_{ij}}\mathcal{L} = -C^{-1}_{ijkq}\left(\rho^{trial}_{kq} - \rho_{kq}\right) + \sum_{\alpha}\Delta\gamma^{\alpha}\frac{\delta f^{\alpha}}{\delta\sigma^{\alpha}_{ij}} = -\varepsilon^{p}_{ij} + \varepsilon^{p,n}_{ij} + \sum_{\alpha}\Delta\gamma^{\alpha}\frac{\delta f^{\alpha}}{\delta\sigma^{\alpha}_{ij}}$$

$$\delta_{\chi_{ij}}\mathcal{L} = -D^{-1}_{ijkq}\left(\chi^{n}_{kq} - \chi_{kq}\right) + \sum_{\alpha}\Delta\gamma^{\alpha}\frac{\delta f^{\alpha}}{\delta\chi_{ij}} = -\chi_{ij} + \chi^{n}_{ij} + \sum_{\alpha}\Delta\gamma^{\alpha}\frac{\delta f^{\alpha}}{\delta\chi_{ij}}$$

$$\delta_{\gamma^{\alpha}}\mathcal{L} = f^{\alpha}$$

The increment in the solution variables are then given by:

$$\begin{bmatrix} \delta_{\rho_{kq}}\left(\delta_{\rho_{ij}}\mathcal{L}\right) & \delta_{\chi_{kq}}\left(\delta_{\rho_{ij}}\mathcal{L}\right) & \delta_{\gamma^{\alpha}}\left(\delta_{\rho_{ij}}\mathcal{L}\right) \\ \delta_{\rho_{kq}}\left(\delta_{\chi_{ij}}\mathcal{L}\right) & \delta_{\chi_{kq}}\left(\delta_{\chi_{ij}}\mathcal{L}\right) & \delta_{\gamma^{\alpha}}\left(\delta_{\chi_{ij}}\mathcal{L}\right) \\ \delta_{\rho_{kq}}\left(\delta_{\gamma^{\theta}}\mathcal{L}\right) & \delta_{\chi_{kq}}\left(\delta_{\gamma^{\theta}}\mathcal{L}\right) & \delta_{\gamma^{\alpha}}\left(\delta_{\gamma^{\theta}}\mathcal{L}\right) \end{bmatrix} \begin{Bmatrix} \Delta\rho_{kq} \\ \Delta\chi_{kq} \\ \Delta^{2}\gamma^{\alpha} \end{Bmatrix} = - \begin{Bmatrix} \delta_{\rho_{ij}}\mathcal{L} \\ \delta_{\chi_{ij}}\mathcal{L} \\ \delta_{\gamma^{\alpha}}\mathcal{L} \end{Bmatrix} \tag{45}$$

where θ , $\phi \in \mathscr{R}_{act}$ and the Hessian matrix is defined as:

$$\mathscr{H} = \begin{bmatrix} \delta_{\rho_{kq}}\left(\delta_{\rho_{ij}}\mathcal{L}\right) & \delta_{\chi_{kq}}\left(\delta_{\rho_{ij}}\mathcal{L}\right) & \delta_{\gamma^{\phi}}\left(\delta_{\rho_{ij}}\mathcal{L}\right) \\ \delta_{\rho_{kq}}\left(\delta_{\chi_{ij}}\mathcal{L}\right) & \delta_{\chi_{kq}}\left(\delta_{\chi_{ij}}\mathcal{L}\right) & \delta_{\gamma^{\phi}}\left(\delta_{\chi_{ij}}\mathcal{L}\right) \\ \delta_{\rho_{kq}}\left(\delta_{\gamma^{\theta}}\mathcal{L}\right) & \delta_{\chi_{kq}}\left(\delta_{\gamma^{\theta}}\mathcal{L}\right) & \delta_{\gamma^{\phi}}\left(\delta_{\gamma^{\theta}}\mathcal{L}\right) \end{bmatrix}$$

Thus

$$\begin{Bmatrix} \Delta\rho_{ij} \\ \Delta\chi_{ij} \\ \Delta^{2}\gamma^{\theta} \end{Bmatrix} = -\mathscr{H}^{-1} \begin{Bmatrix} \delta_{\rho_{kq}}\mathcal{L} \\ \delta_{\chi_{kq}}\mathcal{L} \\ \delta_{\gamma^{\phi}}\mathcal{L} \end{Bmatrix}$$

However $\delta_{\gamma^{\phi}}\left(\delta_{\gamma^{\alpha}}\mathcal{L}\right) = 0$ for all ϕ and α thus the Hessian becomes difficult to invert numerically.

The system in equation 45 is therefore rearranged:

$$\begin{bmatrix} \delta_{\rho_{kq}}\left(\delta_{\rho_{ij}}\mathcal{L}\right) & \delta_{\chi_{kq}}\left(\delta_{\rho_{ij}}\mathcal{L}\right) \\ \delta_{\rho_{kq}}\left(\delta_{\chi_{ij}}\mathcal{L}\right) & \delta_{\chi_{kq}}\left(\delta_{\chi_{ij}}\mathcal{L}\right) \end{bmatrix} \begin{Bmatrix} \Delta\rho_{kq} \\ \Delta\chi_{kq} \end{Bmatrix} + \begin{Bmatrix} \delta_{\gamma^{\phi}}\left(\delta_{\rho_{ij}}\mathcal{L}\right) \\ \delta_{\gamma^{\phi}}\left(\delta_{\chi_{ij}}\mathcal{L}\right) \end{Bmatrix} \left\{\Delta^{2}\gamma^{\phi}\right\} = - \begin{Bmatrix} \delta_{\rho_{ij}}\mathcal{L} \\ \delta_{\chi_{ij}}\mathcal{L} \end{Bmatrix} \tag{46}$$

giving

$$\left\{ \begin{array}{c} \Delta\rho_{kq} \\ \Delta\chi_{kq} \end{array} \right\} = - \left[\begin{array}{cc} \delta_{\rho_{kq}}\left(\delta_{\rho_{ij}}\mathcal{L}\right) & \delta_{\chi_{kq}}\left(\delta_{\rho_{ij}}\mathcal{L}\right) \\ \delta_{\rho_{kq}}\left(\delta_{\chi_{ij}}\mathcal{L}\right) & \delta_{\chi_{kq}}\left(\delta_{\chi_{ij}}\mathcal{L}\right) \end{array} \right]^{-1} \left\{ \begin{array}{c} \delta_{\gamma^\phi}\left(\delta_{\rho_{ij}}\mathcal{L}\right) \\ \delta_{\gamma^\phi}\left(\delta_{\chi_{ij}}\mathcal{L}\right) \end{array} \right\} \left\{\Delta^2\gamma^\phi\right\} - \left[\begin{array}{cc} \delta_{\rho_{kq}}\left(\delta_{\rho_{ij}}\mathcal{L}\right) & \delta_{\chi_{kq}}\left(\delta_{\rho_{ij}}\mathcal{L}\right) \\ \delta_{\rho_{kq}}\left(\delta_{\chi_{ij}}\mathcal{L}\right) & \delta_{\chi_{kq}}\left(\delta_{\chi_{ij}}\mathcal{L}\right) \end{array} \right]^{-1} \left\{ \begin{array}{c} \delta_{\rho_{ij}}\mathcal{L} \\ \delta_{\chi_{ij}}\mathcal{L} \end{array} \right\} \tag{47}$$

Also from equation 45

$$\left\{ \begin{array}{cc} \delta_{\rho_{kq}}\left(\delta_{\gamma^\alpha}\mathcal{L}\right) & \delta_{\chi_{kq}}\left(\delta_{\gamma^\alpha}\mathcal{L}\right) \end{array} \right\} \left\{ \begin{array}{c} \Delta\rho_{kq} \\ \Delta\chi_{kq} \end{array} \right\} = - \left\{\delta_{\gamma^\alpha}\mathcal{L}\right\}$$

giving:

$$[G]_{\alpha\phi}\left\{\Delta^2\gamma^\phi\right\} = \left\{\delta_{\gamma^\alpha}\mathcal{L}\right\} -$$

$$\left\{ \begin{array}{cc} \delta_{\rho_{kq}}\left(\delta_{\gamma^\alpha}\mathcal{L}\right) & \delta_{\chi_{kq}}\left(\delta_{\gamma^\alpha}\mathcal{L}\right) \end{array} \right\} \left[\begin{array}{cc} \delta_{\rho_{kq}}\left(\delta_{\rho_{ij}}\mathcal{L}\right) & \delta_{\chi_{kq}}\left(\delta_{\rho_{ij}}\mathcal{L}\right) \\ \delta_{\rho_{kq}}\left(\delta_{\chi_{ij}}\mathcal{L}\right) & \delta_{\chi_{kq}}\left(\delta_{\chi_{ij}}\mathcal{L}\right) \end{array} \right]^{-1} \left\{ \begin{array}{c} \delta_{\rho_{ij}}\mathcal{L} \\ \delta_{\chi_{ij}}\mathcal{L} \end{array} \right\}$$

Rearranging

$$\left\{\Delta^2\gamma^\phi\right\} = [A]_{\phi\alpha}\left\{\left\{\delta_{\gamma^\alpha}\mathcal{L}\right\} -\right.$$

$$\left.\left\{ \begin{array}{cc} \delta_{\rho_{kq}}\left(\delta_{\gamma^\alpha}\mathcal{L}\right) & \delta_{\chi_{kq}}\left(\delta_{\gamma^\alpha}\mathcal{L}\right) \end{array} \right\} \left[\begin{array}{cc} \delta_{\rho_{kq}}\left(\delta_{\rho_{ij}}\mathcal{L}\right) & \delta_{\chi_{kq}}\left(\delta_{\rho_{ij}}\mathcal{L}\right) \\ \delta_{\rho_{kq}}\left(\delta_{\chi_{ij}}\mathcal{L}\right) & \delta_{\chi_{kq}}\left(\delta_{\chi_{ij}}\mathcal{L}\right) \end{array} \right]^{-1} \left\{ \begin{array}{c} \delta_{\rho_{ij}}\mathcal{L} \\ \delta_{\chi_{ij}}\mathcal{L} \end{array} \right\}\right\} \tag{48}$$

where:

$$[G]_{\alpha\phi} = \left[\left\{ \begin{array}{cc} \delta_{\rho_{kq}}\left(\delta_{\gamma^\alpha}\mathcal{L}\right) & \delta_{\chi_{kq}}\left(\delta_{\gamma^\alpha}\mathcal{L}\right) \end{array} \right\} \left[\begin{array}{cc} \delta_{\rho_{kq}}\left(\delta_{\rho_{ij}}\mathcal{L}\right) & \delta_{\chi_{kq}}\left(\delta_{\rho_{ij}}\mathcal{L}\right) \\ \delta_{\rho_{kq}}\left(\delta_{\chi_{ij}}\mathcal{L}\right) & \delta_{\chi_{kq}}\left(\delta_{\chi_{ij}}\mathcal{L}\right) \end{array} \right]^{-1} \left\{ \begin{array}{c} \delta_{\gamma^\phi\rho_{ij}}\mathcal{L} \\ \delta_{\gamma^\phi\chi_{ij}}\mathcal{L} \end{array} \right\} \right]$$

and

$$[A] = [G]^{-1}$$

Knowing $\Delta^2\gamma^\phi$ allows the calculation of $\Delta\varepsilon^p_{kq}$ and $\Delta\eta_{kq}$:

$$\left\{ \begin{array}{c} \Delta\varepsilon^{p}_{kq} \\ \Delta\eta_{kq} \end{array} \right\} = \left[\begin{array}{cc} C^{-1}_{kqij} & 0 \\ 0 & D^{-1}_{kqij} \end{array} \right] \left[\begin{array}{cc} \delta_{\rho_{kq}}\left(\delta_{\rho_{ij}}\mathcal{L}\right) & \delta_{\chi_{kq}}\left(\delta_{\rho_{ij}}\mathcal{L}\right) \\ \delta_{\rho_{kq}}\left(\delta_{\chi_{ij}}\mathcal{L}\right) & \delta_{\chi_{kq}}\left(\delta_{\chi_{ij}}\mathcal{L}\right) \end{array} \right]^{-1}$$

$$\left\{ \left\{ \begin{array}{c} \delta_{\rho_{ij}}\mathcal{L} \\ \delta_{\chi_{ij}}\mathcal{L} \end{array} \right\} + \left\{\Delta^2\gamma^{\phi}\right\} \left\{ \begin{array}{c} \delta_{\gamma^{\phi}}\left(\delta_{\rho_{ij}}\mathcal{L}\right) \\ \delta_{\gamma^{\phi}}\left(\delta_{\chi_{ij}}\mathcal{L}\right) \end{array} \right\} \right\}$$

Attention is now limited to Mises plasticity in which $\frac{\delta f^{\alpha}}{\delta\chi_{ij}} = -\frac{\delta f^{\alpha}}{\delta\sigma^{\alpha}_{ij}}$

The iterative solution procedure can then be defined:

1. Compute the trial elastic quantities

$$\rho^{trial}_{ij} = C_{ijkq}\left(\varepsilon^{Tr,n+1}_{kq} - \varepsilon^{p,n}_{kq}\right)$$

$$f^{l} = \left|\rho_{ij} + Y\widehat{\sigma}^{l}_{ij} - \chi_{ij}\right| - \sigma^{y} =$$

$$\sqrt{\tfrac{3}{2}\left(\rho'_{ij} + Y\widehat{\sigma}'^{l}_{ij} - \chi_{ij}\right)\left(\rho'_{ij} + Y\widehat{\sigma}'^{l}_{ij} - \chi_{ij}\right)} - \sigma^{y} \;\text{ for}\, l = 1, 2..m$$

2. Check yield conditions

IF $\left|\rho^{trial}_{ij} + Y\widehat{\sigma}^{l}_{ij} - \chi^{n}_{ij}\right| - \sigma^{y} \leq 0$ for $l = 1, 2..m$ THEN

$$\rho^{n+1}_{ij} = \rho^{trial}_{ij}$$

$$\varepsilon^{p,n+1}_{ij} = \varepsilon^{p,n}_{ij}$$

ELSE (system is plastic):

$$\zeta = 0$$

$$Q^{\zeta}_{act} = \left\{\alpha \subset l \,\text{where}\, \left|\rho^{trial}_{ij} + Y\widehat{\sigma}^{n,trial}_{ij} - \chi^{n}_{ij}\right| - \sigma^{y} > 0\right\}$$

$$\rho^{n+1,\zeta}_{ij} = \rho^{trial}_{ij}$$

$$\varepsilon^{p,n+1,\zeta}_{ij} = \varepsilon^{p,n}_{ij}$$

$$\triangle\gamma^{n,\zeta} = 0$$

goto 4

ENDIF

3. RETURN Values back to Solver

4. Evaluate Residuals

$$\rho_{ij}^{n+1,\zeta} = C_{ijkq}\left(\varepsilon_{kq}^{T,n+1} - \varepsilon_{kq}^{p,\zeta}\right)$$

$$R_{ij}^{\zeta} = \left\{ \begin{array}{c} -\varepsilon_{ij}^{p,\zeta} + \varepsilon_{ij}^{p,n} + \sum_{\alpha} \triangle\gamma^{\alpha,\zeta} r_{ij}^{\alpha,\zeta} \\ -\eta_{ij}^{\zeta} + \eta_{ij}^{n} - \sum_{\alpha} \triangle\gamma^{\alpha,\zeta} r_{ij}^{\alpha,\zeta} \end{array} \right\}$$

$$r_{ij}^{l,\zeta} = \frac{3}{2} \frac{\rho_{ij}^{\prime\zeta} + Y\widehat{\sigma}_{ij}^{\prime l,\zeta}}{\left|\rho_{kq}^{\zeta} + Y\widehat{\sigma}_{kq}^{l,\zeta}\right|}$$

$$\alpha \in Q_{act}^{\zeta} \text{ and } \beta \in Q_{act}^{\zeta}$$

5. Check Convergence

$$f^{l,\zeta} = \sqrt{\frac{3}{2}\left(\rho_{ij}^{\prime} + Y\widehat{\sigma}_{ij}^{\prime l} - \chi_{ij}\right)\left(\rho_{ij}^{\prime} + Y\widehat{\sigma}_{ij}^{\prime l} - \chi_{ij}\right)} - \sigma^{y} \text{ for } l = 1, 2..m$$

IF $f^{l,\zeta} \leq \mathrm{TOL}_1$, for $l = 1, 2..m$ and $\left\|f^{\alpha,\zeta}\right\| < \mathrm{TOL}_1$

Solution Converged

$$\rho_{ij}^{n+1} = \rho_{ij}^{k}$$

$$\varepsilon_{ij}^{p,n+1} = \varepsilon_{ij}^{p,k}$$

RETURN values to solver

ELSE

Continue

ENDIF

6. Compute Elastic and Tangent Moduli

$$[g]_{\alpha\beta}^{\zeta} = \left\{ \begin{array}{cc} r_{ij}^{\alpha,\zeta} & -r_{ij}^{\alpha,\zeta} \end{array} \right\} \left[A^{\zeta}\right]_{\alpha\beta} \left\{ \begin{array}{c} r_{kq}^{\beta,\zeta} \\ -r_{kq}^{\beta,\zeta} \end{array} \right\}$$

$$[G]^{\zeta} = \left[g^{\zeta}\right]^{-1}$$

$$\left[A_{ijkq}^{\zeta}\right]^{-1} = \left[\begin{array}{cc} C_{ijkq}^{-1} & 0 \\ 0 & D_{ijkq}^{-1} \end{array} \right] + \sum_{\alpha} \triangle\gamma^{\alpha} \left[\begin{array}{cc} \frac{\delta r_{ij}^{\alpha,\zeta}}{\delta\left(\rho_{kq}^{k} + X\widehat{\sigma}_{kq}^{\alpha}\right)} & \frac{\delta r_{ij}^{\alpha,\zeta}}{\delta\left(\chi_{kq}\right)} \\ \frac{-\delta r_{ij}^{\alpha,\zeta}}{\delta\left(\rho_{kq}^{k} + X\widehat{\sigma}_{kq}^{\alpha}\right)} & \frac{-\delta r_{ij}^{\alpha,\zeta}}{\delta\left(\chi_{kq}\right)} \end{array} \right]$$

7. Calculate the increment to the plastic consistency parameters

$$\triangle^{2}\gamma^{\alpha,\zeta} = \sum_{\beta} [G]_{\alpha\beta}^{\zeta}\left(f^{\beta,\zeta} - r_{ij}^{\beta,\zeta} A_{ijkq}^{\zeta} R_{kq}^{\zeta}\right)$$

$$\triangle\bar{\gamma}^{\alpha,\zeta+1} = \triangle\gamma^{\alpha,\zeta} + \triangle^2\gamma^{\alpha,\zeta}$$

IF $\triangle\gamma^{\alpha,\zeta+1} < 0$

Remove α from Q_{act}

Goto 4

ENDIF

8. Calculate Increment to plastic strains

$$\left\{ \begin{array}{c} \triangle\varepsilon_{ij}^{p,\zeta+1} \\ \triangle\eta_{ij}^{k+1} \end{array} \right\} = \left[\begin{array}{cc} C_{ijkq}^{-1} & 0 \\ 0 & D_{ijkq}^{-1} \end{array} \right] \left[A_{kqop}^{\zeta}\right] \left(R_{op} + \sum \triangle^2\gamma^{\beta,\zeta} \left\{ \begin{array}{c} r_{op}^{\beta,\zeta} \\ -r_{op}^{\beta,\zeta} \end{array} \right\} \right)$$

9. Update iterative quantities

$$\triangle\gamma^{\alpha,\zeta+1} = \triangle\gamma^{\alpha,\zeta} + \triangle^2\gamma^{\alpha,\zeta}$$

$$\varepsilon_{ij}^{p,n+1} = \varepsilon_{ij}^{p,n} + \triangle\varepsilon_{ij}^{p,\zeta+1}$$

$$\eta_{ij}^{p,n+1} = \eta_{ij}^{p,n} + \triangle\eta_{ij}^{p,\zeta+1}$$

$$\text{set } \zeta = \zeta + 1$$

Goto 3

An approximate form of the consistent tangent modulus can be defined as follows, by ignoring the coupling between the residual stress and the back stress.

Differentiating the algorithmic form of the stress update (equation 44):

$$d\rho_{ij}^{n+1} = C_{ijkq} \left(d\varepsilon_{kq}^{Tr} - \sum_{\alpha} d\Delta\gamma^{\alpha} \frac{\delta f^{\alpha,n+1}}{\delta\sigma_{kq}^{\alpha,n+1}} - \sum_{\alpha} \Delta\gamma^{\alpha} \frac{\delta\left(\frac{\delta f^{\alpha,n+1}}{\delta\sigma_{kq}^{\alpha,n+1^2}}\right)}{\delta\sigma_{ij}^{\alpha,n+1}} d\sigma_{ij}^{\alpha,n+1} \right) \tag{49}$$

$$\left(C_{ijkq}^{-1} + \sum_{\alpha} \Delta\gamma^{\alpha} \frac{\delta\left(\frac{\delta f^{\alpha,n+1}}{\delta\sigma_{kq}^{\alpha,n+1^2}}\right)}{\delta\sigma_{ij}^{\alpha,n+1}} \right) d\rho_{ij}^{n+1} = d\varepsilon_{ij}^{Tr} - \sum_{\alpha} d\Delta\gamma^{\alpha} \frac{\delta f^{\alpha,n+1}}{\delta\sigma_{ij}^{\alpha,n+1}}$$

$$d\rho_{ij}^{n+1} = \left(C_{ijkq}^{-1} + \sum_{\alpha} \Delta\gamma^{\alpha} \frac{\delta\left(\frac{\delta f^{\alpha,n+1}}{\delta\sigma_{kq}^{\alpha,n+1^2}}\right)}{\delta\sigma_{ij}^{\alpha,n+1}} \right)^{-1} \left(d\varepsilon_{kq}^{Tr} - \sum_{\alpha} d\Delta\gamma^{\alpha} \frac{\delta f^{\alpha,n+1}}{\delta\sigma_{kq}^{\alpha,n+1}} \right) \tag{50}$$

let

$$\left(C_{ijkq}^{-1} + \sum_{\alpha} \Delta\gamma^{\alpha} \frac{\delta\left(\frac{\delta f^{\alpha,n+1}}{\delta \sigma_{kq}^{\alpha,n+1^2}}\right)}{\delta \sigma_{ij}^{\alpha,n+1}} \right)^{-1} = \Xi_{ijkq}^{n+1}$$

Differentiating the backstress update algorithm:

$$d\chi_{ij}^{n+1} = d\chi_{ij}^{n} - D_{ijkq} \left(\sum_{\alpha} d\Delta\gamma^{\alpha} \frac{\delta f^{\alpha,n+1}}{\delta \chi_{kq}^{\alpha+1}} + \sum_{\alpha} \Delta\gamma^{\alpha} \frac{\delta\left(\frac{\delta f^{\alpha,n+1}}{\delta \chi_{kq}^{n+1}}\right)}{\delta \chi_{ij}^{n+1}} d\chi_{ij}^{n+1} \right) \tag{51}$$

with $d\chi_{ij}^{n} = 0$

$$d\chi_{ij}^{n+1} = \left(D_{ijkq}^{-1} + \sum_{\alpha} \Delta\gamma^{\alpha} \frac{\delta\left(\frac{\delta f^{\alpha,n+1}}{\delta \chi_{kq}^{n+1}}\right)}{\delta \chi_{ij}^{n+1}} \right)^{-1} \left(- \sum_{\alpha} d\Delta\gamma^{\alpha} \frac{\delta f^{\alpha,n+1}}{\delta \chi_{kq}^{n+1}} \right) \tag{52}$$

let

$$\left(D_{ijkq}^{-1} + \sum_{\alpha} \Delta\gamma^{\alpha} \frac{\delta\left(\frac{\delta f^{\alpha,n+1}}{\delta \chi_{kq}^{n+1}}\right)}{\delta \chi_{ij}^{n+1}} \right)^{-1} = \varphi_{ijkq}^{n+1}$$

Differentiating the algorithmic form of the consistency condition i.e.

$$\frac{\delta\left(f^{\beta}\right)}{\delta \sigma_{ij}^{\beta,n+1}} + \frac{\delta\left(f^{\beta}\right)}{\delta \chi_{ij}^{n+1}} = 0$$

gives:

$$\frac{\delta f^{\beta,n+1}}{\delta \sigma_{ij}^{\beta,n+1}} d\sigma_{ij}^{\beta,n+1} + \frac{\delta f^{\beta,n+1}}{\delta \chi_{ij}^{n+1}} d\chi_{ij}^{n+1} = 0 \tag{53}$$

with $X\widehat{\sigma}_{ij}^{\prime\alpha}$ being constant over the step

$$d\sigma_{ij}^{\alpha,n+1} = \delta\rho_{ij}^{n+1}$$

Substituting equations 50 and 52 into 53:

$$\frac{\delta f^{\beta,n+1}}{\delta \sigma_{ij}^{\beta,n+1}} \Xi_{ijkq}^{n+1} \left(d\varepsilon_{kq}^{Tr} - \sum_{\alpha} d\Delta\gamma^{\alpha} \frac{\delta f^{\alpha,n+1}}{\delta \sigma_{kq}^{\alpha,n+1}} \right) + \frac{\delta f^{\beta,n+1}}{\delta \chi_{ij}} \varphi_{ijkq}^{n+1} \left(- \sum_{\alpha} d\Delta\gamma^{\alpha} \frac{\delta f^{\alpha,n+1}}{\delta \chi_{kq}^{n+1}} \right) = 0$$

giving

$$\frac{\delta f^{\beta,n+1}}{\delta \sigma_{ij}^{\beta,n+1}} \Xi_{ijkq}^{n+1} \left(\sum_{\alpha} d\Delta\gamma^{\alpha} \frac{\delta f^{\alpha,n+1}}{\delta \sigma_{kq}^{\alpha,n+1}} \right) + \frac{\delta f^{\beta,n+1}}{\delta \chi_{ij}} \varphi_{ijkq}^{n+1} \left(\sum_{\alpha} d\Delta\gamma^{\alpha} \frac{\delta f^{\alpha,n+1}}{\delta \chi_{kq}^{\alpha+1}} \right) = \frac{\delta f^{\beta,n+1}}{\delta \sigma_{ij}^{\beta,n+1}} \Xi_{ijkq}^{n+1} d\varepsilon_{kq}^{Tr}$$

This gives

$$[g] \left\{ d\triangle\gamma^{n} \right\} = \left\{ \frac{\delta f^{\beta,n+1}}{\delta \sigma_{ij}^{\beta,n+1}} \Xi_{ijkq}^{n+1} \right\} d\varepsilon_{kq}^{Tr}$$

where

$$[g]_{\alpha\beta} = \frac{\delta f^{\beta,n+1}}{\delta \sigma_{ij}^{\beta,n+1}} \Xi_{ijkq}^{n+1} d\Delta\gamma^{n} \frac{\delta f^{\alpha,n+1}}{\delta \sigma_{kq}^{\alpha,n+1}} + \frac{\delta f^{\beta,n+1}}{\delta \chi_{ij}^{n+1}} \varphi_{ijkq}^{n+1} \frac{\delta f^{\alpha,n+1}}{\delta \chi_{kq}^{n+1}}$$

Thus

$$\left\{ d\triangle\gamma^{n} \right\} = [G] \left\{ \frac{\delta f^{\beta,n+1}}{\delta \sigma_{ij}^{\beta,n+1}} \Xi_{ijkq}^{n+1} \right\} d\varepsilon_{kq}^{T}$$

giving

$$d\triangle\gamma^{\alpha} = \sum_{\beta} [G]_{\alpha\beta} \frac{\delta f^{\beta,n+1}}{\delta \sigma_{ij}^{\beta,n+1}} \Xi_{ijkq}^{n+1} d\varepsilon_{kq}^{Tr} \tag{54}$$

where

$$[G] = [g]^{-1}$$

Substituting 54 into 50

$$d\rho_{ij}^{n+1} = \Xi_{ijkq}^{n+1} \left(d\varepsilon_{kq}^{Tr} - \sum_{\alpha} \sum_{\beta} [G]_{\alpha\beta} \frac{\delta f^{\beta,n+1}}{\delta \sigma_{ij}^{\beta,n+1}} \Xi_{ijkq}^{n+1} d\varepsilon_{kq}^{Tr} \frac{\delta f^{\alpha,n+1}}{\delta \sigma_{kq}^{\alpha,n+1}} \right)$$

thus

$$\frac{d\rho_{ij}^{n+1}}{d\varepsilon_{kq}^{Tr}} = \Xi_{ijkq}^{n+1} \left(1 - \sum_{\alpha} \sum_{\beta} [G]_{\alpha\beta} \frac{\delta f^{\beta,n+1}}{\delta \sigma_{ij}^{\beta,n+1}} \Xi_{ijkq}^{n+1} \frac{\delta f^{\alpha,n+1}}{\delta \sigma_{kq}^{\alpha,n+1}} \right)$$

Rearranged gives:

$$\frac{d\rho_{ij}^{n+1}}{d\varepsilon_{kq}^{Tr}} = \Xi_{ijkq}^{n+1} - \sum_{\alpha}^{\alpha} \sum_{\beta} [G]_{\alpha\beta} \left\{ \varpi_{kl}^{\beta} \right\} \varpi_{ij}^{\alpha} \tag{55}$$

where

$$\varpi_{ij}^{\alpha} = \Xi_{ijkq}^{n+1} \frac{\delta f^{\alpha,n+1}}{\delta \sigma_{kq}^{\alpha,n+1}}$$

and

$$\varpi_{kq}^{\beta} = \frac{\delta f^{\beta,n+1}}{\delta \sigma_{ij}^{\beta,n+1}} \Xi_{ijkq}^{n+1}$$

Example

The hardening model was implemented in ABAQUS using the user subroutine UMAT (other FEA packages could also be suitable). The example problem chosen was the plate with uniform cyclic temperature and pressure studied in (Heitzer et al. 2000). The geometry consists of a square plate fixed in the vertical direction on the top and bottom edges. The load cycle is defined by a surface traction P and uniform cyclic temperature T. The loads are assumed to vary both in and out of phase resulting in a four point load cycle which may be expressed in pressure temperature space as $(0,0)$, $(0,T)$, (P,T) and $(P,0)$. The thermal loads are assumed to be applied slowly enough that they may be considered quasi-static. The problem is summarised in figure 27.

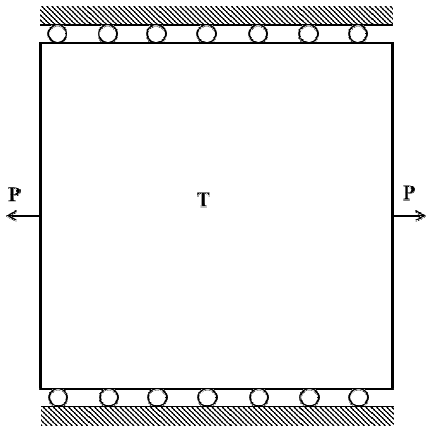

Figure 27: Hardening Model Schematic

The problem as studied in (Heitzer et al. 2000) considers the hardening effects in a different manner to the proposed model. In (Heitzer et al. 2000) the hardening is not related to the plastic strain through a hardening modulus, rather the back stress is bounded. The result is that the plastic strain at the ultimate tensile strength is not given in the material data. Thus the hardening modulus cannot be defined in the current problem. Here two arbitrary equivalent plastic strains are chosen to coincide with the ultimate tensile strength to show it has little or no impact on the resulting ratchet boundaries. The material models defined in (Heitzer et al. 2000) are Young's modulus 200GPa, Poisson's ratio 0.3, yield strength 205MPa and thermal expansion coefficient of $1.6\text{x}10^{-5}{}^{\circ}\text{C}^{-1}$. The hardening model is a bilinear kinematic model, which varies from the initial yield strength at zero plastic strain to a maximum equivalent backstress of $0.5\sigma^y$, at an assumed equivalent plastic strain of 0.05. For completeness, unlimited kinematic hardening is also considered with a hardening modulus of 2GPa and the results for perfect plasticity are given for comparison. The shakedown boundaries given by EMSP and Hietzer et al. (2000) are shown in figure 28.

From figure 28, the hardening form of the EMSP method agrees closely with the results given by Hiezter et al. (2000). In this particular problem the backstress-plastic strain relationship does not have an impact on the resulting boundaries. However

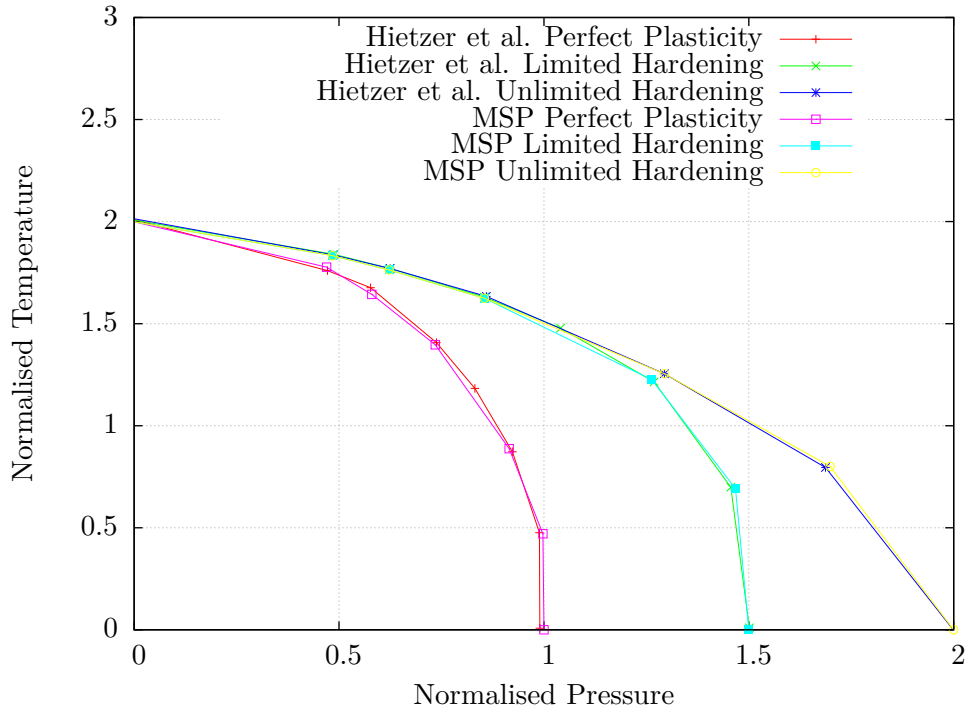

Figure 28: Shakedown Boundaries for Hardening Materials

in problems with displacement controlled loading and/or inplane constraints, the backstress-plastic strain relationship could have an impact on the resulting boundaries which could be an advantage to the hardening model used in the EMSP method. Further research is required in this area to fully understand the potential impact on the backstress-plastic strain relationship.

5.6.3 Non-linear Geometry

Non-linear geometry is of interest in a number of engineering components, for instance pipe bends. In such geometries, changes in the shape of the component could significantly alter the load path. It was shown in (Maier et al. 1993) that this could affect shakedown and ratchet boundaries. To consider possible non-linear geometry effects requires the component shape to be simulated at all of the cyclic load points. As with temperature dependent material properties, it is difficult to formulate a method which allows for the simulation of all cyclic points and incorporation of the non-linear

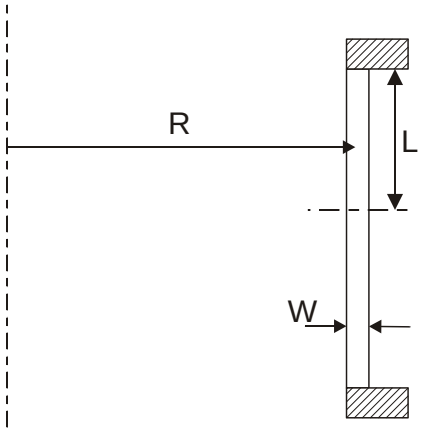

Figure 29: Short Pipe Problem

relationship each imposes on the other whilst using conventional finite elements.

It is however possible to implement the simplified non-linear kinematic shakedown process proposed in (Gross-Weege 1990). In this process the cyclic loads are linearised i.e. the non-linear geometric effects due to the addition of the cyclic loads are assumed to be negligible and may be represented by superposition of elastic stresses. Thus only the deformed configuration of the residual+constant load condition need be simulated and the cyclic stresses may be superimposed onto the residual+constant stresses in the deformed configuration. This is easily achieved using a co-rotational form of the proposed shakedown method. In practice, this requires the rotation of the cyclic stresses to the current configuration. This may be done in ABAQUS using the ABAQUS utility routine ROTSIG. However, under conditions where large thermal strains or large cyclic loads may be present in the structure, the assumption that the cyclic loads result in negligible geometric effects might be tenuous and this approach should be used with caution in such situations.

The method is implemented in ABAQUS via the user subroutine UMAT. To simulated the deformed configuration due to the constant load it is necessary to apply the constant load to the structure. If the constant load is ramped over the analysis step, an increment in the solution "time" can still be used as an increment in the lower bound multiplier.

Example

The example presented here is a short pipe held between two rigid stiffened rings. Figure 29 shows the dimensions of the pipe where W/R=1/200, L/R=1/10. The material properties chosen for the study are perfectly plastic material with Young's modulus=2100GPa, Poisson's ratio=0.3 and yield strength 360MPa. The load cycle under investigation is constant internal pressure P plus varying internal pressure μP(t). The geometric effects, as discussed above, must be simulated by applying the load onto the finite element model. However there are three possible load cases which can be applied to the model i.e. "Case A" P + μP, "Case B" P − μP and "case C" P. For completeness all three cases are examined. The results of the shakedown simulations are presented in figure 30 along with the ratchet boundary found by incremental FEA.

From figure 30 the proposed method agrees closely with the FEA solution for all three cases at lower cyclic loads. As the cyclic load increases, the non-linear geometric effects due to the cyclic loads increase. As the proposed method does not account for the non-linear geometric effects due to the cyclic loads it produces larger errors as the cyclic loads increase. However the close agreement for lower cyclic loads demonstrates

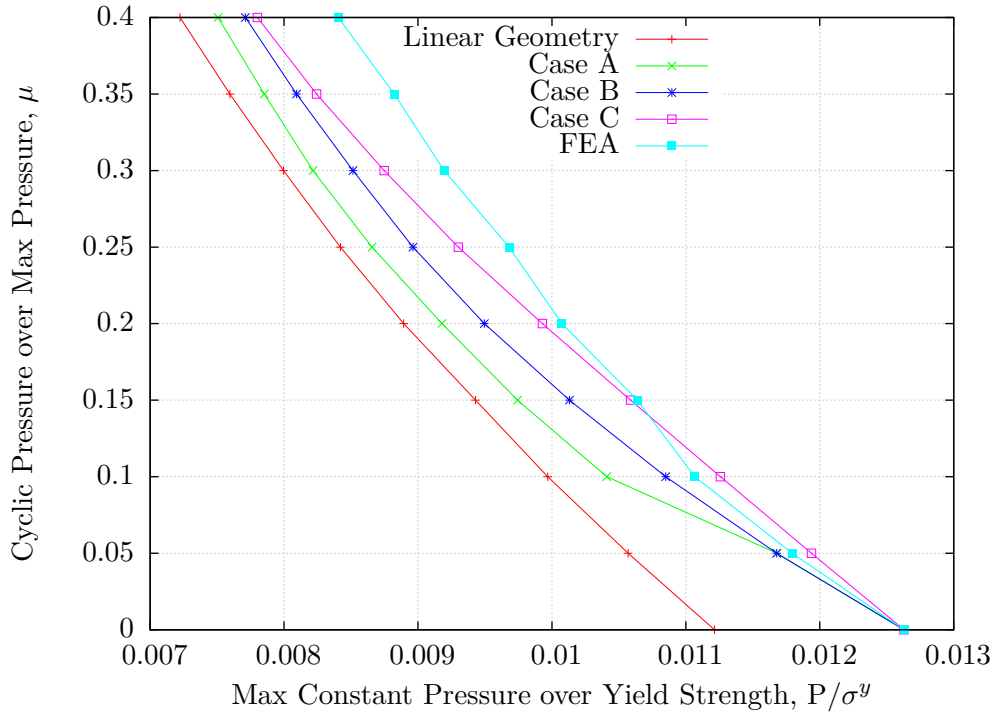

Figure 30: Elastic Shakedown Boundary with Non-linear Geometry for Different Cases

the potential of the method if it can be extended to simulate the geometric effects for all of the points on the load cycle.

5.7 Limitations of the Shakedown Method

The results presented in Sections 5.5 to 5.6.3 show that the EMSP method gives relatively accurate solutions when compared to the LMM and other lower bound methods under the conditions studied. However, as with any numerical method, there are a number of limitations:

Number of load cases The method can consider an arbitrary set of load cases, however due to the method used for integration of the plastic strains only 6 of the load cases can actively require returning to their respective yield surfaces at once. If more than six require limiting to their respective yield surfaces the problem becomes indeterminate. This does not necessarily limit the EMSP method to only consider load cycles with six or less load points. In many cases where there are more than 6 points in the load cycle a bounding result could be gained for each material point by using appropriate filters in the UMAT routine to select the 6 most onerous points in the load cycle, which would allow bounding of the result. Also if the combined residual plus superimposed stresses at two or more load points have a similar normal direction only the load point with greater magnitude of stress need be considered as this will bound the behaviour of the

other points.

Geometric non-linearity The method can consider a simplified version of non-linear geometry adjusted shakedown as demonstrated in Section 5.6.3. However the proposed method does require the linearisation of the cyclic stresses. This limits the proposed method to the consideration of cyclic loads which do not result in significant geometry changes. It was demonstrated that this can result in large errors for higher cyclic loads.

Temperature dependent material properties It is possible to consider a temperature dependent yield strength, as in the case of the LMM method (see Section 5.6.1). However any temperature effects on the stresses resulting from that temperature are ignored (for example, both the Young's modulus and Poisson's ratio of a material vary with temperature). This can result in a number of important interactions which can effect the resulting shakedown and ratchet boundaries (this is demonstrated in Appendix B). The inability of the method to account for temperature dependent material properties could be a significant limitation for use in practice. However, no other shakedown method is currently able to account for this effect either, so it is not a limitation when compared with other methods.

5.8 Benefits of the Shakedown Method

The EMSP method has a number of advantages over other direct shakedown methods.

Maintaining the constitutive model Many , if not all, of the other direct shakedown methods are based on a purely mathematical interpretation of Melan's theorem. Whilst this allows for determination of the loads at the shakedown boundary, the solution methods usually result in the loss of the underlying assumed material response. When attempting to incorporate effects of additional non-linear behaviour (beyond perfect plasticity) the loss of the underlying material model makes it difficult to incorporate those effects. The EMSP method preserves the underlying constitutive model and as such it has been demonstrated that the EMSP method is easily extended to consider additional non-linear effects, such as hardening.

Direct calculation of plastic strains Melan's theorem does not require the calculation of plastic strains, however knowledge of the plastic strains and estimates of the displaced shape of the structure can be useful. Due to the EMSP

method directly calculating the plastic strains during the shakedown analysis these estimates are readily available as output from the material routines.

Strictness in the lower bound result The stresses calculated by the EMSP method, due to the elastic plastic formulation, are strictly limited to be equal to or below the assumed yield strength of the material at all load points considered. This is not necessarily true of other methods. As such the EMSP methods is one of the few direct methods which can consider an arbitrary load cycle that is also a strictly lower bound method.

Stress range The EMSP method calculates a stress solution which satisfies both yield and equilibrium at every increment in the solution. These stress solutions can be used to calculate the stress range at each point in the solution and provide estimates of the mean stress value used in many fatigue assessments.

Familiar solution behaviour Many of the current direct shakedown methods are based on relatively abstract solution methods, which engineers in general are not familiar with. The EMSP method is an elastic plastic method which behaves like a limit solution. Thus if an engineer is familure with the use of plasticty in finite element software, the application and solution behaviour of the EMSP would be familiar.

The EMSP method also has a number of benefits over the more conventional methods used for design against and assessment of ratchetting. For example, consider the simplified methods used in many pressure vessel design standards. These methods are usually based on elastic analysis and an interaction diagram based on the Bree problem. When performing an assessment it is necessary to determine the ratchet plane and two limiting points in the load cycle. This may result in a number of practical problems for the engineer:

1. Are two load points adequate: Complex load cycles may not be fully bounded by just two load points. Consider a load cycle where the principle stress at four points form a perfect tetrahedron in principle stress space. In such a scenario all four points in the load cycle will lie on the yield surface, thus reverse plasticity may occur for stress ranges less than twice yield. When using the EMSP method it is possible to consider an arbitrary number of load points and easily capture this behaviour.

2. Where is the ratchet plane: The elastic analysis performed to obtain stresses for a shakedown assessment may provide a set of stresses for which the position

and orientation of the ratchet plane is not at first obvious. The position and orientation of the ratchet plane does not need to be known when using the EMSP method as it is naturally calculated during the solution of the EMSP method.

Much of the ambiguity which can result from the application of simplified design/assessment methodology may be avoided when using the EMSP method. Further the calculation of redistributed stresses over the ratchet plane will probably result in greater accuracy in components which do not have a single axis of symmetry (e.g. a pipe intersection).

5.9 Discussion

In this Section, a new shakedown method based on non-smooth multi-surface plasticity has been proposed. This method has been shown to be a strict lower bound method which gives reliable results for multiple load points. The method utilises a material model which maintains a constitutively consistent description of the plastic strains in the structure/components: in this aspect the method is unique. Through a number of common benchmark problems and some more complex problems, the method has previously been shown to give good agreement to the upper bound LMM, which has been verified against non-linear FEA. Several extensions to the base EMSP method have been proposed and implemented. Extensions include: the use of temperature dependent yield strength; the consideration of non-linear geometry and hardening.

Despite the accuracy and reliability of this method, it still has several limitations. These limitations originate from the use of a user programmed material model. When using this approach it is only possible to solve for one stress-strain relationship at a time; i.e. the residual stress and strain. However to solve for effects such as full non-linear geometry and temperature dependent material effects in a computationally efficient manner, it is necessary to consider several stress-strain relationships simultaneously. However, at present, this is a limitation to most shakedown methods.

6 Non-smooth Yield Surface for Ratchet

In Section 5 non-smooth multi yield surface plasticity was used to define a lower bound direct shakedown method. The method is now extended to a lower bound direct ratchet method. The ratchet method allows the elastic ratchet and the plastic ratchet boundary (beyond the alternating plasticity boundary) to be determined. The extension of the method is based on the separation of constant and cyclic loads given in (Gokhfeld 1980).

6.1 The Material Model

Throughout this Section a number of additional assumptions are made. These assumptions are as follows:

Assumption 10 The load history can be partitioned into cyclic and constant parts

Assumption 11 The cyclic loads lie within the ratchet boundary

Assumption 12 The constant load is applied under load control

In cases where the varying stresses are large enough to cause alternating plasticity, it is necessary to find a set of varying plastic strains and stresses which vanish over the cycle. This is difficult to solve for at the same time as finding the constant residual stress. If an elastic-perfectly plastic structure is subject to both a constant load and varying load it is possible to consider the cyclic loads separately from the constant load (Gokhfeld 1980). This allows a separate solution to find a set of varying residual stresses and strains which vanish over the cycle and thus satisfy the supplementary condition of the extended Melan's theorem given in equation 17.

The use of simplified cyclic stresses to solve for the varying component of the residual stress is suggested in (Gokhfeld 1980). The simplified measure was to ignore cyclic stress above yield, although it is noted that the use of such simplified cyclic stresses can be non-conservative in cases where the regions of application in the structure are "large".

In (1993c,d) Polizzotto gave a more complete treatment of cyclic strains and stresses in which post transient strains and stresses must be found whilst taking account of the redistribution which occurs during the cycle. The post transient strains and stresses may be found by repeated cycling of the fixed values of cyclic loads, i.e. a fixed value of Z, in a full non-linear FEA. They can then be used in a modified shakedown procedure to give the full ratchet boundary using an incrementally larger value of the ratchet multiplier Y. It is possible for cyclic loads alone to cause either limit or ratchet failure in which case no stabilised reverse plasticity cycle can exist. In this case the magnitudes of the cyclic load must be decreased and the cyclic analysis must be started again.

The cyclic stresses and strains for the ratchet solution proposed in this Section can be found using the Stage 1 solution method used in Methods 1 and 2 of Section 3. In this case the strains at the end of the cyclic solution form the starting point of the ratchet solution. Thus the constant residual strains are the combined strains from both the constant residual strain found in the cyclic solutions and the contribution to the constant residual from the constant load found during the ratchet analysis, i.e

$$\rho_{ij}^{c} + \overline{\rho}_{ij} = E_{ijkq}\left(\varepsilon_{kq}^{Tr} - \varepsilon_{kq}^{p}\right)$$

where

$$C_{ijkq} = \lambda\delta_{ij}\delta_{kq} + \mu(\delta_{ik}\delta_{jq} + \delta_{iq}\delta_{jk}) \tag{56}$$

with:

$$\lambda = \frac{vE}{(1+v)(1-2v)} \text{ and } \mu = \frac{E}{2(1+v)}$$

Using this and the solutions from Stage 1, the ratchet solution material model may be defined as follows.

The loaded stresses are given by

$$\sigma_{ij}^{l} = \rho_{ij}^{c} + \overline{\rho}_{ij} + Y\hat{\sigma}_{ij}^{c} + Z\widehat{\sigma}_{ij}^{l} + \sum_{\theta=1}^{\theta=l}\rho_{ij}^{\Delta,\theta} \tag{57}$$

where Z is a fixed cyclic load multiplier.

The yield conditions are:

$$f^{l} = \left|\rho_{ij}^{c} + \overline{\rho}_{ij} + Y\hat{\sigma}_{ij}^{c} + Z\widehat{\sigma}_{ij}^{l} + \sum_{\theta=1}^{\theta=l}\rho_{ij}^{\Delta,\theta}\right| - \sigma^{y} \leq 0 \text{ for } l = 1, 2..m$$

with:

$$\left|\rho_{ij}^{c} + \overline{\rho}_{ij} + Y\hat{\sigma}_{ij}^{c} + Z\widehat{\sigma}_{ij}^{l} + \sum_{\theta=1}^{\theta=l}\rho_{ij}^{\Delta,\theta}\right| =$$

$$\sqrt{\frac{3}{2}\left(\rho_{ij}^{\prime c} + \overline{\rho}_{ij}^{\prime} + Y\hat{\sigma}_{ij}^{\prime c} + Z\widehat{\sigma}_{ij}^{\prime l} + \sum_{\theta=1}^{\theta=l}\rho_{ij}^{\prime\Delta,\theta}\right)\left(\rho_{ij}^{\prime c} + \overline{\rho}_{ij}^{\prime} + Y\hat{\sigma}_{ij}^{\prime c} + Z\widehat{\sigma}_{ij}^{\prime l} + \sum_{\theta=1}^{\theta=l}\rho_{ij}^{\prime\Delta,\theta}\right)} \tag{58}$$

and the net plastic strain rate is assumed to be due to all load cases and given by Koiter's Rule:

$$\dot{\varepsilon}^p_{ij} = \sum_{\alpha} \dot{\gamma}^{\alpha} \frac{\delta f^{\alpha}}{\sigma^{\alpha}_{ij}} \tag{59}$$

where

$$Q_{act} \text{ where } f = 0 \text{ and } \gamma \geq 0 \tag{60}$$

and

$$\alpha \in Q_{act} \text{ and } \beta \in Q_{act}$$

The necessary constraints on the system become

$$\gamma^l \geq 0 \quad , \quad f^l \leq 0 \quad , \quad \gamma^l f^l = 0 \quad and \quad \gamma^l \dot{f}^l = 0$$

For Mises plasticity:

$$\begin{aligned} \frac{\delta f^l}{\sigma^l_{ij}} = r^l_{ij} &= \frac{\delta\left(\left|\rho^c_{kq}+\overline{\rho}_{kq}+Y\hat{\sigma}^c_{kq}+Z\widehat{\sigma}^l_{kq}+\sum_{\theta=1}^{\theta=l}\rho^{\Delta,\theta}_{kq}\right|-\sigma^y\right)}{\delta\left(\rho^c_{ij}+\overline{\rho}_{ij}+Y\hat{\sigma}^c_{ij}+Z\widehat{\sigma}^l_{ij}+\sum_{\theta=1}^{\theta=l}\rho^{\Delta,\theta}_{ij}\right)} \\ &= \frac{3}{2}\frac{\rho'^c_{ij}+\overline{\rho}'_{ij}+Y\hat{\sigma}'^c_{ij}+Z\widehat{\sigma}'^l_{ij}+\sum_{\theta=1}^{\theta=l}\rho'^{\Delta,\theta}_{ij}}{\left|\rho^c_{kq}+\overline{\rho}_{kq}+Y\hat{\sigma}^c_{kq}+Z\widehat{\sigma}^l_{kq}+\sum_{\theta=1}^{\theta=l}\rho^{\Delta,\theta}_{kq}\right|} \end{aligned} \tag{61}$$

Let the set of yield surfaces at which yielding occurs be defined as the set of active yield criteria:

Following the works of Simo and Hughes, it is assumed that:

$$[g_{\alpha\beta}] = \left[r^{\alpha}_{ij} E_{ijkq} r^{\beta}_{kq}\right] \tag{62}$$

is positive definite which gives the tangent modulus as:

$$E^{ep}_{ijkq} = C_{ijkq} - \sum_{\alpha}\sum_{\beta} [G]_{\alpha\beta} \left(E_{ijop} r^{\alpha}_{op}\right)\left(E_{kqrs} r^{\beta}_{rs}\right) \tag{63}$$

where

$$\sum_{\alpha,\beta,\varsigma} [G]_{\alpha\beta} [g]_{\beta\varsigma} = \delta_{\alpha\varsigma} \tag{64}$$

6.2 Solution Scheme: CMSP

The numerical method based on the material model given in Section 6.1 is given the name CMSP, were the "MSP" parts stands for multi surface plasticity and the "C" is cyclic for the cyclic stage 1 analysis. The ratchet solution may be thought of as a shakedown solution in which the stress at the loaded points σ_{ij}^m is modified to include the effect of any varying residual component from an alternating plasticity mechanism. The integration and solution algorithms for this model are the same as for shakedown, with the loaded stresses modified to take account of any cyclic varying residual stresses and thus will not be repeated here. The general solution procedure is outlined below. In step $m+3$ the cyclic and ratchet solution occur one after the other. If the time at which the cyclic solution finish is t^c then the multiplier Y may be defined as Y =steptime-t^c. In defining the ratchet multiplier Y in this way the automatic time stepping procedure in the FEA may be used to control the convergence of the ratchet multiplier. The largest value of Y for which the solver can find a stable equilibrium solution is taken as the ratchet multiplier at the ratchet boundary. During the cyclic solutions it is important to make sure the solver solves for the extremes in the load case. To do this, time points may be set at every unit of time during the ratchet step $m+3$ and using 1 unit in time as the difference between the last cyclic load to the next. This also allows for interpolating the superimposed cyclic stress from one state to the other as necessary if the solver cannot pass from one load point to the next in a single increment. The general solution method can then be summarised as follows.

Step 1 Load the model with the constant load, write stresses to state variable array.

Step 2 to $m+1$ Load the model with the loads for critical cyclic load case n and solve for the elastic stresses. Write these stresses to the state variable array.

Step $m+2$ Return model back to unstressed state.

Step $m+3$

Cyclic Solution Perform cyclic solution using results from steps 2 to $m+1$. If constant residual has converged store step time as t^c.

Ratchet Solution Y =Step time$-t^c$. Perform Ratchet analysis to find maximum value of Y.

6.3 Examples

6.3.1 Axi-symmetric Bree Cylinder

The CMSP method was applied to the Bree problem introduced in Section 3. The results presented in figure 31 shows that the CMSP produces a ratchet boundary that agrees to within fractions of a percent with the upper bound LMM. The LMM results have been found using (Ure 2013) with the same FE mesh with a convergence of 0.00001. The agreement is better than that of the Hybrid Method and Methods 1 and 2 (see figure 17). This suggests that the problems identified with plastic strain direction and compatibility in Section 3.6 were the cause of the poor agreement between the LMM and the Hybrid Method and Methods 1 and 2.

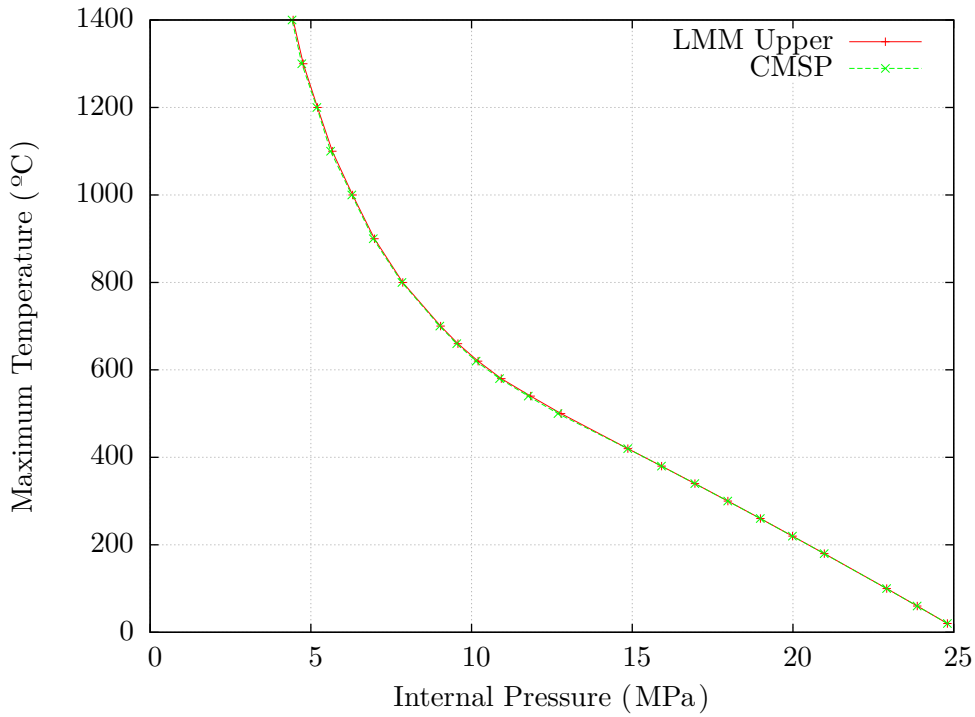

Figure 31: Bree Cylinder Ratchet Boundaries from Various Methods

6.3.2 Pressurised Two Bar

To test the CMSP method under varying degrees of multi-axial stresses, it was applied to the pressurised two bar problem introduced in Section 3.5.3. The results presented in figures 32 to 34 show that the CMSP agrees closely with the upper bound LMM for all loads and the various extents of multi-axial stress studied. The LMM solutions have been found using the LMM GUI developed by Ure using the same FE mesh with a convergence tolerance of 0.00001. The slight difference close to the alternating plasticity boundary is attributed to slight differences in job setup between the two methods. In general the CMSP method gives better agreement with the LMM than the Hybrid Method and Methods 1 and 2, see figures 18 to 20.

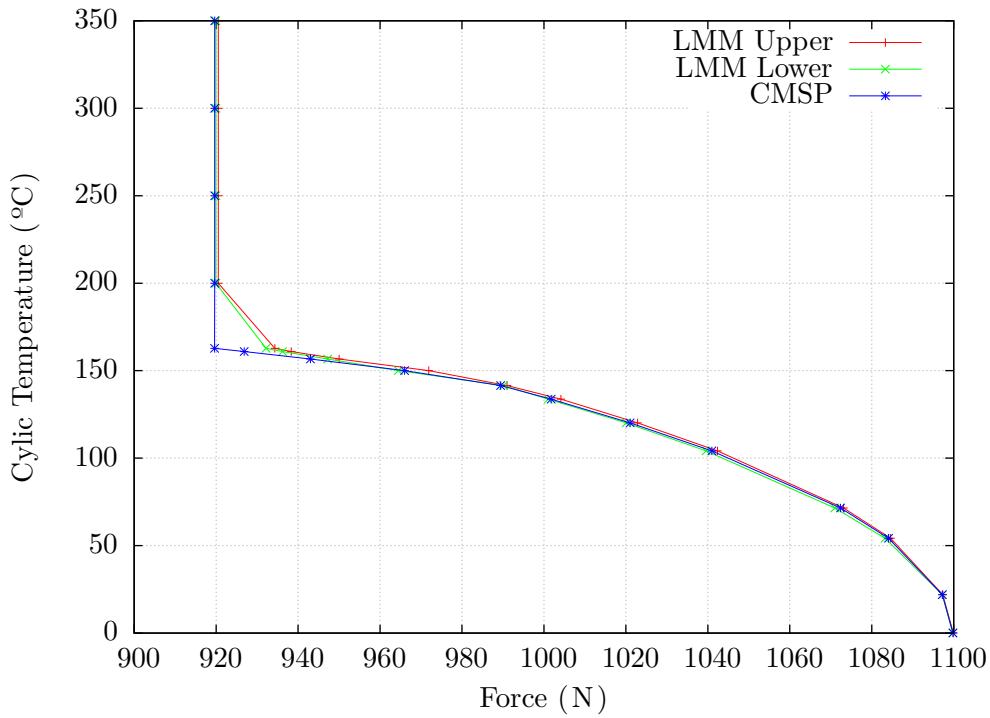

Figure 32: Pressurised Two Bar Ratchet Boundaries by Various Methods with F/P=10

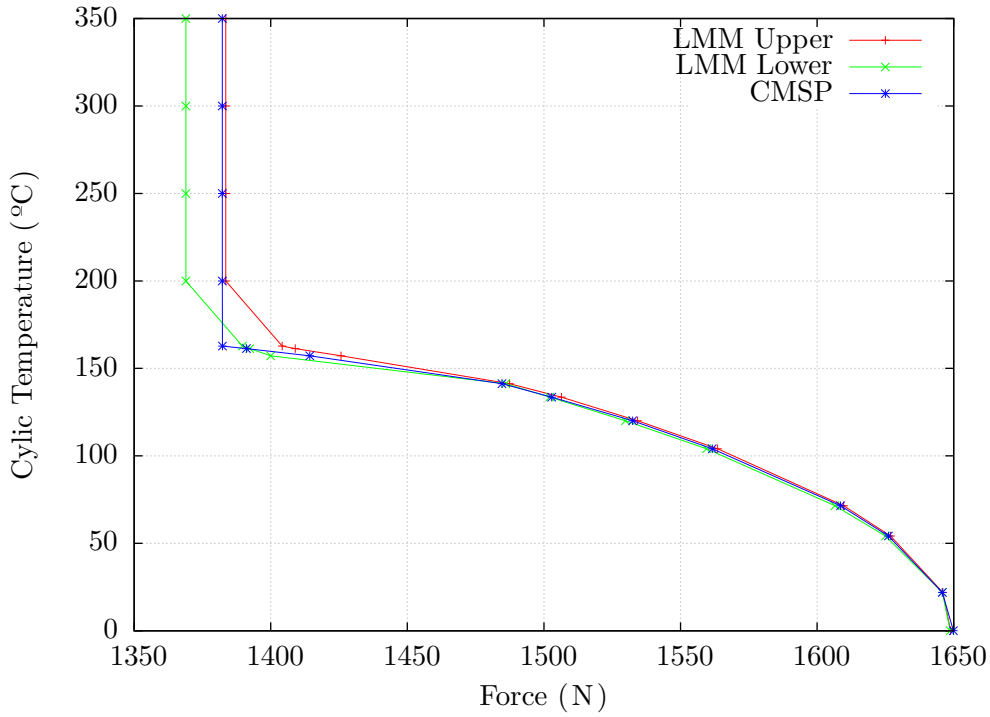

Figure 33: Pressurised Two Bar Ratchet Boundaries by Various Methods with F/P=15

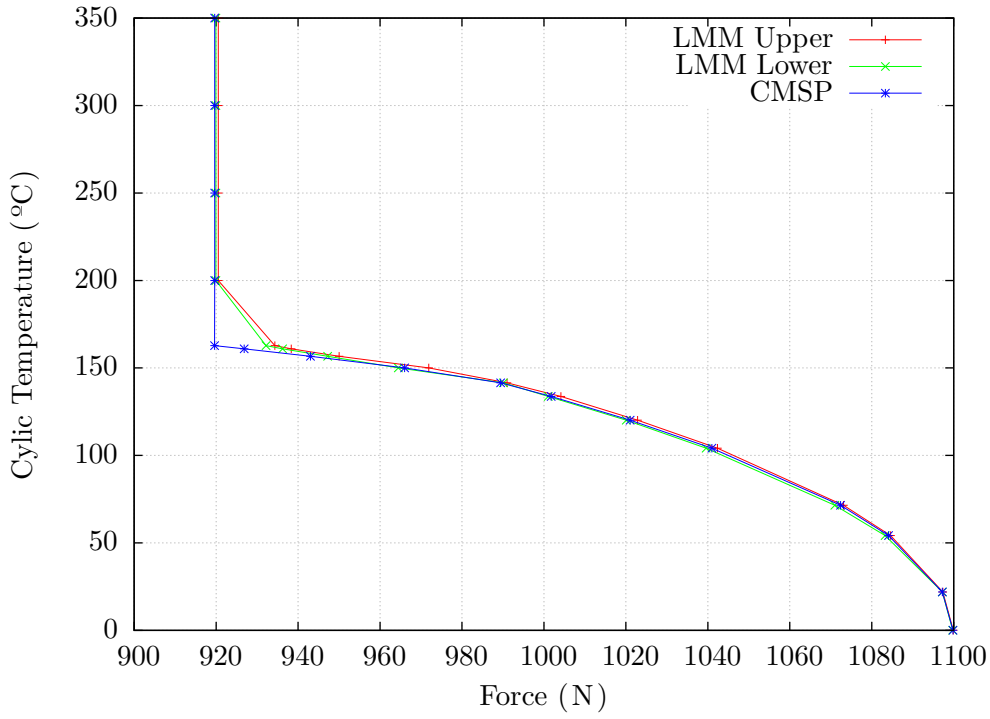

Figure 34: Pressurised Two Bar Ratchet Boundaries by Various Methods with F/P=20

6.3.3 Plate With Hole

The CMSP method was applied to the plate with hole problem introduced in Section 3.5.4. The results in figure 35 show that the CMSP method agrees closely with the upper bound LMM method. The LMM results have been found using the LMM GUI developed by Ure using the same FE mesh. The convergence parameter used was 0.00001 and the number of cyclic solutions doubled over the default value to gain convergence on the cyclic solutions. For this problem the CMSP gives results between the lower and upper bound LMM boundaries over the range of cyclic temperature studied.

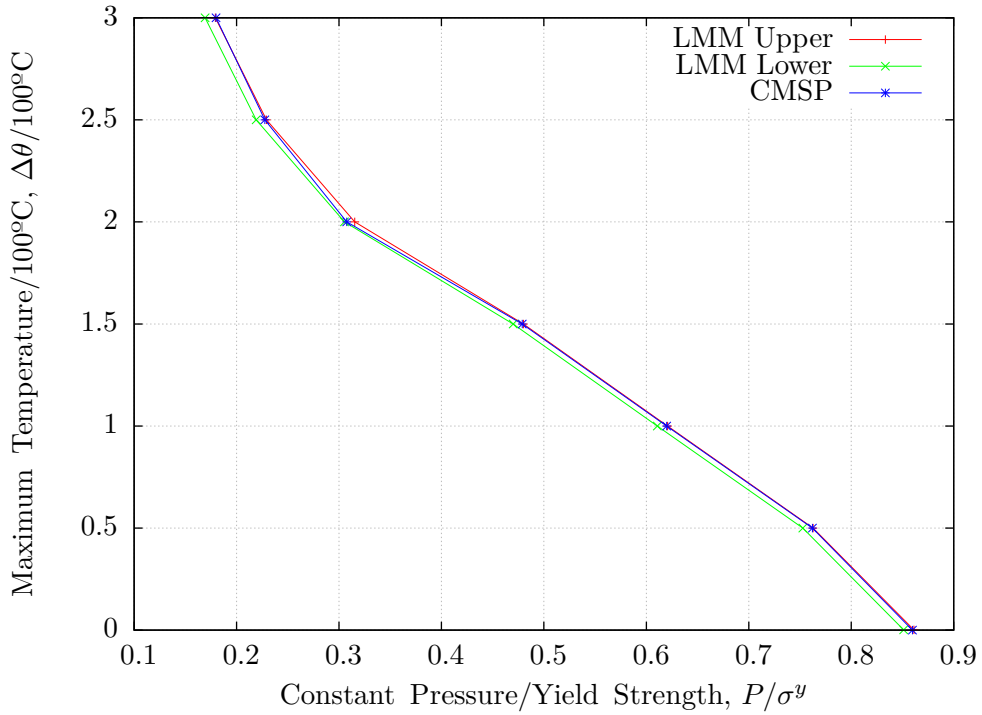

Figure 35: Plate with Hole Ratchet Boundaries from Various methods

6.3.4 Pipe Intersection

The CMSP method is applied to the pipe intersection problem introduced in Section 5.5.5. For this problem the agreement with the upper bound LMM is not as good as the previous benchmark problems studied. This is attributed to the poor accuracy of the cyclic solutions given by the incremental FEA used in Stage 1. The accuracy of the CMSP method can be significantly impacted by the convergence of the cyclic solutions. In this problem strict convergence on the cyclic solutions was never achieved despite the simulation of 1000s of load cycles. This illustrated the greatest limitation of the CMSP method: it is reliant on incremental FEA to find the cyclic stresses. However it is, theoretically, possible to find the cyclic solutions directly, at the same time as solving for the constant residual stress, without the need for incremental finite element solutions. This however would require significant changes to the solution process and is outside the scope of the current research.

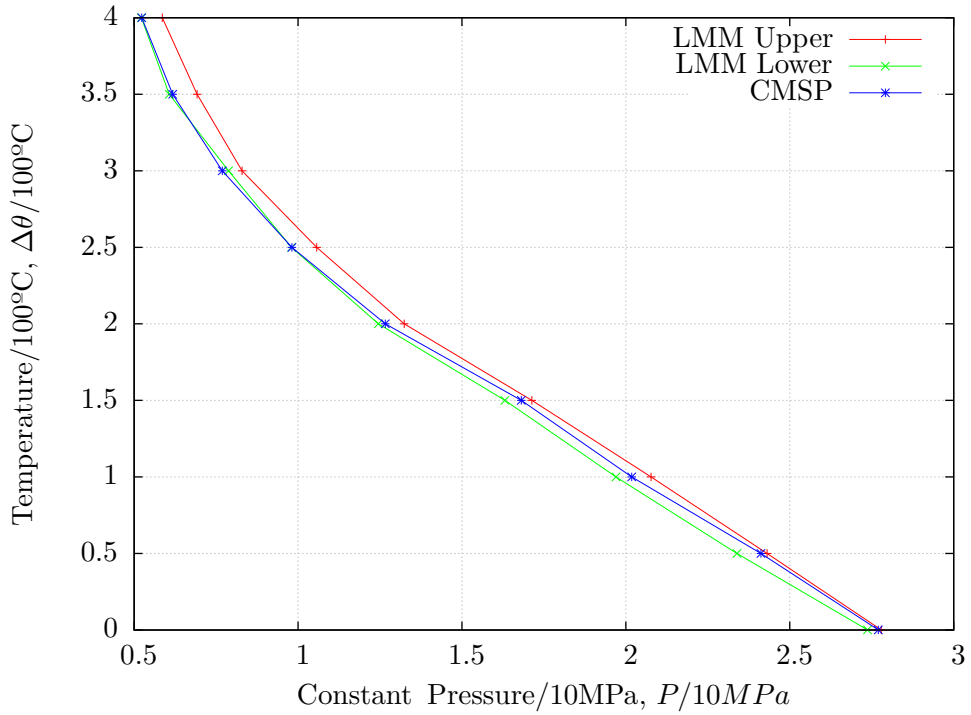

Figure 36: Pipe Intersection Ratchet Boundaries by Various Methods

6.4 Extension of the Ratchet Method

6.4.1 Temperature dependent yield strength

One of the further developments possible in the CMSP is incorporation of temperature dependent yield strength. However any constant temperature must be included in the cyclic solutions: i.e., a constant temperature may not be included in the constant load case and scaled with the constant load to find the ratchet boundary, as the cyclic solutions would require changing if the constant temperature they take place about changes during the analysis. Thus the incorporation of temperature dependent yield strength may be achieved without noticeable change in the computation cost. Whilst it is possible to account for temperate dependent yield strength it is not possible to account for full temperature dependence of material properties (see appendix B).

6.4.2 Pressurised Two Bar: Temperature Dependent Yield

The pressurized two bar structure is shown below in figure 37. Bar 1 has an internal radius of 2.00mm and an external radius of 2.68mm. Bar 2 has an internal radius of 2.00mm and an external radius of 3.22mm. Bar 2 is twice the length of bar 1 and both have the same material properties: Young's modulus of 210GPa , Poisson's ratio of 0.3, the yield strength is assumed to be temperature dependent and varies according to $\sigma^y(T) = 200\text{MPa} - 0.2857 \times T$ and a thermal expansion coefficient of 1.17x10^{-5} $^\circ$C^{-1}. The ends of the cylinders are constrained to remain in plane section at all times. The model was defined in 3D with second order reduced integration elements, with six elements through the thickness of bar 2 and 3 through the thickness of bar 1.

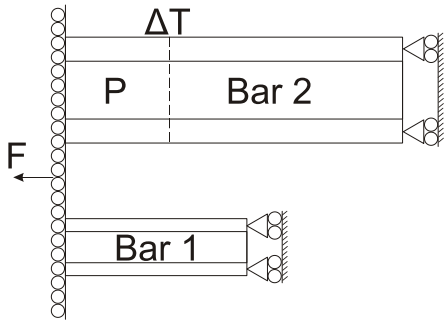

Figure 37: schematic

The load cycle is described by a constant load which consists of internal pressure, P, applied to bar 2 and axial force, F, distributed between both bars by a plane section constraint. The cyclic load is applied as a varying temperature, above the reference temperature, in bar 2, with the temperature being uniform throughout the bar. Bar 1 remains at all times at the reference temperature. The pressure and axial force are considered for three separate conditions: where the force in Newtons divided by the pressure in MPa, F/P, equals 10, 15 and 20. This is done to test the proposed method under varying extents of multi-axial stress conditions.

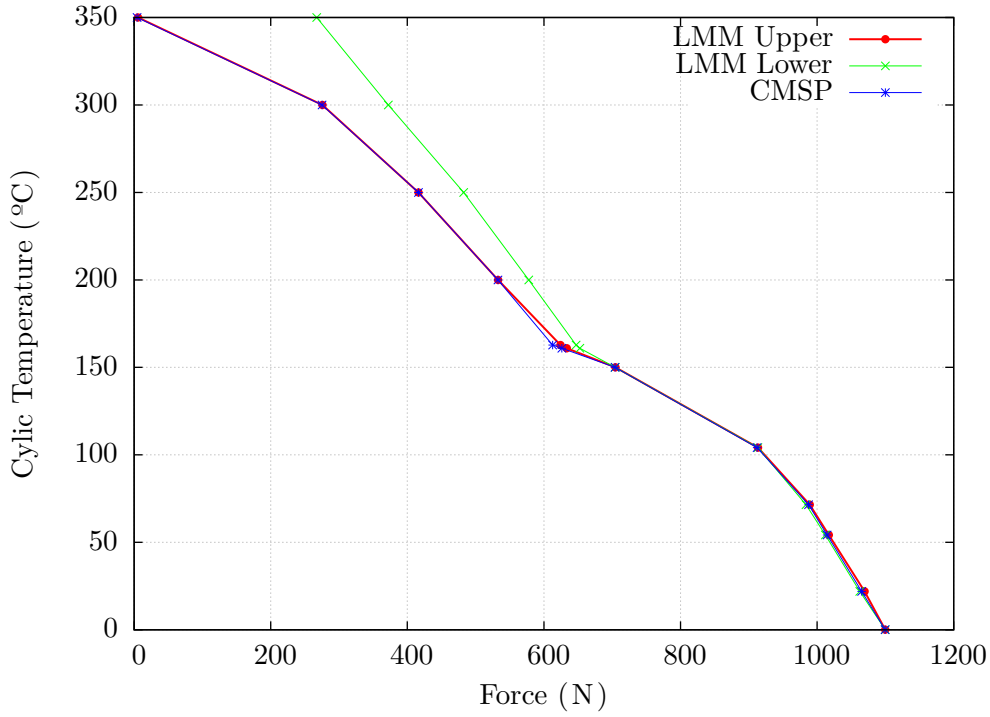

Figure 38: Pressurised Two Bar Ratchet Boundaries by Various Methods with Temperature Dependent Yield and F/P=10

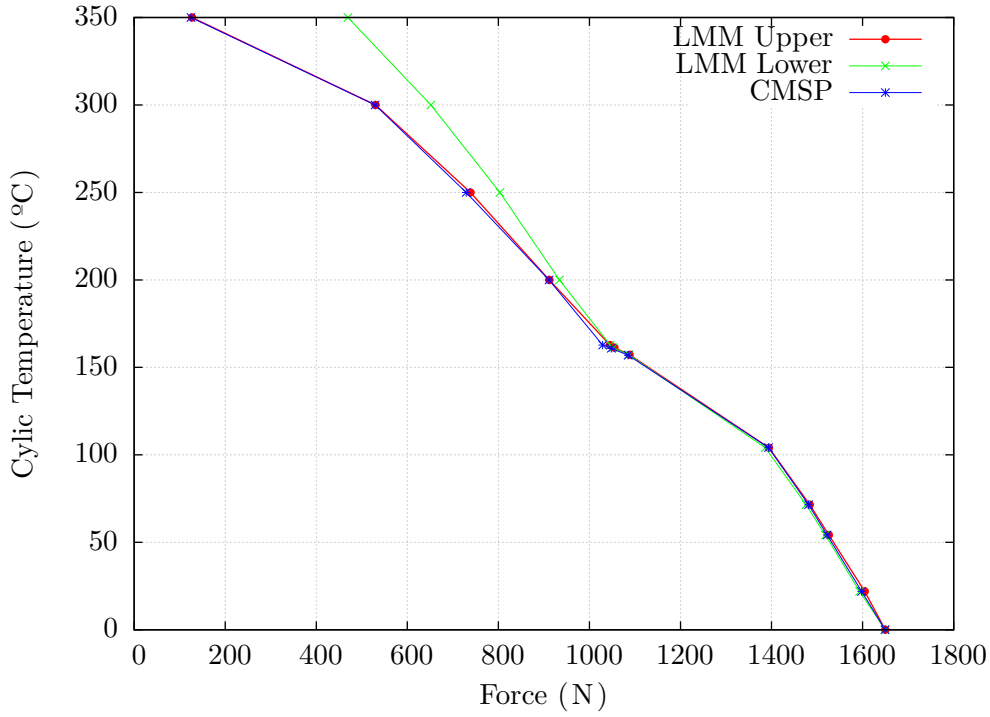

Figure 39: Pressurised Two Bar Ratchet Boundaries by Various Methods with Temperature Dependent Yield and F/P=15

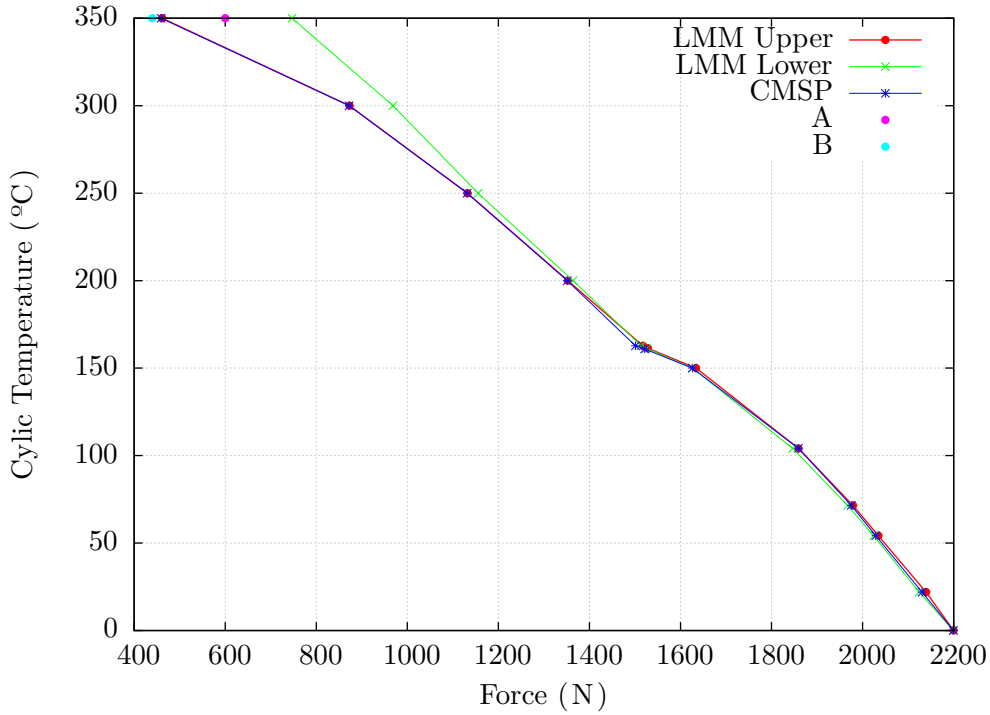

Figure 40: Pressurised Two Bar Ratchet Boundaries by Various Methods with Temperature Dependent Yield and F/P=20

The results presented in figures 38 to 40 show that the CMSP and Upper bound LMM result agree closely. The LMM results were obtained using (Ure 2013) using the same finite element model with a convergence parameter as 0.00001. Note the change in ratchet behaviour compared to the temperature independent results given in figures 18 to 20. This is due to the reduction in the yield strength in the thicker bar, reducing the constant load that it can support at elevated temperature. Also from figures 38 to 40, the lower bound LMM results exceed the CMSP and upper bound LMM results beyond the alternating plasticity boundary.

To verify the boundary given by the CMSP and upper bound LMM, two points at 350 $^\circ$C for F/P=20 at F=440 and F=600 were simulated with incremental FEA. The results of the incremental FEA are presented in figures 41 and 42. Figure 41 shows that there is a stabilised ratchet strain for F=600 at 350 $^\circ$C for F/P=20. This indicates that the lower bound LMM results are non-conservative indicating a non-strictness in the lower bound LMM formulation, (see Appendix A for further discussion on this). The results presented in figure 42 indicates a plastic shakedown solution verifying the CMSP and LMM upper bound results.

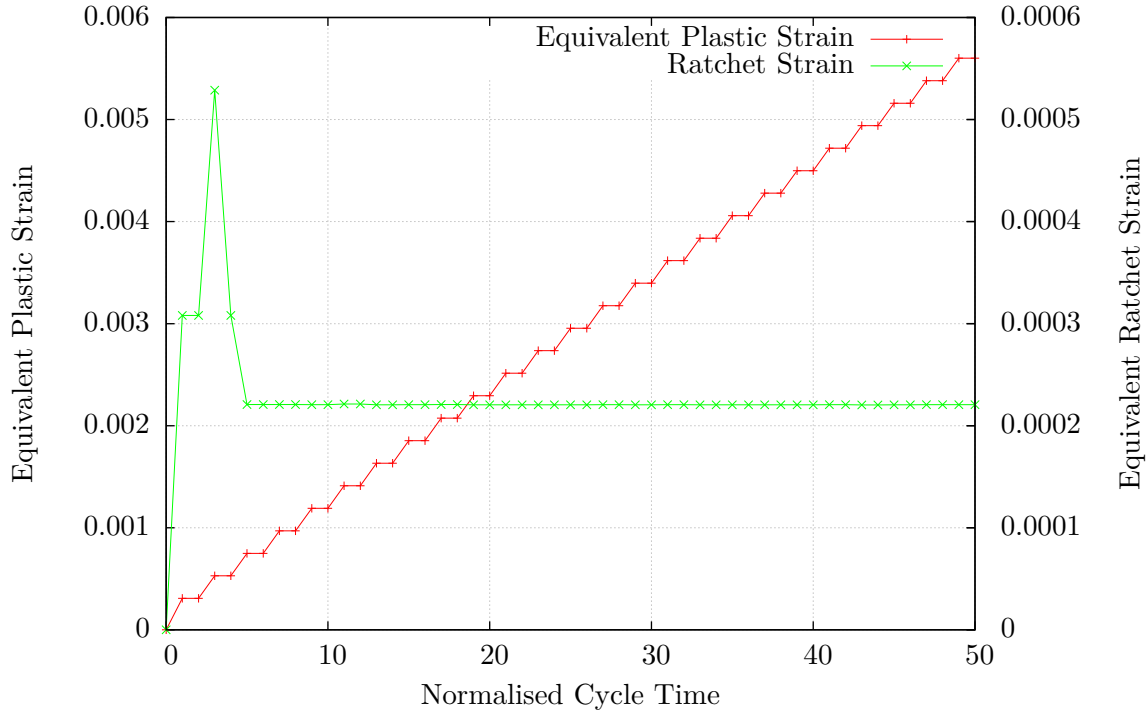

Figure 41: Strain Response Point A, F/P=20

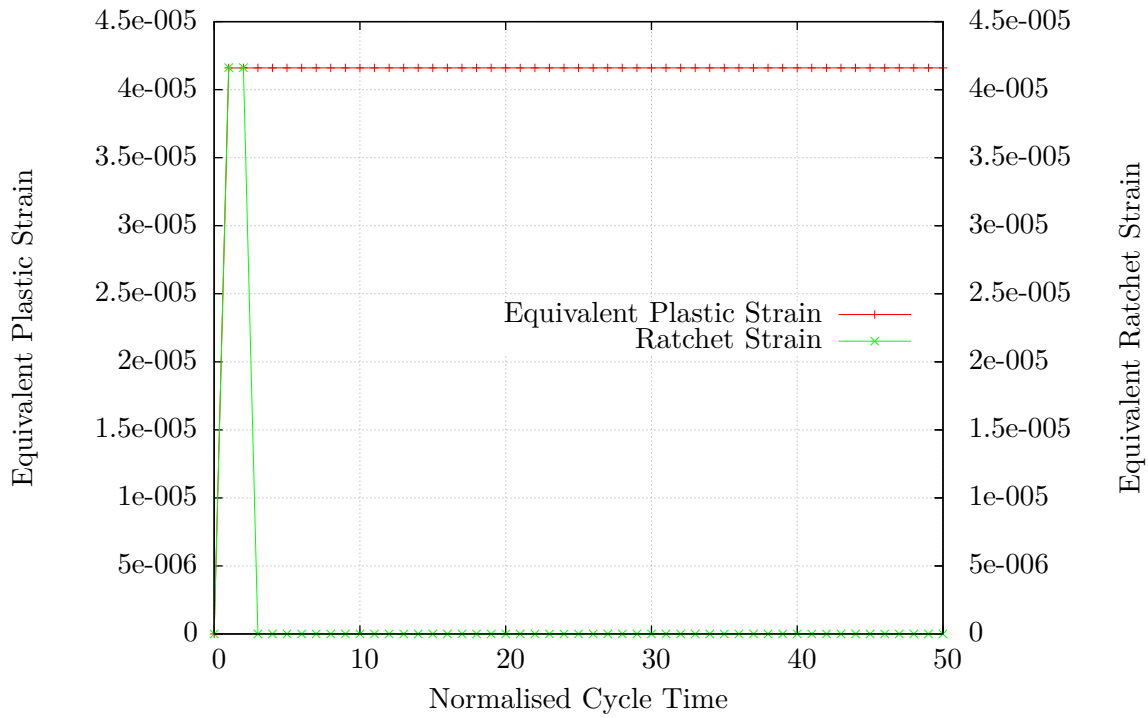

Figure 42: Strain Response Point B, F/P=20

6.5 Simplified Variants of the Ratchet Method

Whilst the CMSP can give close agreement with the upper bound LMM, the cyclic solutions can require a large number of cycles to be solved to obtain a closed plastic strain cycle. Obtaining a closed plastic strain cycle is important for the convergence of the ratchet method as illustrated in Section 6.3.4. Thus the requirement of an incremental finite element solution to find the closed plastic strains can represent a significant computational cost. In this Section a number of simplified cyclic stresses, used in other methods, are explored.

The simplified cyclic stresses proposed here will have computational saving over incremental cyclic solutions used in section 6.2. However the simplification of the cyclic stresses may result in ratchet boundaries which are not as accurate as for the complete cyclic solutions used in the CMSP. Other limitations may also result from the use of the simplified stresses. Thus the aim of this Section is not to carry out computational comparisons, but rather, to assess the accuracy and reliability of the simplified cyclic stresses when used in conjunction with non-smooth multi yield surface plasticity models for the ratchet solution.

6.5.1 Gokhfeld's Cyclic Stress

When introducing the extended ratchet method in (Gokhfled 1980), Gokhfeld also introduced a simplified cyclic stress description to allow for analytical solution for complex components. When the stress in a structure exceeds yield, plastic strains develop within the structure. These plastic strains act to redistribute the stress in the structure such as to satisfy both yield and equilibrium, if possible. This redistribution is non-linear in nature and is a complex function of component shape, material properties and applied loading.

When the cyclic stresses go beyond the alternating plasticity boundary and reverse plasticity cycles result, analytical solutions for the reversed plastic strain and the resulting changing residual stress $\rho_{ij}^{\Delta}(t)$ are difficult to define. To overcome this problem Gokhfeld introduced a simplification for the treatment of the cyclic stresses.

Consider a structure subject to an arbitrary load case. It is assumed that the load case may be separated into constant and cyclic parts, P^c and $P(t)$, and the cyclic load may be decomposed further into a mean load and a fully reversed cyclic amplitude, P^{mean} and $P^A(t)$. These loads result in corresponding elastic stresses (which maintain equilibrium with the load) $\hat{\sigma}_{ij}^c$, $\hat{\sigma}_{ij}^{mean}$ and $\hat{\sigma}_{ij}^A(t)$. The simplification in the cyclic stresses is then:

$$\sigma_{ij}^{A,adj}(t) = \begin{cases} \hat{\sigma}_{ij}^{A}(t) \quad \text{for} \quad \left|\hat{\sigma}_{ij}^{A}(t)\right| \leq \sigma^{y} \\ \\ V\hat{\sigma}_{ij}^{A}(t) \quad \text{for} \quad \left|\hat{\sigma}_{ij}^{A}(t)\right| > \sigma^{y} \quad \text{where} \quad V = \frac{\sigma^{y}}{\left|\hat{\sigma}_{ij}^{A}(t)\right|} \end{cases} \tag{65}$$

i.e. when the cyclic stress amplitude at a particular material point exceeds yield it is assumed equal to yield, thus no elastic plastic analysis is required. Because the stress cycle has to be separated into a mean and a fully reversed cyclic stress amplitude, it limits the number of points which can be considered in the load cycle to 2.

The cyclic stresses must then satisfy the extended Melan's theorem i.e.

$$\left|\left(\rho_{ij}^{c} + \bar{\rho}_{ij}\right) + \hat{\sigma}_{ij}^{c} + \hat{\sigma}_{ij}^{mean} + \sigma_{ij}^{A,adj}\right| \leq \sigma^{y} \text{ and } \left|\left(\rho_{ij}^{c} + \bar{\rho}_{ij}\right) + \hat{\sigma}_{ij}^{c} + \hat{\sigma}_{ij}^{mean} - \sigma_{ij}^{A,adj}\right| \leq \sigma^{y}$$

However, scaling down the stress for a particular set of material points, where the equivalent cyclic stress amplitude exceeds yield, will result in a local violation of equilibrium in the structure and may also lead to a loss of equilibrium with the applied surface traction. This theoretically results in a cyclic stress description which does not satisfy the stringent requirements of a lower bound solution. Scaling down the stress at particular material points results in a portion of the energy in the structure being lost. From Koiter's theorem, this will theoretically lead to an over estimation of the constant load at ratchet. It was, however, noted by Gokhfled that if the region of the structure for which the assumption, in equation 65, is applied is small, the resulting over estimation of the constant load at ratchet is likely to be limited.

Material Model and Solution Method: SMSP

The numerical method based on Gokhfeld's simplified cyclic stress is given the name SMSP, were the "MSP" parts stands for multi surface plasticity and the "S" is simplified for the simplified cyclic stress. The cyclic stresses are found using an elastic analysis, for both the mean stress and the cyclic stress amplitude. The simplified cyclic stress amplitude, $\pm\sigma_{ij}^{A,adj}$, as given in equation 65, can be calculated during the elastic solution. The cyclic solution is then found by applying the cyclic stress amplitude and the mean cyclic stress to the component whist satisfying Melan's theorem i.e. the cyclic solution is given by the following model.

Having found $\pm\sigma_{ij}^{A,adj}$ and $\hat{\sigma}_{ij}^{mean}$ using an elastic analysis and the function given in equation 65 the constant residual stress due to cyclic loading is given by:

$$\bar{\rho}_{ij} = C_{ijkq}\left(\varepsilon_{kq}^{Tr} - \varepsilon_{kq}^{p}\right)$$

The stresses at the loaded condition s are given by:

$$\sigma_{ij}^{1} = \overline{\rho}_{ij} + \hat{\sigma}_{ij}^{mean} + \sigma_{ij}^{A,adj} \ , \ \sigma_{ij}^{2} = \overline{\rho}_{ij} + \hat{\sigma}_{ij}^{mean} - \sigma_{ij}^{A,adj}$$

The yield conditions are:

$$f^{1} = \left|\overline{\rho}_{ij} + \hat{\sigma}_{ij}^{mean} + \sigma_{ij}^{A,adj}\right| - \sigma^{y} \leq 0 \ ,$$

$$f^{2} = \left|\overline{\rho}_{ij} + \hat{\sigma}_{ij}^{mean} - \sigma_{ij}^{A,adj}\right| - \sigma^{y} \leq 0$$

and the net plastic strain rate is assumed to be due to all load cases and given by Koiter's Rule:

$$\dot{\varepsilon}_{ij}^{p} = \sum_{\theta=1}^{\theta=2} \dot{\gamma}^{\theta} \frac{\delta f^{\theta}}{\delta \sigma_{ij}^{\theta}} = \dot{\gamma}^{1} \frac{\delta f^{1}}{\delta \sigma_{ij}^{1}} + \dot{\gamma}^{2} \frac{\delta f^{2}}{\delta \sigma_{ij}^{2}}$$

with

$$\gamma^{l} \geq 0 \quad , \quad f^{l} \leq 0 \quad , \quad \gamma^{l} f^{l} = 0 \quad and \quad \gamma^{l} \dot{f}^{l} = 0 \ \text{ for } l = 1, 2$$

This model can be integrated in the same manner as shown in Section 5.6.2.

The constant load is then added to the structure whilst satisfying Melan's theorem using the following procedure. The plastic strain is carried over from the cyclic solutions to preserve as much of the compatibility as possible. The constant residual stress due to cyclic loading is given by:

$$\rho_{ij}^{c} + \overline{\rho}_{ij} = C_{ijkq}\left(\varepsilon_{kq}^{Tr} - \varepsilon_{kq}^{p}\right)$$

The stresses at the loaded conditions are given by:

$$\sigma_{ij}^{1} = \rho_{ij}^{c} + \overline{\rho}_{ij} + \hat{\sigma}_{ij}^{c} + \hat{\sigma}_{ij}^{mean} + \sigma_{ij}^{A,adj} \ , \ \sigma_{ij}^{2} = \rho_{ij}^{c} + \overline{\rho}_{ij} + \hat{\sigma}_{ij}^{c} + \hat{\sigma}_{ij}^{mean} - \sigma_{ij}^{A,adj}$$

The yield conditions are:

$$f^{1} = \left|\rho_{ij}^{c} + \overline{\rho}_{ij} + \hat{\sigma}_{ij}^{c} + \hat{\sigma}_{ij}^{mean} + \sigma_{ij}^{A,adj}\right| - \sigma^{y} \leq 0 \ ,$$

$$f^{2} = \left|\rho_{ij}^{c} + \overline{\rho}_{ij} + \hat{\sigma}_{ij}^{c} + \hat{\sigma}_{ij}^{mean} - \sigma_{ij}^{A,adj}\right| - \sigma^{y} \leq 0$$

and the net plastic strain rate is assumed to be due to all load cases and given by Koiter's Rule:

$$\dot{\varepsilon}^{p}_{ij} = \sum_{\theta=1}^{\theta=2} \dot{\gamma}^{\theta} \frac{\delta f^{\theta}}{\delta \sigma^{\theta}_{ij}} = \dot{\gamma}^{1} \frac{\delta f^{1}}{\delta \sigma^{1}_{ij}} + \dot{\gamma}^{2} \frac{\delta f^{2}}{\delta \sigma^{2}_{ij}}$$

with

$$\gamma^{l} \geq 0 \quad , \quad f^{l} \leq 0 \quad , \quad \gamma^{l} f^{l} = 0 \quad and \quad \gamma^{l} \dot{f}^{l} = 0 \ \text{ for } l = 1, 2$$

This model is integrated using the same method as given in Section 5.6.2 thus the procedure is not repeated here.

Examples

The material models and solution methods given in Section 6.5.2 were implemented in ABAQUS using the user subroutine UMAT. The example problems studied were the axi-symmetric Bree cylinder and plate with hole examples given in Sections 5 and 6. See Section 5 for details of geometry and material properties.

Discussion

The results for the Bree cylinder given in figure 43 show that, as expected, for higher values of cyclic load beyond the alternating plasticity boundary the method becomes non-conservative. The results show a non-conservatism of 7% at the highest cyclic load considered here. However, the method shows over conservatism for the plate with hole example (see figure 43). In this case, the simplified cyclic stress fails to capture the redistributed stress due to the plastic strains at the in-plane constraints which result due to the cyclic loads. On addition of the constant load, this results in an error in the direction of constant stress resulting in excess straining in this region of the component. This reduces load carrying capacity, which in turn reduces the constant load at the ratchet boundary. Whilst this cyclic stress description results in computational savings, it generally shows relatively widely scattered results compared to the CMSP and LMM boundaries. It is also limited to considering only two points on the load cycle, which may not be sufficient to describe the ratchet mechanism.

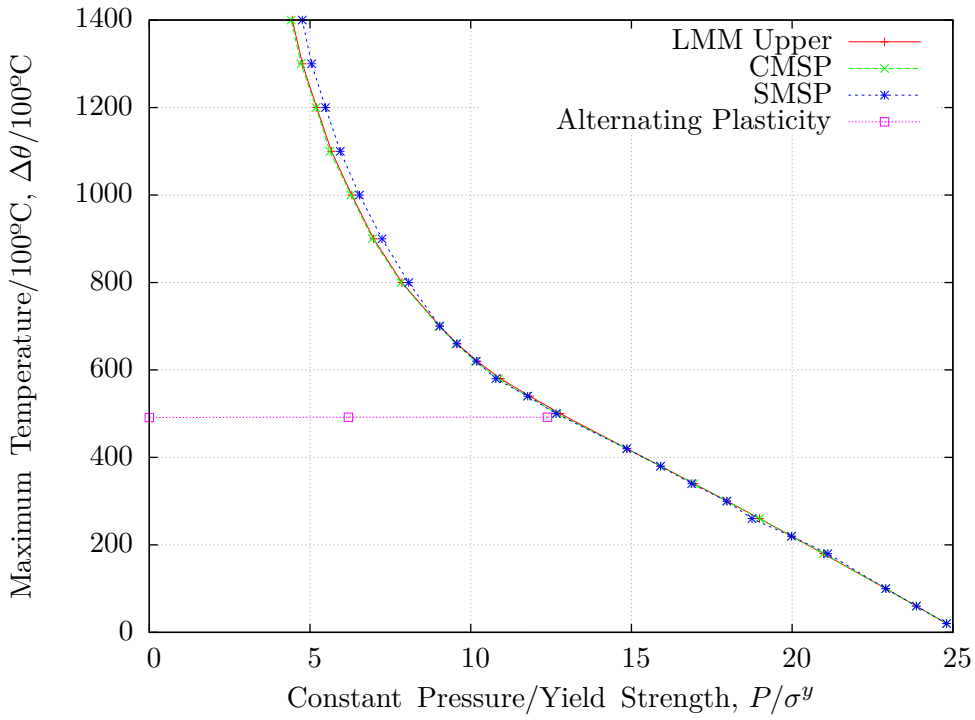

(a) Bree Cylinder Ratchet Diagram from Various Methods

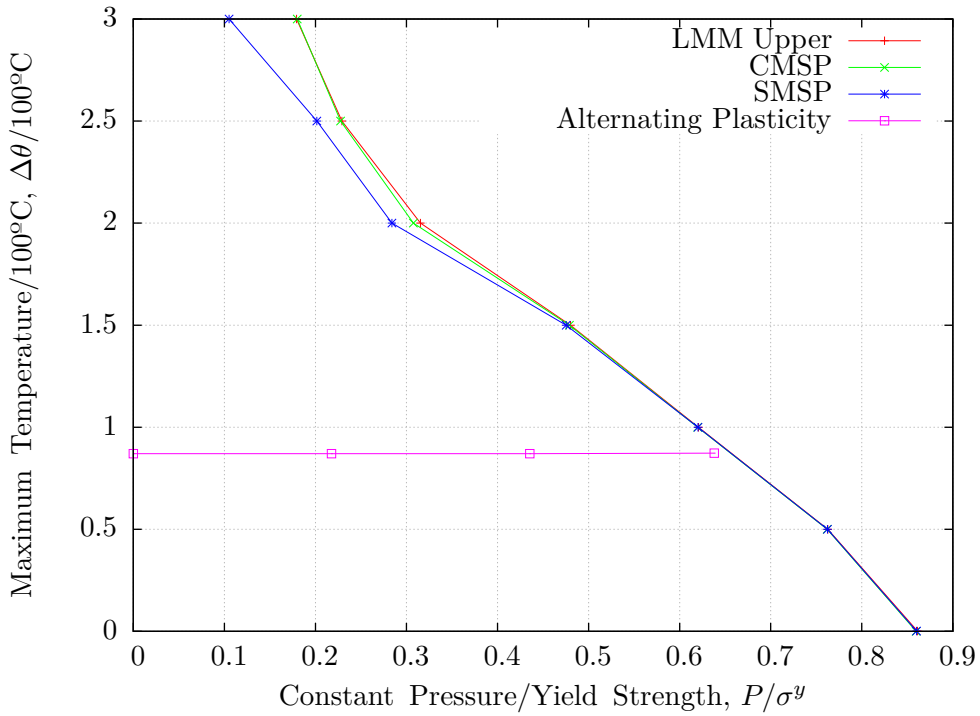

(b) Plate with Hole Ratchet Diagram from Various Methods

Figure 43: SMSP Results

6.5.2 Non-Cyclic Stress

Whilst the simplified cyclic stress proposed by Gokhfeld does not require the use of non-linear analysis techniques to find the "stabilised" cyclic stresses, the resulting boundaries show scattered results compared to the more accurate solution given by the CMSP method. A more serious problem is the possibility of a non-conservative result. This is due to the stresses being simply scaled down in magnitude, resulting in stress fields which do not maintain equilibrium. Here the stress measure used in the non-cyclic method is implemented.

The non-cyclic simplification follows the same basic assumptions as for Gohkfeld's simplified cyclic stress i.e. the cyclic part of the load cycle may be separated into a mean part and a fully reversed cyclic stress amplitude. In this case however, the cyclic stress amplitude is applied in a non-linear elastic plastic analysis. By doing this, if the stress exceeds yield it is allowed to redistribute in a manner which maintains equilibrium throughout the structure. This should result in stresses which satisfy the more stringent conditions of a lower bound method.

Material model and Solution method NMSP

The numerical method based on the non-cyclic stress is given the name NMSP, were the "MSP" parts stands for multi surface plasticity and the "N" is for non-cyclic. The cyclic stress amplitude is found using an elastic-perfectly plastic analysis, to allow redistribution of the stresses if yield is exceeded, thus the first step of the solution procedure is to solve for the cyclic stress amplitude using the following material model:

$$\sigma_{ij}^{A,adj} = C_{ijkq}\left(\varepsilon_{kq}^{Tr} - \varepsilon_{kq}^{p}\right)$$

The yield condition is:

$$f = \left|\sigma_{ij}^{A,adj}\right| - \sigma^{y} \leq 0$$

the plastic strain rate is given by:

$$\dot{\varepsilon}_{ij}^{p} = \dot{\gamma}\frac{\delta f}{\delta \sigma_{ij}}$$

with

$$\gamma \geq 0 \quad , \quad f \leq 0 \quad , \quad \gamma f = 0 \quad and \quad \gamma \dot{f} = 0$$

Note that it is assumed that:

$$\sigma_{ij}^{A,adj} = -\left(-\sigma_{ij}^{A,adj}\right)$$

This model is integrated and implemented using the radial return method. For a detailed discussion on this process see, for example, (Simo and Hughes 2000). Consider that if the cyclic load amplitude was to be reversed at this point the structure would not return to zero strains as the addition of the plastic strain will result in a different unload path in most complex components. Thus the plastic strain calculated at this condition is a mix between a constant residual plastic strain and a varying residual plastic strain. It is not possible to determine at this stage how much of the plastic strain is constant and how much is varying. To find that the load would need to be cycled, which is what the simplified stress is design to avoid.

Having found $\pm\sigma_{ij}^{A,adj}$ the, steady state cyclic stresses and strains can be calculated. The steady state residual stress due to cyclic loading is given by:

$$\bar{\rho}_{ij} = C_{ijkq}\left(\varepsilon_{kq}^{Tr} - \varepsilon_{kq}^{p}\right)$$

The stresses at the loaded conditions are given by:

$$\sigma_{ij}^{1} = \overline{\rho}_{ij} + \hat{\sigma}_{ij}^{mean} + \sigma_{ij}^{A,adj} \ , \ \sigma_{ij}^{2} = \overline{\rho}_{ij} + \hat{\sigma}_{ij}^{mean} - \sigma_{ij}^{A,adj}$$

where $\hat{\sigma}_{ij}^{mean}$ is an optional mean stress that can be added to alter the cyclic profile of the cyclic stresses.

The yield conditions are:

$$f^{1} = \left|\overline{\rho}_{ij} + \hat{\sigma}_{ij}^{mean} + \sigma_{ij}^{A,adj}\right| - \sigma^{y} \leq 0 \ ,$$

$$f^{2} = \left|\overline{\rho}_{ij} + \hat{\sigma}_{ij}^{mean} - \sigma_{ij}^{A,adj}\right| - \sigma^{y} \leq 0$$

and the net plastic strain rate is assumed to be due to all load cases and given by Koiters Rule:

$$\dot{\varepsilon}_{ij}^{p} = \sum_{\theta=1}^{\theta=2} \dot{\gamma}^{\theta} \frac{\delta f^{\theta}}{\delta \sigma_{ij}^{\theta}} = \dot{\gamma}^{1} \frac{\delta f^{1}}{\delta \sigma_{ij}^{1}} + \dot{\gamma}^{2} \frac{\delta f^{2}}{\delta \sigma_{ij}^{2}}$$

with

$$\gamma^{l} \geq 0 \quad , \quad f^{l} \leq 0 \quad , \quad \gamma^{l} f^{l} = 0 \quad and \quad \gamma^{l} \dot{f}^{l} = 0 \ \text{ for} \, l = 1, 2$$

This model can be integrated in the same manner as shown in Section 5.6.2, thus it is not repeated here.

The constant load at the ratchet boundary can then be calculated. The steady state resiudal stress due to all loading is given by:

$$\rho_{ij}^{c} + \overline{\rho}_{ij} = C_{ijkq}\left(\varepsilon_{kq}^{Tr} - \varepsilon_{kq}^{p}\right)$$

The stresses at the loaded conditions are given by:

$$\sigma_{ij}^{1} = \rho_{ij}^{c} + \overline{\rho}_{ij} + \hat{\sigma}_{ij}^{c} + \hat{\sigma}_{ij}^{mean} + \sigma_{ij}^{A,adj} \ , \ \sigma_{ij}^{2} = \rho_{ij}^{c} + \overline{\rho}_{ij} + \hat{\sigma}_{ij}^{c} + \hat{\sigma}_{ij}^{mean} - \sigma_{ij}^{A,adj}$$

The yield conditions are:

$$f^{1} = \left|\rho_{ij}^{c} + \overline{\rho}_{ij} + \hat{\sigma}_{ij}^{c} + \hat{\sigma}_{ij}^{mean} + \sigma_{ij}^{A,adj}\right| - \sigma^{y} \leq 0 \ ,$$

$$f^{2} = \left|\rho_{ij}^{c} + \overline{\rho}_{ij} + \hat{\sigma}_{ij}^{c} + \hat{\sigma}_{ij}^{mean} - \sigma_{ij}^{A,adj}\right| - \sigma^{y} \leq 0$$

and the net plastic strain rate is assumed to be due to all load cases and given by Koiter's Rule:

$$\dot{\varepsilon}_{ij}^{p} = \sum_{\theta=1}^{\theta=2} \dot{\gamma}^{\theta} \frac{\delta f^{\theta}}{\delta \sigma_{ij}^{\theta}} = \dot{\gamma}^{1} \frac{\delta f^{1}}{\delta \sigma_{ij}^{1}} + \dot{\gamma}^{2} \frac{\delta f^{2}}{\delta \sigma_{ij}^{2}}$$

with

$$\gamma^{l} \geq 0 \quad , \quad f^{l} \leq 0 \quad , \quad \gamma^{l} f^{l} = 0 \quad and \quad \gamma^{l} \dot{f}^{l} = 0 \ \text{ for } l = 1, 2$$

This model is integrated using the same method as given in Section 5.6.2 thus is not repeated here.

Examples

The material models and solution methods given in Section 6.5.2 were implemented in ABAQUS using the user subroutine UMAT. The example problems studied were the axi-symmetric Bree cylinder and plate with hole examples given in Sections 5 and 6. See Section 5 for details of geometry and material properties.

Discussion

The results of both the Bree cylinder and plate with hole examples (see figure 44) indicate that the NMSP produces a more consistent ratchet boundary than the Gokhfled

simplified cyclic stress, generally between 1% to 4% of the CMSP method. This is attributed to the redistribution of stress being simulated in the non-linear calculation of $\sigma_{ij}^{A,adj}$. The discrepancies in the calculated boundary may be explained by the loss of the constant residual plastic strain, caused by the simplified cyclic stress solution, which does not simulate the redistribution fully. From compatibility, this will alter the redistribution of constant stress through the structure but to a lesser extent than the Gokhfled simplified stress, as a change in direction of the cyclic stress is partially accounted for. Thus the total stress used in the non-cyclic stress simulation has less error than in the case of Gokhfled simplified stress, resulting in ratchet boundary solutions in closer agreement with the CMSP and LMM. The error shown here is relatively small (<4% and conservative), however it is not possible to say if this is the general case and the simplified stress is limited to considering only two point load cycles, which in the general case may not be sufficient to describe the ratchet mechanism.

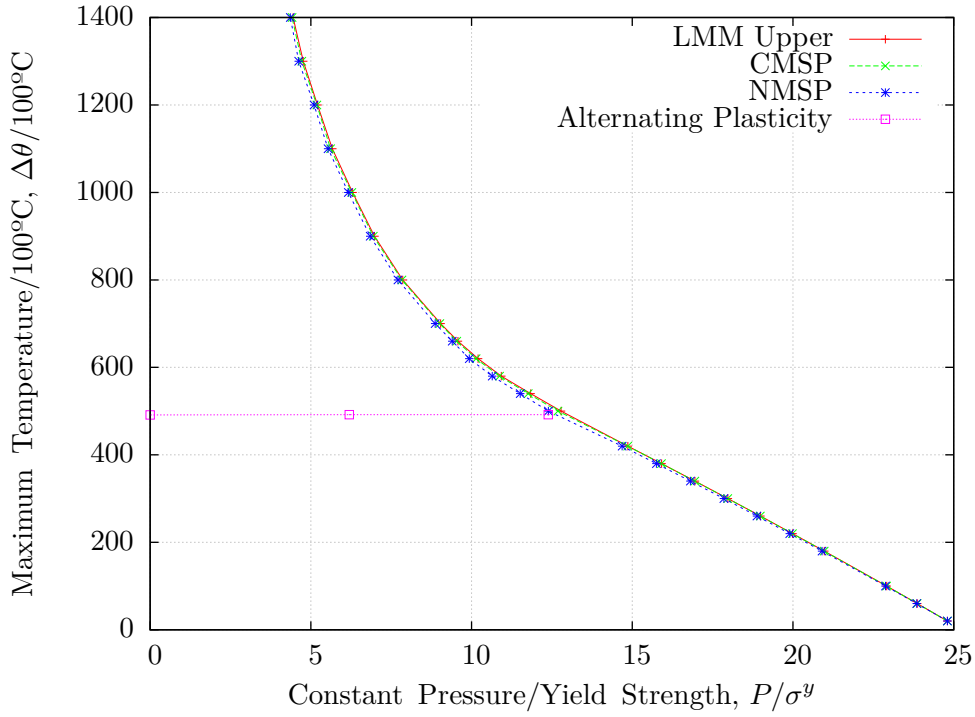

(a) Bree Cylinder Ratchet Diagram from Various Methods

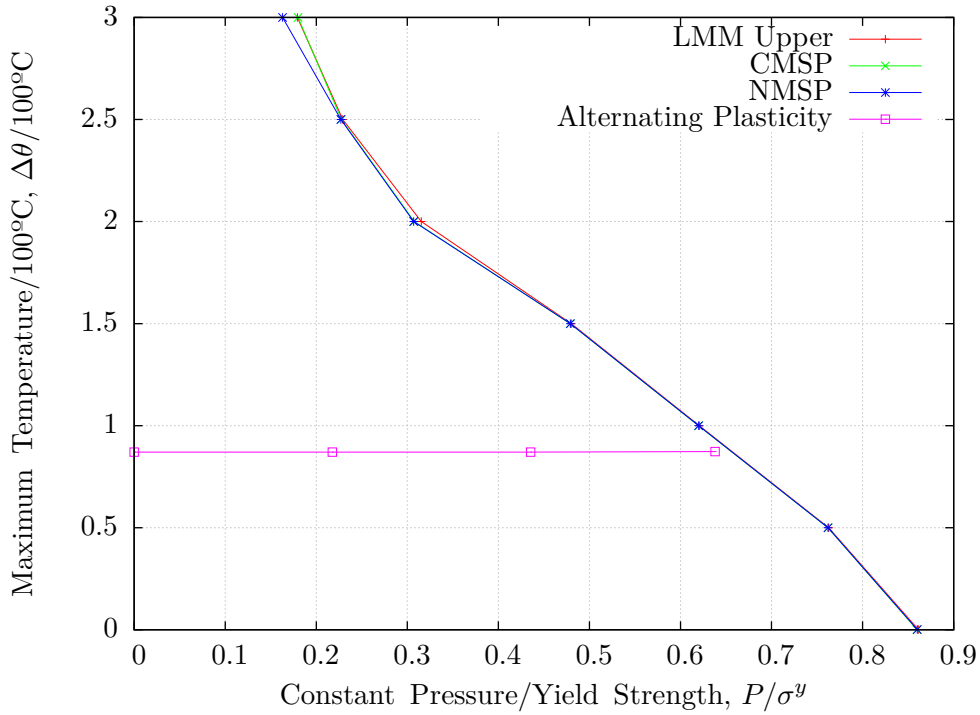

(b) Plate with Hole Ratchet Diagram from Various Methods

Figure 44: NMSP Results

6.6 Current Limitations of the Ratchet Method

The results presented in Sections 6.3 to 6.5.2 show that the CMSP method gives relatively accurate solutions when compared to the LMM and other lower bound methods under the conditions studied. However as with any numerical method there are a number of limitations:

Number of load cases The method can consider an arbitrary set of load cases, however only 6 of the load cases can actively require returning to their respective yield surfaces at once. If more than six require limiting to their respective yield surfaces the problem becomes indeterminate.

Separation of constant and cyclic loads As with all current ratchet methods the proposed ratchet methods require the separation of the constant and cyclic load cases to allow the two stage procedure to work. However many load cases may not have a discernible constant load and it may be impossible to define a constant load to show a suitable safety factor against ratchet. However using the CMSP method as a basis and coupling this with element level formulations it is theoretically possible to overcome this limitation and several others.

Hardening It is possible to consider hardening in the shakedown method as discussed in Section 5.6.2, however in the ratchet method the separation of the constant and cyclic load cases makes it difficult to consider the hardening behaviour of the cycle. As the constant load is added the cycle will take place about a different plastic strain (i.e. the residual plastic strain will change due to the addition of the constant load). This means that the hardening variables will change, making the cyclic solutions invalid. The cyclic solutions would require recomputing after each iteration of the constant load solution to account for the change in the plastic strains. This would result in a relatively computationally expensive method. However the development of a method which solves the cyclic and constant parts of the problem is theoretically possible utilising element level formulations.

Quality of the Cyclic Solutions The quality of the ratchet solutions are susceptible to the quality of the cyclic solutions. This is demonstrated by the solutions for the pipe intersection example (see figure 36). The results for $\Delta\theta/100$ higher than 2.0 showed reduced accuracy. The number of cycles can be relatively high for complex components such as the pipe intersection, and given the highly non-linear nature of the plastic straining and stress redistribution the method may be seen as computationally expensive compared to other methods. However the simplified

cyclic stress descriptions used by other methods could be used in place of the Stage 1 analysis. As with hardening and separation of the load case, the possibility of extending this method using element level formulations could theoretically overcome this limitation

6.7 Discussion

In this Section a new ratchet method has been proposed. This method is unique in that it has been shown to be a strictly lower bound method which gives reliable results for multiple load points, which has not been demonstrated for other lower bound methods. The method utilises a material model that maintains a constitutively consistent description of the plastic strains in the structure, and is again unique in this aspect. Through a number of common benchmark problems and some more complex examples, the method has been shown to give good agreement with the upper bound LMM, which has previously been shown to be an accurate and reliable upper bound method.

Despite the accuracy and reliability of this method, it still has several limitations. These ultimately stem from the use of user programmed material models. When using this approach it is only possible to solve for 1 stress-strain relationship at a time i.e. the residual stress and strain during the shakedown and ratchet solutions. However to solve for effects such as fully non-linear geometry and temperature dependent material effects, in a computationally efficient manner, it is necessary to consider several stress-strain relationships and their non-linear relationship to each other at the same time.

The separation of cyclic and constant parts of the cycle also makes it impossible to consider fully cyclic load conditions that may cause ratchet. Again it is necessary to separate the cyclic and constant parts because it is not possible to solve for multiple stress-strain relationships at once. If element level formulations were used, with a shakedown/ratchet method based on the EMSP/CMSP methods, it is theoretically possible for the constant and cyclic parts of the structures response to be solved simultaneously resulting in a more flexible and potentially more computationally efficient method.

7 Conclusion

Previously proposed modified yield ratchet methods have been revisited and two alternative modified yield methods proposed, formulated and implimented. By investigating the performance of these methods in benchmark problems, two basic limitations in this approach to determining the ratchet boundary were identified: The loss of compatability between solution stages and errors in the direction of plastic strain on the addition of constant load.

Following this investigation, Melan's theorem was reinterpreted in terms of plasticity modelling. Melan's theorem was shown to have the same form as a non smooth multi yield surface plasticity model. A new lower bound direct shakedown method has been proposed, the MSP method, based on non smooth multi yield surface plasticity.

The EMSP method utilises a non-linear finite element material model based on non smooth multi yield surface plasticity. The EMSP method was demonstrated to give good agreement with the upper bound LMM for the benchmark problems studied. The method was extended to allow incorporation of simplified hardening models and the incorporation of approximate non-linear geometry effects.

The EMSP method was then extended to give the ratchet boundary beyond the alternating plasticity boundary. The CMSP method utilises cyclic FEA and the MSP method. The CMSP method was demonstrated to give good agreement with the upper bound LMM.

Two simplified variants of the CMSP method were developed to reduce the computational cost of the method. The SMSP utilises Gokhfeld's simplified cyclic stress. The NMSP method utilises the non-cyclic stresses proposed by Reinhardt.

The EMSP and CMSP methods are unique in that they are strict lower bound methods, reliable and capable of solving for more than two load points. The strict lower bound and reliability of the method are due to maintaining a constitutively accurate description of the assumed material response.

Whilst some limitation have been identified with both the MSP and CMSP methods, it is theoretically possible to overcome all of the current limitations. This could be achieved through the use of element level formulations and a material model based on the MSP and CMSP methods.

The research presented here has developed lower bound shakedown and ratchet methods which allow the determination of both accurate and reliable ratchet boundaries.

8 References

Abdalla, H.F., Megahed, M.M., Younan, M.Y., 2006, "Determination of shakedown limit load for a 90 degree pipe bend using a simplified technique." ASME Journal of Pressure Vessel Technology, 128, 618–624.

Abdalla, H.F., Megahed, M.M., Younan, M.Y., 2007a, "A simplified technique for shakedown limit load determination." Nuclear Engineering and Design 237, 1231–1240.

Abdalla, H.F., Megahed, M.M., Younan, M.Y., 2007b, "Shakedown limit load determination for a kinematically hardening 90-degree pipe bend subjected to constant internal pressure and cyclic bending." In: Proceedings of the ASME – PVP Division Conference , San Antonio, Texas, USA.

Abdalla, H.F., Megahed, M.M., Younan, M.Y., 2007c, "Shakedown limits of a 90-degree pipe bend using small and large displacement formulations." ASME Journal of Pressure Vessel Technology 129, 287–295.

Abdalla, H.F., Megahed, M.M., Younan, M.Y., 2008, "Shakedown limit loads for 90- degree scheduled pipe bends subjected to constant internal pressure and cyclic bending moments". In: Proceedings of the ASME – PVP Division Conference , Chicago, Illinois, USA.

Abdalla, H.F., Megahed, M.M., Younan, M.Y., 2009, "Comparison of pipe bend ratchetting/ shakedown test results with the shakedown boundary determined via a simplified technique." In: Proceedings of the ASME – PVP Division Conference, Prague, Czech Republic.

Abou-Hanna, J., McGreevy, T.E., 2011, "A simplified ratcheting limit method based on limit analysis using modified yield surface." Int. J. Pressure Vessels and Piping, 88, pp.11-18

Adibi-Asl, R., Reinhardt, W., 2008, "The Elastic Modulus Adjustment Procedure (EMAP) for Shakedown" ASME PVP Conference, Chicago, IL

Adibi-Asl, R., Reinhardt, W., 2011a, "Non-cyclic shakedown/ratcheting boundary determination-part 1: analytical approach." Int. J. Pressure Vessels Piping, 88, (8-9), pp.311-320

Adibi-Asl, R., Reinhardt, W., 2011b, "Non-cyclic shakedown/ratcheting boundary determination-part 1: numerical implimentation." Int. J. Pressure

Vessels Piping, 88, (8-9), pp.321-329

Belouchrani, M.A., Weichert, D., Hachemi, A., 2000, "Fatigue threshold computation by shakedown theory." Mech. Res. Comm., 27, pp.287–293.

Bree, J., 1967, "Elasto-plastic behaviour of thin tubes subjected to internal pressure and intermittent heat fluxes with application to fast reactor fuel elements," J. Strain. Analysis, 2, pp.226-238.

Boulbibane, M., Weichert, D., 1997, "Application of shakedown theory to soils with nonassociated flow rules." Mech. Res. Comm., 24, pp.513–519.

Carvelli, V., Maier, G., Taliercio, A., 2000, "Kinematic limit analysis of periodic heterogeneous media." Comp. Mod. Eng. Sci., 1, 19–30.

Chen, H.F. Chen, W., Ure, J.M., 2012, "Linear matching method on the evaluation of cyclic behaviour with creep effect." In: ASME Pressure Vessels and Piping Conference, July 15-20, Toronto.

Chen, H.F., Engelhardt, M.J., Ponter, A.R.S., 2003, "Linear matching method for creep rupture assessment." Int. J. of Pressure Vessels and Piping, 80, pp.213-220.

Chen, H.F., Ponter, A.R.S., 2001a, "A method for the evaluation of a ratchet limit and the amplitude of plastic strain for bodies subjected to cyclic loading." European Journal of Mechanics - A/Solids, 20 (4), pp. 555-571.

Chen, H.F., Ponter, A.R.S. 2001b, "Shakedown and limit analyses for 3-D structures using the linear matching method." International Journal of Pressure Vessels and Piping, 78, pp. 443-451

Chen, H.F., Ponter, A.R.S. 2004, "A simplified creep-reverse plasticity solution method for bodies subjected to cyclic loading." Eur. J. of Mechanics - A/Solids, 23 (4), pp.561-577.

Chen, H.F., Ponter,A.R.S., 2005a, "Integrity assessment of a 3D tubeplate using the linear matching method. Part 2: creep relaxation and reverse plasticity." Int. J. of Pressure Vessels and Piping, 82 (2), pp.95-104.

Chen, H.F., Ponter,A.R.S., 2005b, "The linear matching method for shakedown and limit analyses applied to rolling and sliding point contact problems." Road Materials and Pavement Design, 6, pp.9-30.

Chen, H.F., Ponter,A.R.S., 2006, "Linear matching method on the evaluation of plastic and creep behaviours for bodies subjected to cyclic thermal and mechanical loading." Int. J. for Numerical Methods in Engineering, 68 (1). pp.13-32.

Chen, L., Liu, Y., Yang, P., Cen, Z., 2008, "Limit analysis of structures containing flaws based on a modified elastic compensation method." European J. of Mechanics - A/Solids, 27, pp.195-209

Chen, H.F., Ure, J.M., Tipping, D., 2013, "Calculation of a lower bound ratchet limit part 1 – Theory, numerical implementation and verification." Eur. J. of Mechanics / A Solids,37, pp.361-368

Corigliano, A., Maier, G., Pyckp, S., 1995a. "Kinematic criteria of dynamic shakedown extended to nonassociative constitutive laws with saturation nonlinear hardening." Rend. Mat. Ace. Lincei, 5

Corigliano, A., Maier, G., Pyckp, S., 1995b. "Dynamic shakedown analysis and bounds for elastoplastic structures with nonassociative, internal variable constitutive laws." Int. J. Solids and Structures, 32, 21, pp.3145-3166

Gokhfeld, D.A., 1980, *Limit analysis of structures at thermal cycling.* Sijthoff & Noordhoff.

Gorash, Y., Chen, H.F., 2012, "Creep-fatigue life assessment of high-temperature weldments using the linear matching method." In: RAMS: Recent Appointees in Materials Science, Spetember 5-7, Glasgow. (Unpublished)

Gross-Weege, J., 1990, "A unified formulation of statical shakedown criteria for geometrically nonlinear problems." Int. J. Plasticity, 6, pp.433–447.

Hachemi, A., Weichert, D., 1992, "An extension of the static shakedown theorem to a certain class of inelastic materials with damage." Arch. Mech., 44, pp.491–498.

Heitzer M., Pop, G., Staat, M., 2000, "Basis Reduction for the Shakedown Problem for Bounded Kinematic Hardening Material.", Journal of Global Optimization, 17, pp.185-200

Heitzer, M., Staat, M., Reiners, H., Schubert, F., 2003, "Shakedown and ratchetting under tension–torsion loadings: analysis and experiments." Nuclear Engineering and Design, 225, pp.11-26

Huang, Y., Stein, E., 1996, "Shakedown of a cracked body consisting of kinematic hardening material." Eng. Fract. Mech., 54, pp.107–112.

Koiter, W.T., 1960, "General theorems for elastic plastic solids." *Progress in solid mechanics*, J.N. Sneddon and R. Hill, eds., North Holland, Amsterdam, 1, pp.167-221.

Indermohan, H., Reinhardt, W., 2012 "Ratchet boundary Evaluation and Comparison with Ratcheting Experiments Involving Strain Hardening Material Models." ASME Pressure Vessel and Piping Conference, Toronto, Ontatio, Canada. July 15-19, PVP2012-78516

Lang H., Wirtz, K., Heitzer, M., Staat, M., Oettel, R., 2001, "Cyclic plastic deformation tests to verify FEM-based shakedown analyses." Nuclear Engineering and Design, 2-3, pp.235-247

Lubliner, J., 1990, *Plasticity Theory*, Macmillan, London.

Mackenzie, D., Boyle, J.T., 1993, "A method of estimating limit loads by iterative elastic analysis. I-Simple examples." Int. J. Pres. Yes. Piping 53, pp.77-95

Mackenzie, D., Boyle, J.T., Hamilton, R., 1993, "The elastic compensation method for limit and shakedown analysis: a review." J. of Strain Analysis, 35, pp.171-188

Maier, G., 1969, "Shakedown theory in perfect elastoplasticity with associated and nonassociated flow-laws: a finite element, linear programming approach." Meccanica, 4, pp.250–260.

Maier, G., 1972. "A shakedown theory allowing for workhardening and second-order geometric effects." In: Sawczuk, A. (Ed.), Foundations of Plasticity. Noordhoff.

Maier, G., Carvelli, V., Taliercio, A., 2001, "Limit and shakedown analysis of periodic heterogeneous media." *Handbook of Materials Behaviour Models*, ed. Lemaitre, J,. Academic Press, London, pp. 1025–1036.

Maier, G., Pan, L.G., Perego, U., 1993, "Geometric effects on shakedown and ratchetting of axisymmetric cylindrical shells subjected to variable thermal loading." Engineering Structures, 15 (6), pp.453-465

Marriott, D.L., 1998 "Evaluation of deformation or load control of stresses under inelastic conditions using elastic finite element stress analysis." Proceedings of the ASME Pressure Vessels and Piping Conference, Pittsburgh, Pennsylvania, PVP, 136, pp.3-9

Martin, J.B., 1975, *Plasticity*, MIT Press

Martin, M., Rice, D., 2009, "A Hybrid Procedure for Ratchet Boundary Prediction." ASME PVP Conference, Prague, Czech Republic.

Melan, E., 1936, "Theorie Statisch Unbestimmter Systeme aus Ideal-Plastischem Bastoff." Sitzungsberichte der Akademie der Wissenschaft. Wien, Abtiia;145, pp.195–218.

Muscat, M., Hamilton, R., Boyle J.T., 2002 "Shakedown analysis for complex loading using superposition." J. Strain analysis, 37 (5), pp.399-412

Muscat, M., Mackenzie, D., Hamilton, R., 2003 "Evaluating shakedown under proportional loading by non-linear static analysis." Computers and Strucutres, 81 (17), pp.1727-1737

Nadarajah, C., Mackenzie, D., Boyle, J. T., 1993, "A method of estimating limit loads by iterative elastic analysis. II-Nozzle sphere intersections with internal pressure and radial load." Int. J. Pres. Ves. Piping, 53, pp.97-119

Nguyen, Q., Pham, D., 2001. "On shakedown theorems in hardening plasticity." C. R. Acad. Sci. 329, pp.307– 314.

Nguyen-Tajan, T.M.L., Pommer, B., Maitournam, H., Houari, M., Verger, L., Du, Z.Z., Snyman, M., 2003 "Determination of the stabilized response of a structure undergoing cyclic thermal-mechanical loads by a direct method." Abaqus Users Conference Proceedings.

Pham, D.C., 2005 "Shakedown static and kinematic theorems for elastic-plastic limited linear kinematic-hardening solids." European J. of Mechanics - A/Solids 24, pp.35-45

Polizzotto, C., 1993a, "On the Conditions to Prevent Plastic Shakedown of Structures: Part I- Theory," Trans. ASME, J. Applied Mechanics, 60, pp.15-19.

Polizzotto, C., 1993b, "On the Conditions to Prevent Plastic Shakedown of Structures: Part II- The Plastic Shakedown Limit Load," Trans. ASME, J. Applied Mechanics, 60, pp.20-25.

Polizzotto, C., 1993c, "A Study on Plastic Shakedown of Structures: Part I- Basic Properties," Trans. ASME, J. Applied Mechanics, 60, pp.318-323

Polizzotto, C., 1993d, "A Study on Plastic Shakedown of Structures: Part II- Theorems," Trans. ASME, J. Applied Mechanics, 60, pp.324-330

Polizzotto, C., Borino, G., Cademi, S., Fuschi, P., 1991. Shakedown problems for mechanical models with internal variables. Eur. J. Mech. A 10, pp.621–639.

Ponter, A.R.S., 1975. "A general shakedown theorem for elastic plastic bodies with work hardening." Proc. SMIRT-3

Ponter, A.R.S., Carter K.F., 1996, "Limit state solutions, based upon linear elastic solutions with a spatially varying elastic modulus." Computer Methods in Applied Mechanics and Engineering, 140, pp.237-258

Ponter, A.R.S., Carter K.F., 1997, "Shakedown state simulation techniques based on linear elastic solutions." Computer Methods in Applied Mechanics and Engineering, 140, pp.259-279

Ponter, A.R.S., Chen, H., 2001, "A Minimum theorem for cyclic load in excess of shakedown, with applications to the evaluation of a ratchet limit." Euro. J. Mech. A/Solids, 20, pp.539–553.

Ponter, A.R.S. Chen, H.F., Ciavarella, M., Specchia, G., 2006, "Shakedown analysis for rolling and sliding contact problems." Int. J. of Solids and Structures, 43 (14-15). pp.4201-4219

Ponter, A.R.S., Fuschi, P., Engelhardt, M., 2000, "Limit analysis for a general class of yield conditions." Eur. J. Mech. A/Solids, 19, pp.401–421

Reinhardt, W., 2008, "A Noncyclic Method for Plastic Shakedown Analysis." J. of Pressure Vessel Technology, 130, (3).

Simo, J.C., Hughes, T.J.R, 2000, "Computational Inelasticity." Springer, New York

Simon, J., Weichert, D., 2011, "Numerical lower bound shakedown analysis of engineering structures." Computational. Methods in Applied Mechanics and Enginerring, 200, pp.2828-2839

Staat, M., Heitzer, M., 2001, "LISA - a European project for FEM-based limit and shakedown analysis." Nuclear Engineering and Design, 206, pp.151–166

Shi, J., Mackenzie, D., Boyle, J.T., 1993, "A method of estimating limit loads by iterative elastic analysis. III-Torispherical heads under internal pressure." Int. J. Pres. Ves. Piping, 53, pp.97-119 .

Ure, J., 2013, LMM GUI for ABAQUS CAE, provided via personal comunication.

Ure, J.M., Chen, H.F., Chen, W., Li, T., Tipping, D.J., Mackenzie, D., 2011, "A direct method for the evaluation of lower and upper bound ratchet limits." In: 11th International Conference on Mechanical Behaviour of Materials, June 5-9, Lake Como,.

Ure, J.M., Chen, H.F., Tipping, D., 2013 "Calculation of a lower bound ratchet limit part 2 : Application to a pipe intersection and dissimilar material join." Eur. J. of Mechanics - A/Solids, 37, pp.369-378.

Vu, D.K., Staat, M., 2007, "Shakedown analysis of structures made of materials with temperature-dependent yield stress." International Journal of Solids and Structures, 44, pp.4524–4540

Weichert, D., 1986, "On the influence of geometrical nonlinearities on the shakedown of elastic–plastic structures." Int. J. Plasticity, 2, pp.135–148.

Weichert, D., Gross-Weege, J., 1988. "The numerical assessment of elastic-plastic sheets under variable mechanical and thermal loads using a simplified two-surface yield condition." Int. J. Mech. Sci. 30, pp.757–767.

Yang, P., Liu, Y., Ohtake, H., Yuan, H., Cen, Z., 2005, "Limit analysis based on a modified elastic compensation method for nozzel-to-cylinder junctions." Int. J. Pressure Vessels and Piping, 82, pp.770-776

A LMM Observations

The LMM is an upper and lower bound shakedown and ratchet method, see section 2.5.2 for a more detailed description of the method. The original form of the LMM was an upper bound. Whilst the upper bound form of the LMM has a convergence proof there can be a number of problems when using the method for assessments.

Due to the upper bound nature of the method the results will, theoretically, always be non-conservative. Thus for assessment purposes the method must be shown to be fully converged in order to have confidence in the identified upper bound load multiplier. However the convergence parameter used in the LMM is based on the difference between consecutive multipliers. Thus if a convergence of 0.001 is set, if the multiplier changes by less than 0.001 for 5 iterations in a row the solutions is deemed to be converged. However the multiplier may change by 0.00099 for each of the five iterations. Therefore a convergence parameter of 0.001 is set but the multiplier could have theoretically changed by as much as 0.00495 over the five iterations and a similar change could continue to occur for a significant number of iterations. Thus it is not always easy to determine whether the upper bound method has converged. This is illustrated by use of the plate with hole example studied in section 3.5.4, however for this study the free edges of the plate are not constrained to remain plane. Figure A.1 shows the identified ratchet boundary for converge parameters of 0.001 and 0.0001. Note that a significant difference between the two boundaries can exist, more than the change in converge parameters suggests would be the case.

The lower bound form of the LMM was added to provide a complementary lower bound multiplier to aid in the assessment of whether the upper bound had fully converged and thus increase confidence in the upper bound multiplier. In the case of shakedown the linearity of the problem allowed for scaling of the stresses to give a strict lower bound multiplier that has been demonstrated to be reliable and capable of close agreement with the upper bound multiplier. It has been shown however, that in general the lower bound takes longer to converge to the "actual" solution.

In the case of ratchet the problem is less well defined. The addition of the varying residual stresses that occur due to reverse plasticity results in a series of yield surfaces offset from each other. Thus the stresses are not necessarily being scaled down to the same yield surface, or along the same load path depending on the choice of stresses being scaled. In the case of a single stress being scaled along a single direction it may not be possible to satisfy all of the yield criteria at the same time, thus the problem becomes non-linear.

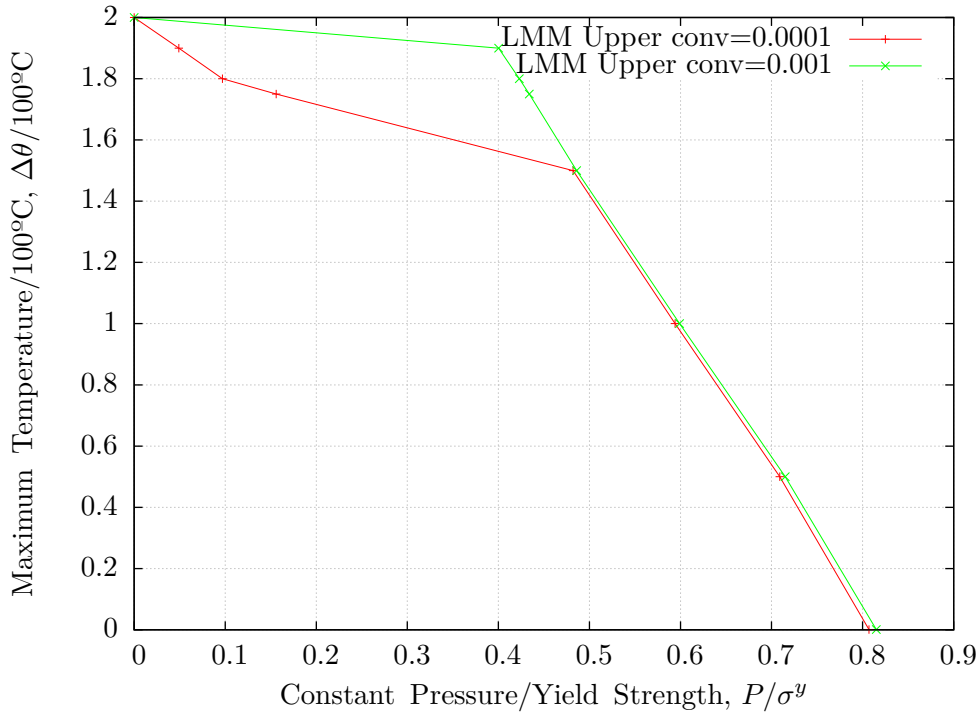

Figure A.1: Upper Bound LMM Convergence

In the latest form of the lower bound LMM presented in (Chen et al. 2013) the constant load alone is scaled down. However in doing so the resulting expression for the lower bound multiplier does not give a single result. It results in a range for the multiplier which will satisfy Melan's theorem for a given point on the load cycle, all points in the load cycle will have a different range of the multiplier which will satisfy Melan's theorem at that load point. However contrary to the claim in (Chen et al. 2013) there is no guarantee that these ranges overlap for all of the load cases and thus it may not be possible to identify a single lower bound multiplier that satisfies all load instances simultaneously. This is illustrated in figure A.2.

In figure A.2 the yield surfaces for the two load points are offset from each other by the varying residual + cyclic stresses. The total stress (given by CD) lies within the red solid yield surface associated with the second load instance, which is possible due to redistribution in the stress during solution. In the case shown $1 \lesssim X_2 \lesssim 1$. However to satisfy the first load case the constant load (vector given by AB) must be scaled

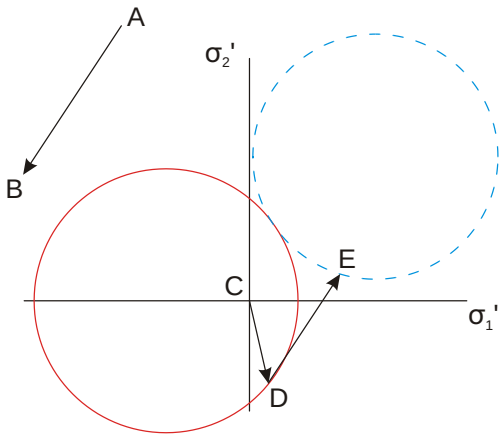

Figure A.2: Impossible Lower Bound Configuration

down along the constant load vector (i.e.
along DE) thus $X_1 \ll 1$. Thus both load cases cannot be satisfied by a single multiplier thus the resulting multiplier should be $X = 0$, however by the current method $X = X_1 \gg 0$. Thus the method if a condition such as this arises in the solution does not represent a strict lower bound solution.

To illustrate this the plate with hole example studied at the start of this section is repeated, without the in plane constraint on the free edges, whilst calculating the lower bound multiplier, the results are presented in figure A.3. A further example of this behaviour was observed in section 6.4.2 in which the lower bound gave excessively non-conservative results. It is clear that the lower bound is capable of giving multipliers that far exceed the upper bound, clearly illustrating the non-strictness of the lower bound LMM. Thus it is difficult to have increased confidence in the upper bound multiplier when using the lower bound multiplier, as the lower bound may be producing a non-conservative result.

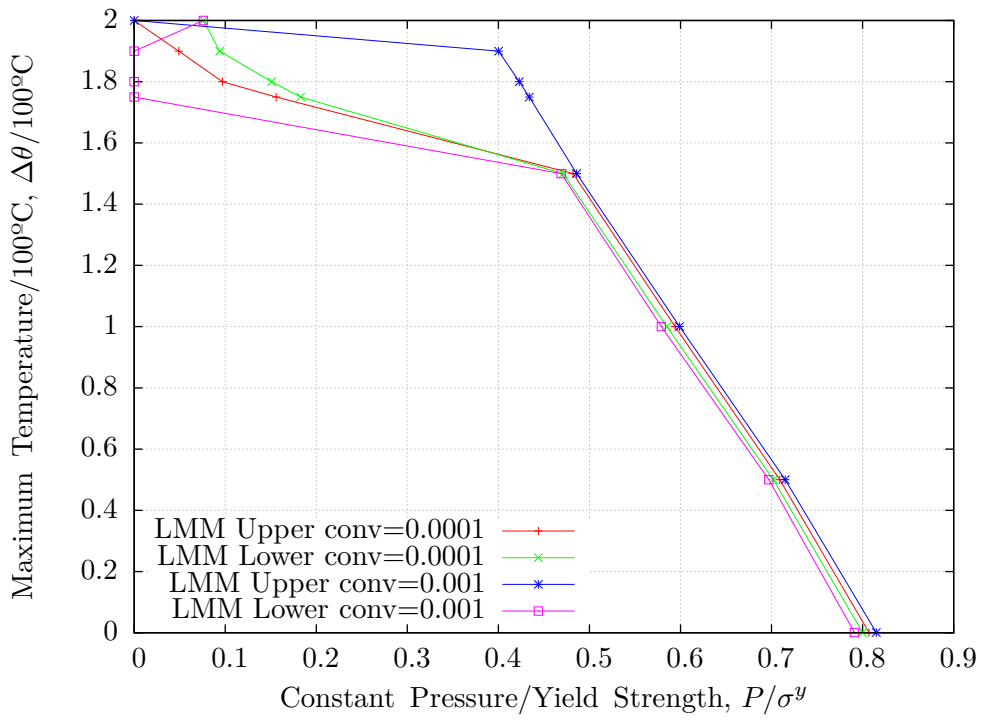

Figure A.3: Lower Bound LMM Non-strictness

B A Study of the effects of Temperature dependent material properties

Temperature dependent material properties, specifically Young's modulus and Poisson's ratio, could have a significant effect on the shakedown or ratchet boundary. Consider that the demonstration of elastic shakedown is fundamentally the demonstration that there exists a time invariant plastic strain in the structure. Consider then, that at a particular temperature there is a non-uniform residual plastic strain in the structure and this results in a given residual stress. On increasing the temperature in a non-uniform manner throughout the structure the shear modulus of the material at the plasticity strained region will reduce, thus unloading this region to part of the structure where the shear modulus reduces by a lesser amount. Thus whilst there is a time invariant residual plastic strain, the residual stress is not necessarily time invariant. This fact is in contradiction to the assumptions in both the upper and lower bound shakedown theorems that there is a time invariant residual stress. Thus the bounding theorems may not be sufficient in cases where a change in temperature could induce a change in the residual stress through a change in material properties.

To demonstrate this a 2D plane stress Bree cylinder, with the same dimensions as in section 5.5.2, and meshed with 10 second order reduced integration elements, with aspect ratio 1, through thickness is studied. The yield strength 402.7MPa, the thermal expansion coefficient 1.335x10^{-5}. The Young's modulus is assumed to be temperature dependent and varies according to $E = 201GPa - 0.0729\frac{GPa}{^{\circ}C} \times (T - T^0)\,^{\circ}C$ and a Poisson's ratio 0.26. An immediate difference, to the temperature independent case, is observed in the elastic stresses resulting from the use of the temperature dependent material properties. These stresses are not linear through thickness due to the non-linear change in Young's modulus through the thickness of the plate. Also the point of zero elastic stress shifts toward the heated side of the plate. The effect on elastic stresses is easily incorporated into current shakedown and ratchet methods as the elastic solutions could be calculated using the temperature dependent material properties and thus account for the asymmetry. Currently the LMM can account of temperature dependent Young's modulus on the elastic stress solutions.

Further to the change in elastic stresses caused by the temperature dependent Young's modulus is the aforementioned effect of a change in residual stress. The Bree cylinder is loaded with the cyclic temperature equal to 900°C with the expansion coefficient of 1.335x10^{-5}. This induces a residual plastic strain into the plate similar to the residual plastic strain which would be present in the Bree cylinder. The plate

is then cooled to find the residual stress at 0°C. The expansion coefficient is then set to zero, by use of the user subroutine UEXPAN and the plate reheated to 900°C. As the expansion coefficient is zero during the reheating any change in the residual stress is induced by the change in material properties. Figure B.1 shows the residual stress state across the thickness of the cylinder for varying temperatures during the reheating process. This clearly indicates that a change in the residual stress is possible due to a change in the elastic material properties of the material caused by a change in temperature. This effect can not, currently, be simulated in any of the direct shakedown or ratchet methods. This is due to the current methods being based on the assumption of a constant residual stress and the use of conventional finite elements.

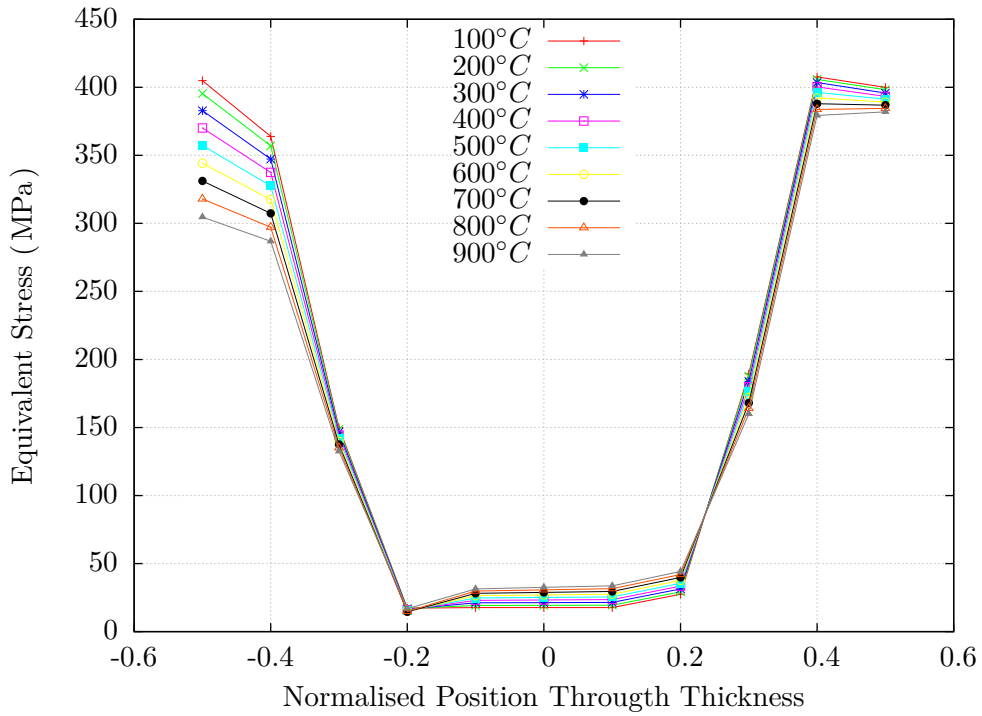

Figure B.1: Change in Residual Stress Due to Temperature Dependent Young's Modulus

To ascertain whether these temperature induced changes in the stress states affect the shakedown or ratchet boundary, incremental FEA was used to obtain the shakedown and ratchet boundaries for the Bree cylinder. The results of the analysis are presented in figure B.2. For comparison the analytical solution for temperature independent properties are also included in figure B.2. As shown in the figure after the initial yield at approximately 300°C there is a gradual deviation of the temperature dependent boundary away from the analytical temperature independent solution. At the analytical shakedown boundary the difference is 3%. The ratchet boundary as given by the temperature dependent Young's modulus adjusted LMM is also given in figure B.2. This shows a ratchet boundary that consistently predicts greater constant load at ratchet

than the temperature independent solutions. This can be explained by the reduction in thermal stress caused by the softening of the high temperature material, resulting in less elastic strain energy for a given temperature. However the incremental finite element results give a boundary which predicts a lower constant load at ratchet than the LMM, this suggests that temperature dependent Young's modulus has a further effect on the resulting boundaries through some other mechanism than the elastic loads. If the results are normalised in the usual manner, i.e. against yield stress the resulting boundaries are shown in figure B.3. The ratchet boundary as found by the incremental finite element solution is consistently lower than the analytical boundary with the difference growing for the greater temperatures.

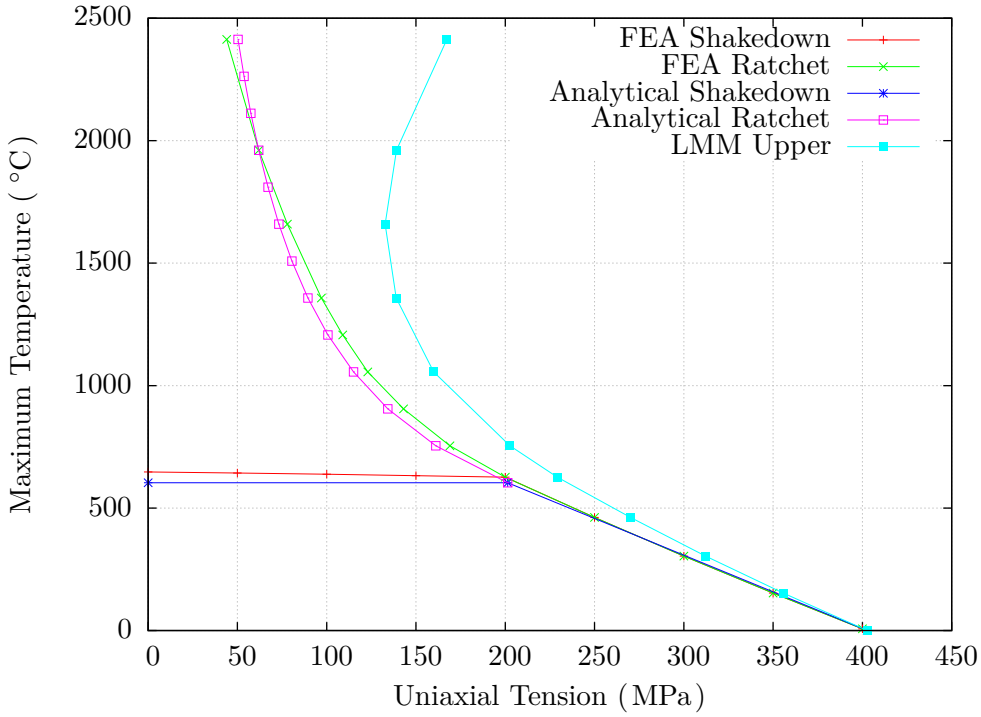

Figure B.2: Bree Boundaries Temperature dependent Properties

A marked difference in the alternating plasticity boundary is also observed in both figures B.2 and B.3 further demonstrating the complex interactions that takes place due to the temperature dependent material properties. In this particular example the difference is slight between the two boundaries. However the difference is sufficient to allow an investigation of the reasons for the difference. If the only cyclic stress was induced by the cyclic thermal load the alternating plasticity boundary should, theoretically, be flat. The downward slope of the alternating plasticity boundary observed for the incremental finite element solutions suggests that there are additional cyclic stresses occurring during the load cyclic. Two possible sources of these additional cyclic effects are a change in the constant load due to changing material properties and

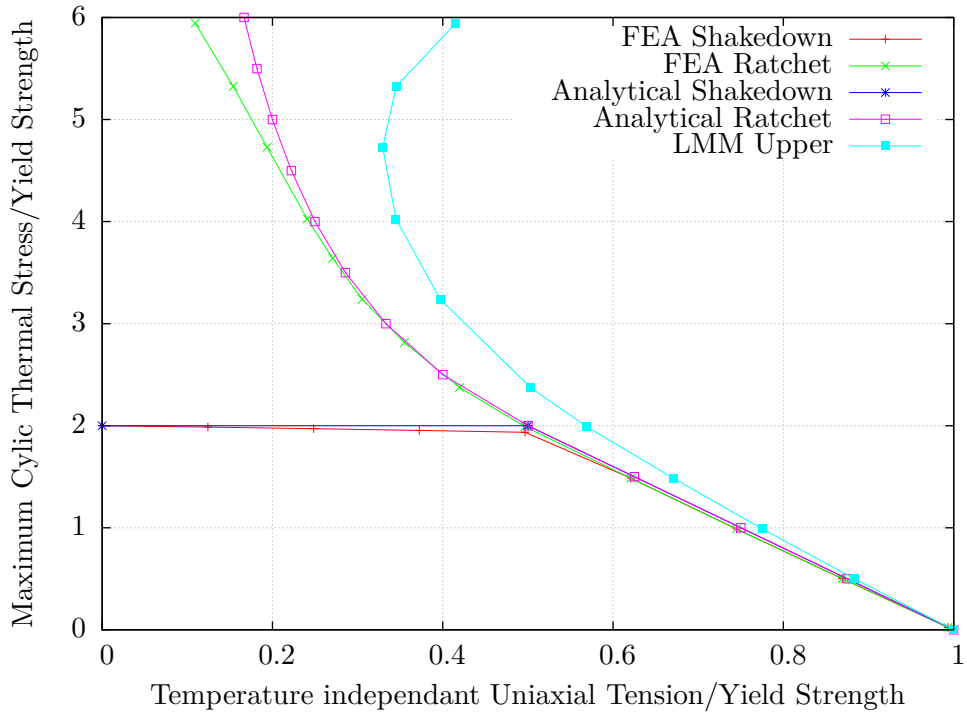

Figure B.3: Normalised Bree Boundaries Temperature dependent Properties

a change in the constant residual stress due to changes in the material properties.

For this study a constant load of 200MPa is chosen and the corresponding temperature of 626°C which lies inside the elastic shakedown domain for this particular problem. The constant load is applied to a finite element model of the Bree cylinder, the model is then heated with the linear temperature gradient whilst ignoring expansion effects i.e. a thermal expansion coefficient of 0. The resulting stresses and the variation in constant load, over the cycle, induced by the changing material properties is shown in figure B.4. To explore the residual stress the Bree cylinder in loaded with the constant load and cyclic temperature whilst accounting for expansion effects until the cycle stabilises, approximately 4 cycles. The cylinder in then unloaded of all loads and temperature. The cylinder in then reheated whilst ignoring the effects of thermal expansion (through the use of user subroutine UEXPAN). The residual stress at 0°C and at 626°C and the resulting variation in residual stress, over the cycle, induced by temperature dependent properties is shown in figure B.4. From figure B.4 it is clear that additional cyclic stresses occur due to the "constant" tensile load and the "constant" residual stress. To find the total cyclic stress these additional cyclic stresses must be added to the cyclic thermal load. From figure B.4 it can also be seen that the variation in the stresses act in the same direction as the cyclic load, thus the additional variations will result in a more damaging case for this particular problem.

From the incremental finite element model the total cyclic stress, over the cycle, is

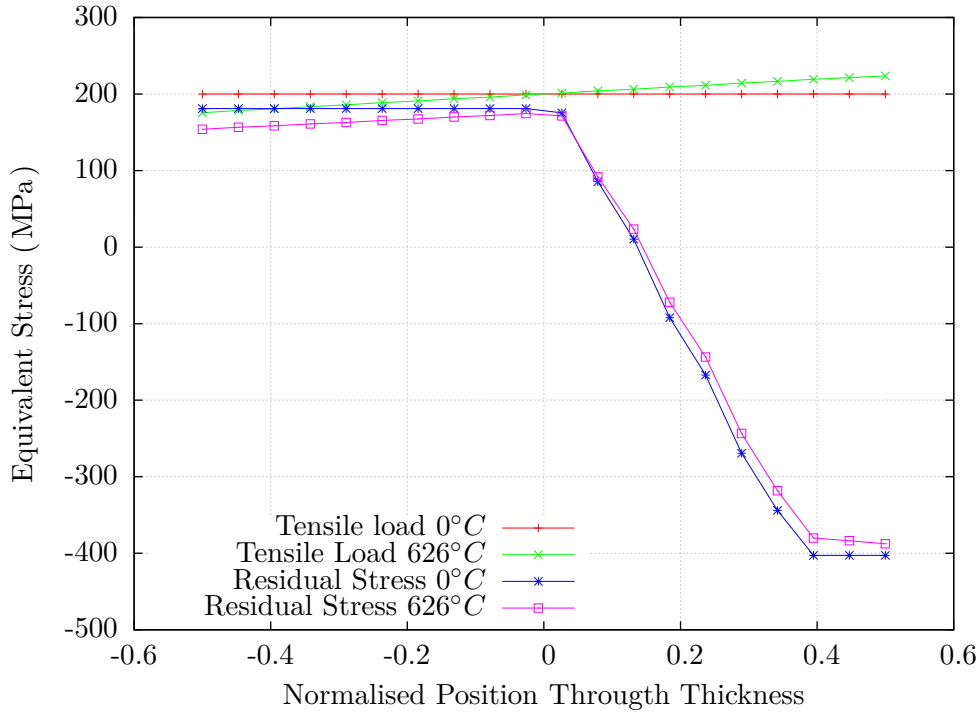

Figure B.4: Bree Cylinder Additional Temperature Induced Variations in Stress

found and shown in figure B.5. The cyclic stress from the cyclic temperature is found by elastic plastic analysis and is shown in figure B.5. It can be seen that the total cyclic stress is greater than the cyclic thermal stress from cyclic temperature alone. If the effect of the variation in constant stress during the cycle is added to the cyclic thermal stress, the resulting total cyclic stress is still less than the total cyclic stress found by incremental FEA. If the variation in residual stress is added to sum of the cyclic thermal stress and the variation in constant stress then the total cyclic stress matches that of the incremental finite element model closely. This suggests that the change in residual stress and constant stress over the cycle induced by temperature dependent properties is an important factor in the determination of the shakedown and ratchet boundaries.

Further to the effects descried by this point on the alternating plasticity boundary, the change in material properties with temperature results in the elastic stress solutions not being linearly related. That is an elastic stress solution at 100°C cannot be scaled to give the elastic stress solution at 200°C. The same is true for temperature effects on the constant load and residual stress.

A number of conclusions can be made from the example studied.

- Temperature dependent properties can result in a variation in the constant and residual stresses during the load cycle
- In the case of the Bree cylinder studied here the variation induced in both the

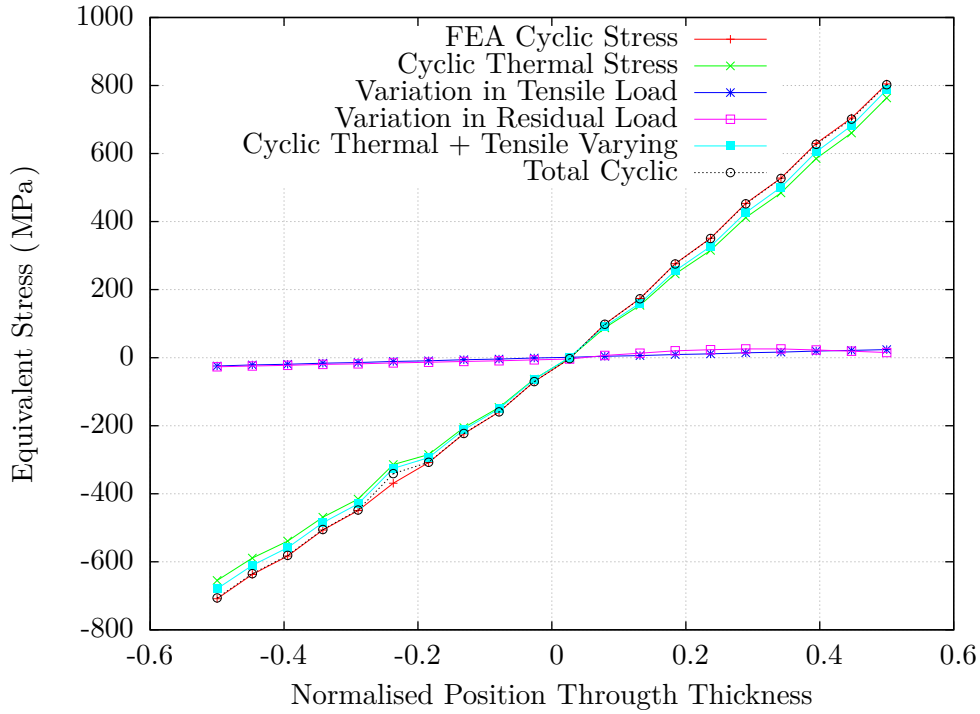

Figure B.5: Bree Cylinder Cyclic Stress with temperature dependent effects

constant and residual stresses are detrimental to the addition of constant load, i.e. it adds to the total cyclic load reducing the size of the elastic core.

- Incorporation of the temperature dependent properties on the elastic loads only can result in non-conservative results as the temperature dependent properties tend to cause lower elastic strain energies in the thermal loads, as demonstrated by the LMM results.

- The possibility of a variation in the residual stress during the cycle, not caused by a change in plastic strain, results in the bounding theorem being invalid under the effects of temperature dependent properties.

- The inability to scale elastic stress solutions for different temperatures requires a new elastic solution for each temperature in the shakedown solutions. The same argument may be extended to the calculation of the variation in constant load and residual stress in a ratchet solution. Requiring a new analysis to determine the temperature effects on the constant and residual stress at every point of the ratchet analysis.

The above example has shown the importance of re-assessing the constant, thermal and residual stresses at each point in the load cycle for every iteration of a shakedown and ratchet solution where temperature dependent material properties are used. However the current solution methodology used in shakedown and ratchet methods does not

allow for the variation in residual stress during the cycle without an accompanying change in plastic strain, nor do they allow for re-assessment of the superimposed stresses during the solution. Thus at present the current methods cannot account of the effects of temperature dependent material properties in a complete sense. Whilst the effect of temperature on the example studied was slight this may not be representative of the general case. The effect on the resulting boundaries is likely to be a function of the geometry, boundary conditions, constraints and the rate of change of material properties w.r.t temperature. Further research on this topic is required to gain an understanding of the general case and the possible effects of temperature dependent material properties on more complex structures and load cycles.

C Nomenclature

Nomenclature

C_{ijkl}	Elastic Modulus
C^{con}	Consistent tangent modulus
D	Hardening modulus
E	Youngs Modulus
E^{ep}	Tangent modulus
f	Yield function
$\mathcal{H}$	Hassian matrix
$\mathcal{L}$	Lagrangian
l	A point in the load cycle
m	Number of points in the load cycle
P	Set of externally applied loads
P^c	Constant loads
$\hat{P}$	Cyclic loads
r	Normal directions
S	The external surfaces of a strucutre
T	Temperature
t	Time
u_i	displacement
V	Volume of the structure
W	Work done
Y	Lower bound multiplier
Z	Fixed Cyclic load multiplier
α	Coefficient of thermal expansion

χ	backstress
δ_{ij}	Kronecker Delta
ε^{Δ}	Varying residual plastic strain
ε^{er}	Elastic residual strain
ε^{p}	Plastic Strain
$\varepsilon^{p\theta}$	Kinemmatically admissable plastic strains
ε^{r}	Compatable residual strain
ε^{T}	Total mechanical strain
ε^{Tr}	Total residual strain
Γ	Energy function
γ	Plastic consistenty parameter
λ	Lamme's constant
μ	Shear modulus
ν	Poiosson's ratio
ρ	residual stress
$\overline{\rho}$	Constant residual due to cyclic loads
ρ^{c}	Constant residual stress
ρ^{Δ}	Varying residual stress due to alternating plasticity
$\rho_{ij}^{\nabla,trial}$	Accumulated varying residual stress at a given point in the load cycle
ρ^{r}	Total residual stress due to cyclic loads
σ	Total stress (i.e. resdiaul + elastic)
σ^{A}	Cyclic stress amplitude
$\sigma^{A,adj}$	Adjusted cyclic stress amplitude
σ^{e}	elastic stress in eequilibrium with the applied load case
$\hat{\sigma}$	elastic stress in equilibrium with the cyclic load

$\hat{\sigma}^c$	elastic stress in equilibrium with the constant load
$\hat{\sigma}^{mean}$	Mean cyclic stress
σ^r	Normalised Stress
σ^y	Yield stress
φ	Period of a load cycle
ζ	Local itteration number in plasticity algorithims